

## 5. Drilling of GTE-8 and Results Obtained

### 5.1 Selection of Drilling Site

The results of the fault tracing survey around the geothermal manifestations and subterranean temperature survey at the depth of 100 meters conducted in 1985 revealed that northwest to southeast trending faults exist at both sides of the geothermal manifestation area, and the distribution of the temperature coincides well with the distribution of the faults. Judging from the data, especially the distribution of subterranean temperature above 70 degrees in centigrade, the size of the presumed geothermal reservoir is more than 500 meters width and 1,000 meters length.

It is necessary to drill investigation wells, and to measure temperature and hydraulic conductivity of fluid for evaluation of geothermal reservoirs in the San Kampaeng area. The results of the surveys conducted this time also suggested that further investigation wells were necessary. Accordingly the drill site for GTE-8 was selected at a quarry near the subterranean temperature survey hole No. 9. For the selection of the site, the survey results by the fingerprint method played a very important role.

### 5.2 Drilling Work

#### 5.2.1 Generalization

##### (1) Outline of the drilling

- 1) Site: San Kampaeng Area, Thailand (Fig. 5.2-1)
- 2) Drill No.: GTE-8  
Inclination: vertical  
Depth: 1,049.84 m  
Final bore hole size: HQ (98.7 mm)

##### (2) Procedure

Site preparation and setting of the drilling equipment were conducted by EGAT. Drilling works were conducted by the EGAT drilling team under the instruction of JICA engineers. The drilling was started on November 13, 1986, and temporarily stopped at the depth of 518.07 meters on March 15, 1987, then resumed on May 29, 1987. The hole was finally completed at the depth of 1,049.84 meters on December 4, 1987.

Fig. 5.2-2 and Tables 5.2-1 and 5.2-2 show the principal data on the drilling process and the works.

#### 5.2.2 Drilling Work

##### (1) Layout of the site

Fig. 5.2-3 shows the layout of the site.





Volume : 4,942 liters  
 Specific Gravity : 1.80  
 Mixing rate : Cement 4,391 liters of cement

After casing pipes were fixed, an inner and outer tube pressure test were done. No pressure decrease was confirmed after 10 minutes under the conditions of 20 kg/cm<sup>2</sup> pressure.

4) 424.00 to 518.07 meters

The hole was drilled by 5 5/8 inches toricone bits up to the depth of 499.00 meters. Rocks in the hole are mainly hard, fine-grained sandstone. Hardness thereof tends to increase with depth.

At the depth of 435.94 meters, 6 liters per minute lost circulation was encountered. Squeeze was done because the depth was close to the bottom of the 6 inch casing pipes.

This was effective for prevention of lost circulation.

HQ-WL coring was conducted below the depth of 499.00 meters.

At the depth of 501.69 meters, 250 liters per minute hot water outpour occurred. As a result of logging test, it was clarified that the water was gushing from the point of lost circulation at the depth of 480.00 meters. It was decided to block the point of lost circulation since it was shallow and the temperature of the fluid was low at 117°C. Then squeeze cementing was done two times.

Specification of the drilling using 5 5/8 inch toricone bits is as follows:

Mud Water : Volume ; 380 liters/min.  
                   Pressure ; 10 ~ 15 kg/cm<sup>2</sup>  
 Bit : Bit load ; 2.5 ~ 4 tons  
                   Rotation: ; 40 - 45 rpm

Specification of the drilling using HQ-WL diamond is as follows.

Mud Water : Volume ; 110 liters/min.  
                   Pressure ; 10 ~ 20 kg/cm<sup>2</sup>  
 Bit : Bit load ; 1.5 tons  
                   Rotation ; 100 ~ 150 rpm

The mud temperature shown in centigrade is as follows.

Depth (m)	450	480	510
Entering (°C)	49.9	50.3	46.2
Outflow (°C)	55.9	57.1	60.3

5) 518.07 to 755.00 meters

The hole was drilled by the HQ-WL method. At the depth of 643.24 meters, a total circulation loss was encountered. Therefore, the mud water was replaced with pure water. However, continuous water outflow was encountered at the depth of 653.44 meters. Outflow pressure was 4 to 5 kilograms per square centimeter. Accordingly, it became impossible to drill further because the inner tubes could not be inserted into outer tubes. Therefore, reaming using 5 5/8 inches toricone bits was done, after which various bore hole loggings were performed. As the result of these loggings, it was decided to perform squeeze cementing, because the outflow volume of the fluid was 630 liters per minute, although the temperature of the fluid was relatively low at 120°C. Cementing was done two times.

Afterwards, drilling was resumed using 5 5/8 inches toricone bit. Rocks changed to quartzose fine-grained sandstone, after which drilling speed significantly declined. At the depth of 706.92 meters, total circulation loss was encountered. Accordingly, the mud water was replaced with pure water. Subsequently, lost circulation drilling was done up to the depth of 755.00 meters. Results of various bore hole loggings showed that the outflow volume was 1,140 liters per minute and the temperature of the fluid was 120°C. Accordingly, squeeze cementing was done three times, and the section blocked.

Specification of the drilling using 5 5/8 inch toricone bits is as follows :

Mud water	: Volume	; 380 liters/min.
	Pressure	; 10 ~ 15 kg/cm <sup>2</sup>
Bit	: Bit load	; 3 ~ 4 tons
	Rotation	; 40 ~ 45 rpm

Specification of the drilling using HQ-WL diamond bits is as follows :

Mud Water	: Volume	; 100 ~ 200 liters/min.
	Pressure	; 10 kg/cm <sup>2</sup>
Bit	: Bit load	; 1.5 ~ 2.5 tons
	Rotation	; 100 ~ 200 rpm

Four and a half inch casing pipes were inserted up to the depth of 752.50 meters, then fixed by cementing by the two-plug method.

The volume, specific gravity, and mixing rate of the pressure cement slurry are as follows.

Volume	: 7,196 liters
Specific Gravity	: 1.50
Mixing Rate	: API Class G Cement ; 4,092 kg
	Silica Sinter ; 1,637 kg (4,092 kg × 0.4)
	Fly Ash ; 1,023 kg (4,092 kg × 0.25)
	Bentonite ; 143 kg (4,092 kg × 0.035)
	Dispersion Agents CFR-2 ; 24 kg (4,092 kg × 0.006)
	Dispersion Agents D-19 ; 23 kg (4,092 kg × 0.0055)
	Retarder HR-4 ; 8 kg (4,092 kg × 0.002)

After hardening of cement, an inner and outer tube test were done. No anomaly was found.

6) 755.00 to 1,049.84 meters

The hole was drilled by the HQ-WL coring method. Rocks between 749.20 meters and 894 meters were brecciated, and drilling speed increased. Width depth, quartz veinlets increased in the rocks and bit life was shortened significantly.

At the depth of 907.00 meters a total circulation loss was encountered and thermal water outgush occurred. Therefore, when rods were raised or lowered, high density mud water mixed with barite was poured into the hole to prevent outpour of fluid.

At the depth of 914.59 meters, various borehole loggings were performed as well as a blowout test. Results of those tests revealed that the temperature at the point of 907 meters was 125.9°C, and the volume of the outflow water was 960 liters per minute.

Squeeze cementing to prevent fluid blowout was performed six times, and total volume of consumed cement slurry reached 26,063 liters.

At the depth of 915.45 meters, a total circulation loss was encountered; however, no special countermeasure was done and drilling was continued. At the depth of 1,031.89 meters, drilling was temporarily stopped, then various bore hole loggings and a blowout test were performed.

After finishing the tests, HQ-WL coring was resumed. However, rocks changed to very hard sandstone containing more than 90 per cent quartz, and bit consumption drastically increased. On December 4, the break side drum of the drilling cracked, and water leakage occurred. Therefore, it became very risky to insert drilling equipment into the hole. Drilling was consequently stopped at the depth of 1,049.84 meters.

Specifications of the drilling are as follows :

Mud Water	: Volume	; 100 ~ 250 liters/min.
	Pressure	; 3 ~ 15 kg/cm <sup>2</sup>
Bit	: Bit load	; 1.5 ~ 2.5 tons
	Rotation	; 100 ~ 200 rpm

(4) Mud Water for drilling

The mud water was mixed on the basis of geology, drilling method (reaming or coring), state of well, and temperature of the hole, and was remixed when the foregoing conditions changed drastically. supplementation, or replacement of necessary. The composition of the mud for each section of depth is as follows.

1) 0.0 to 37.00 meters

Mud mainly composed of bentonite was used for the drilling for the overburden and fragile weathered shale.

2) 37.00 to 203.00 meters

Bentonite mud was used for this section; however, it was gradually changed to Telnite BH mud with increase of temperature. Slight circulation loss was sometimes encountered, at which point mud water containing Telstop G (granular) and P (powder), and other organic material were used to stop the lost circulation.

3) 203.00 to 424.00 meters

Mud water mainly composed of Q-B mud was used for this. Because 40 liters per minute outflow of water was encountered at the depth of 274.00 meters, bentonite and asbestos were added to the mud to adjust its specific gravity and viscosity.

4) 424.00 to 755.00 meters

Mud water mainly composed of Telnite BH was used for this section. Outflow of water was also encountered in this section. It was furthermore frequently necessary to supplement the mud. At the depth of 707.00 meters, a total circulation loss was encountered, and mud water was replaced with pure water because mud could not be prepared in time. Pure water drilling was continued up to the depth of 755.00 meters.

5) 755.00 to 1,049.84 meters

After fixed casing pipes, HQ-WL coring was resumed, and it was continued up to the depth of 907.00 meters, where a total circulation loss was encountered. In this section, mud water mainly composed of Telnite BH was used.

Many cracks were encountered below the depth of 907.00 meters, from which point lost circulation occurred constantly. Furthermore, fluid outgush occurred in this section. To prevent outgush high density mud water containing barite was pumped into the hole when bits were replaced.

(5) Cementing

Table 5.2-4 shows the status of casing pipe cementing and maintenance cementing.

(6) Measurement of mud water temperature

Temperature of the mud water upon entering the holes and outflow from the holes was measured, recorded, and referred to in assessing changes of inner hole conditions.

Fig. 5.2-4 shows the results of the measurement.

(7) Status of lost circulation during drilling

Table 5.2-5 shows the status of lost circulation

(8) Status of setting of casing pipes

Fig. 5.2-5 shows the status of casing program.

(9) Penetration rate and core recovery

Fig. 5.2-6 shows the penetration rate and the core recovery rate.

### 5.3 Core Geology

#### 5.3.1 Generalization

Geological study on the drill cuttings and the core was conducted twice, March 4th to 20th, 1987 and October 4th to 20th, 1987, while the drilling of GTE-8 was in progress. The studied section is from 8 m to 1,031.89 m. Geology, alteration and fractured zone were carefully studied in preparation of the geologic column. Representative samples were taken for X-ray diffraction

analysis and fixed inclusion study to define the alteration minerals and to measure the homogenize temperature of minerals. Circulation loss and drilling speed were analysed to study the distribution of fractures.

Geology of GTE-8 is mainly composed of alternation of black shale and quartz sandstone. The geology of this test well is similar to that of GTE-6 but considerably different from the geology of GET-6. No limestone or chert intercalation was seen.

### 5.3.2 Geology

The geology of GTE-8 is composed of alternation of quartzose sandstone and black shale and can be correlated to the Kiu Lom Formation of Permian age. Lithologically, it can be subdivided into four members that is, alternation of shale and sandstone (0 m to 421 m), sandstone dominant member (421 m to 755 m), shale dominant member (755 m to 926m) and sandstone dominant member (926 m to 1,031.89 m). (Fig. 5.3.-1)

#### (1) Alternation of shale and sandstone member (0 m to 421 m)

The thickness of the alternating shale and sandstone is more or less 10 meters in general. However, between 160 m to 240 m, both types become 40 m thick beds.

Shale is generally black to dark grey colored, and rock facies partially change to fine sandy shale and to sandstone. The black shale is highly cleaved and slickenside is partially observed. Pale green grey colored thinly laminated siltstone is found between 64 m to 99 m. This rock type is characteristic among the rocks observed in GTE-8.

Sandstone is quartzose fine grained sandstone and transition to shale is common. In some parts sandstone becomes quartzose and compact resulting in cherty facies.

#### (2) Sandstone dominant member (421 m to 755 m)

This section is mainly composed of quartzose fine grained sandstone and intercalated shale of 10 m thick. Sandstone is fine to medium grained and occasionally muddy sandstone is included. Stratification is weak and appearance is generally massive and less fractured. Silicification is obvious in places and fractures are filled by quartz veining.

#### (3) Shale dominated member (755 m to 926 m)

Mainly composed of shale with partial intercalation of sandstone layer. Shale is highly stratified black shale with thin sandy layers. In some places boudinage or pull-apart type sandstone bed or blocks are contained. Two interpretations can be made for this type of sandstone, that is, the result of contemporaneous pseudo-pebbling during sedimentation or pull-apart structure during orogenic movement.

In the section between 870.00 m to 894.50 m, complicated rock facies such as frequent alternation of sandstone and shale with brecciation and silicification are characteristic. Especially, the 872 m to 876 m section is highly brecciated suggesting fault breccia zone.

#### (4) Sandstone dominant member (926 m to 1,031.89 m)

This section is composed of quartzose fine grain sandstone with few layers of black shale. In



some parts, grain size becomes very fine and silicified lithofacies become similar to chert.

### 5.3.3 Alteration

#### (1) General characteristics

For those sections drilled by the non-core method using tricone bit, that is between 0 m to 499 m and 653.44 m to 755.0 m, only drill cuttings were available for petrological study. Therefore the mode of occurrence and assemblage of vein minerals as well as alteration minerals are not clear in detail for these sections. In this test well, from the surface to the bottom, quartz veining and pyrite dissemination is abundant. Vein quartz is milky white and the width of veins sometimes reaches 1 cm to 2 cm. The quartz vein is more abundant in sandstone than in shale, since sandstone is brittle and susceptible to major fractures, as well as lithologically being rich in  $\text{SiO}_2$  and susceptible to leaching, and redeposit.

#### (2) X-ray diffraction analysis

Typical samples are taken from the drill core to conduct X-ray diffraction analysis. Number of detected minerals is limited, being quartz, K-feldspar (microcline), chlorite, sericite and pyrite. (Table 5.3-1)

Quartz and K-feldspar (microcline) are quite abundant, and in most cases are considered not to be alteration minerals, but primary minerals. However, some portions of quartz are evidently quartz vein with druse cavities sometimes serving as passages for hydrothermal solution, suggesting that recent hydrothermal activity may have formed the vein. Secondary quartz formed by silicification is also observed.

Judging from their genesis, there are two types of chlorite and sericite, the one is the product of vein-forming hydrothermal alteration and the other is the result of diagenetic alteration. The amount of these minerals is less than the quartz and K-feldspar.

The sample taken from the depth of 872.10 m is alternated, no chlorite and pyrite were detectable, while sericite was common. The sericite is considered to be a vein-forming hydrothermal alteration mineral along the fracture in the sheared zone.

Pyrite is mostly disseminated along microfractures or hair cracks. In some places, the pyrite occurs as veins along the major fractures or as small masses crystalized in druse cavities.

#### (3) Homogenized temperature of fluid inclusion.

The homogenized temperature was measured in the vein minerals taken from typical core samples. Those are two samples of vein quartz from the sheared zone of 87.10 m depth and from the sandstone of 1,023.59 m deep (Fig. 5.3.-2, Table 5.3-2).

Measured homogenized temperature ranges from  $119^\circ\text{C}$  to  $134^\circ\text{C}$ . The minimum homogenized temperature is  $121^\circ\text{C}$  at 872.1 m and  $119^\circ\text{C}$  at 1,023.59 m. These temperatures roughly agree with the results of temperature logging conducted after 51 hours of standing time on October 9th, 1987. Vein quartz observed in the core included druse cavities.

Judging from above-mentioned two facts, coincidence of temperature and existence of druse cavities, fluid inclusion bearing quartz veins are being formed by the present hydrothermal activity.

#### 5.3.4 Fractures

Drilled cores appropriate for the fracture study were taken from the depth of 499.00 m to 653.44 m and 755.00 m to 1,031.89 m, respectively.

The geology of the former, from 499.00 m to 653.44 m, is hard compact quartzose fine tuff and the drilled core forms a perfect bar or long cylinder meaning less fractured rock. Steeply dipping sharp fracture is common. Most of those fractures are filled with quartz and are partially observed.

In the latter section, 755.00 m to 1,031.89 m, the geology between 871.54 m and 876.04 m is highly brecciated alternation of sandstone and shale. Quartz vein is abundant. Brecciated shale occurs sometimes in quartz vein. Around 9,820 m, frequent alternation of shale and sandstone occurs and rock is highly fractured. Vertical quartz vein is abundant and generally highly silicified. Crystals of needle quartz and/or prismatic (columnar) quartz were observed in the druse of quartz vein. At the depth of 920 m and deeper, the recovered cores are brecciated, and only a limited length of cylindrical or bar shaped core was recovered. Core recovery ratio was also low, suggesting that fracturing is highly developed and rocks are easy fragmentized in this section.

The lost circulation during drill operation indicates permeable fracturing. When GTE-8 was drilled, lost circulation and groundwater outpour are often encountered. The main lost circulation was observed at the following five zones (Fig. 5.3-1).

① Lost circulation zone at 100 m

Lost circulation was observed at the top and bottom boundary of pale grey siltstone distributed 64 to 99 m depth. At the depth of 119.22 m to 121.50 m, the amount of lost circulation was 40 l/min to 50 l/min suggesting the fracture is major.

The zone coincides with the high anomaly detected by temperature logging and is considered to be the result of influence of active geothermal fluid.

② Lost circulation zone at 250 m

The volume of lost circulation in this zone is not large. At the depth of 272.80 m to 279.34 m, 8 l/min to 17 l/min of outpouring was observed. Temperature logging indicates increasing temperature at this depth suggesting influence of active geothermal fluid.

③ Lost circulation zone at 450 m

Geology of this section is fine to medium grained sandstone with intercalated dark grey shale between 459 m to 467 m. At the depth of 435.94 m, lost circulation of 6 l/min was encountered. Between 472.94 m and 484.00 m, 5 l/min of outpour was found. Temperature logging and flow meter logging revealed that this outpour zone is a supply for geothermal fluid.

④ Lost circulation zone at 600 m to 700 m

The volume of lost circulation is quite large in this zone, i.e., 110 l/min at 643.24 m, and 350 l/min at 706.92. Since lost circulation was great, the tricorner bit was adopted for drilling. Geology is mainly quartzose fine grain sandstone. Fractures are presumably druse type cavities in quartz vein.

⑤ Lost circulation at 900 m

Lost circulation of 100 l/min was recorded at 907.00 m and 150 l/min at 915.45 m.

Geology of this zone is frequent alternation of sandstone and shale. Quartz vein with druse cavities is abundant. Temperature logging and flow meter logging revealed that open fractures at 915.45 m and deeper are the outflow points for geothermal fluid.

## 5.4 Well Logging

When the exploratory well GTE-8 was drilled, the following were performed: well logging during drilling, down-hole measurement during production logging and production test.

These measurements and tests serve to study physical properties of geological formations around the well and to study characteristics of geothermal fluid and geothermal reservoirs, provided that geothermal fluid outflow occurs in the well.

Down-hole measurements performed are well logging under static conditions and production test and production logging under producing conditions.

### 5.4.1 Temperature and Pressure Logging

#### (1) Summary

Well logging was carried out simultaneous to drilling. The first well logging was carried out to 203 m depth in December 1986 before casing pipe (8") was inserted.

The second well logging was carried out to 424 m on February, 1987 under conditions water outpour into the well.

The third well logging was carried out to 501 m depth in March 1987, the fourth to 755 m in July 1987, and the fifth to 1,031 m in October and November 1987.

Equipment used and logging procedure are the same as for GTE-7.

Table 5.4-1 Summary of Well Logging of GTE-8

Stage		Items	Remarks
Stage 1	0 ~ 203 m	Temperature logging, Electrical logging, Pressure logging, Caliper logging	by Thai Team
Stage 2	0 ~ 424 m	Temperature logging, Electrical logging, Pressure logging, Caliper logging, Sonic logging, Flowmeter logging	by Thai Team
Stage 3	0 ~ 501 m	Temperature logging, Electrical logging, Pressure logging, Caliper logging, Flowmeter logging	technical advice
Stage 4	0 ~ 755 m	Temperature logging, Electrical logging, Pressure logging, Caliper logging, Flowmeter logging	by Thai Team
Stage 5	0 ~ 1,031 m	Temperature logging, Electrical logging, Pressure logging, Caliper logging	technical advice

(2) Results

The major results of well logging are as follows:

1) The first well logging

The first well logging was carried out when drilling reached to depth of 203 m, and before casing pipe was inserted (Fig. 5.4-1 and Table 5.4-2).

The results of well logging are as follows:

- ① Temperature increases gently with depth and significant change occurs to 203 m depth (well bottom). The bottom temperature is 85.2°C (Fig. 5.4-3).
- ② Electrical logging shows low resistivity to 100 m depth and some resistivity variations beyond 100 m. There are resistivity peaks at depths of 120 m, 150 m, 170 m, and 190 m with resistivity values of 500 to 550  $\Omega$ -m. SP curve shows sudden change at depths of 130 m and 160 m (Fig. 5.4-2).
- ③ Water level in the well is at about 16 m. Pressure at the bottom of the well (203 m) is 19.3 kg/cm<sup>2</sup>G (Fig. 5.4-4).

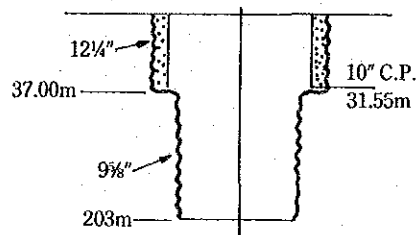


Fig. 5.4-1 Well State in Logging of GTE-8 (Stage 1)

Table 5.4-2 Progress of Well Logging of GTE-8 (Stage 1)

Logging Items	Temperature logging	Electrical logging	Pressure logging	Caliper logging
Date	Dec. 23, 1986	Dec. 23, 1986	Dec. 23, 1986	Dec. 23, 1986
Drilling depth	203 m	203 m	203 m	203 m
Casing	(10") 31.55 m	(10") 31.55 m	(10") 31.55 m	(10") 31.55 m
Shut in	Dec. 23, 1986 17:00	Dec. 23, 1986 17:00	Dec. 23, 1986 17:00	Dec. 23, 1986 17:00
Standing time	—	3 hr	—	—
Time of measurement	21:50 ~ 22:03	19:55 ~ 20:15	—	20:38 ~ 20:52
Depth of measurement	30 ~ 200 m	0 ~ 203 m	0 ~ 200 m	0 ~ 203 m
Others	—	Max temperature 85.2°C (203 m)	Max pressure 19.3 kg/cm <sup>2</sup> G (203 m)	

2) The second well logging

When the drilling reached to depth of 424 m, fluid outpour into the well occurred. Therefore, before casing pipe was inserted, well logging was carried out. (Fig. 5.4-5 and Table 5.4-3)

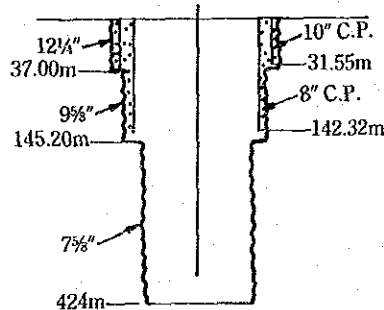


Fig. 5.4-5 Well State in Logging of GTE-8 (Stage 2)

The results are as follows:

- ① After stopping the drilling pump, water continued to spring into the well. Because the maximum temperature of temperature logging is 110°C at 270 m and temperature increases linearly to 270 m, it is clear that water sprang into the well at around 270 m depth. Beyond 270 m, temperature decreases with depth and beyond 360 m, temperature again increases with depth. The temperature at the bottom of the well (424 m)

is 94.2°C. The temperature of spring water at the wellhead is 78.8°C (Fig. 5.4-6)

- ② The well was electrically logged between 140 m and 424 m. Electrical logging to 270 m is applied only for reference because fluid movement was constantly present while logging their well. Resistivity varies largely throughout the logged section and is generally over 100 Ω-m. The maximum resistivity value occurs at around 260 m and 270 m and is over 1,000 Ω-m. The zone between 370 m and 380 m is low resistivity (20 to 60 Ω-m) and corresponds to change of SP curve (Fig. 5.4-7)
- ③ Pressure logging shows linear increase from the wellhead to the bottom. Pressure value at the bottom (424 m) is 40.2 kg/cm<sup>2</sup>G.
- ④ Flow meter logging shows that fluid flows into the well between 260 m and 270 m, which is the same depth as indicated in thermal logging.

Table 5.4-3 Progress of Well Logging of GTE-8 (Stage 2)

Logging Items	Temperature logging	Electrical logging	Pressure logging	Caliper logging	Sonic logging
Date	Feb. 16, 1987	Feb. 16, 1987	Feb. 16, 1987	Feb. 16, 1987	Feb. 16, 1987
Drilling depth	424 m	424 m	424 m	424 m	424 m
Casing	(8'') 142.32 m	(8'') 142.32 m	(8'') 142.32 m	(8'') 142.32 m	(8'') 142.32 m
Shut in	Feb. 16, 1987 6:00	Feb. 16, 1987 6:00	Feb. 16, 1987 6:00	Feb. 16, 1987 6:00	Feb. 16, 1987 6:00
Standing time	Over flow	—	—	—	—
Time of measurement	10:56 ~ 11:40	14:20 ~ 14:42	15:40 ~ 16:17	10:10 ~ 10:37	19:53 ~ 20:32
Depth of measurement	140 ~ 420 m	0 ~ 424 m	0 ~ 424 m	0 ~ 424 m	10 ~ 424 m
Others	Max temperature 110.7°C (273 m)	—	Max pressure 40.2 kg/cm <sup>2</sup> G (424 m)	—	—

### 3) The third well logging

When the well was drilled to depth of 501 m, a large amount of geothermal water outpour occurred into the well. In order to know fluid characteristics, well logging was carried out under conditions of flushing geothermal fluid. The JICA team observed the third well logging and collected and examined data. (Fig. 5.4-8 and Table 5.4-4)

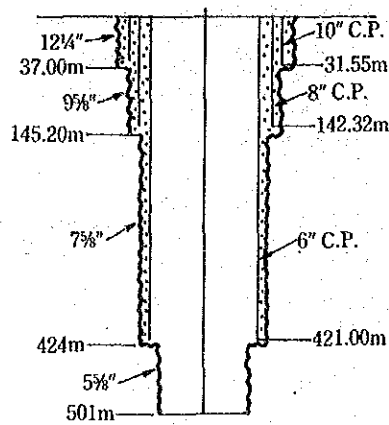


Fig. 5.4-8 Well State in Logging of GTE-8 (Stage 3)

Well logging was carried out under conditions of producing, with the valve completely opened. At the beginning, geothermal fluid poured out continuously, but gradually this changed to intermittent outpour. Amount of geothermal fluid outpour is assumed to be about 5 t/h.

The results are as follows:

- ① Temperature logging was carried out to 499 m under static conditions and under producing conditions. Under static conditions, temperature distribution (standing time: 15 hr) does not show large change. Temperature at around 380 m was rather high and that at the well bottom (499 m) was 113.8°C. Under producing conditions temperature increases linearly from the wellhead to the bottom. The maximum temperature is 117°C measured at the well bottom (500 m) (Figs. 5.4-9 and 10).
- ② Electrical logging is applied only as a reference because of measurement under producing conditions. Resistivity values change greatly beyond 470 m and the value is 2,000 Ω-m at 495 m. Resistivity in the zone shallower than 470 m is low and that between 45 m and 470 m is 100 Ω-m (Fig. 5.4-11).
- ③ Pressure logging shows 46 kg/cm<sup>2</sup>G of pressure at 500 m depth. The results of well logging show that geothermal water intermittently flows into the well at around 477 m and temperature is about 117°C. No fluid flow is seen beyond 480 m.
- ④ Flow meter logging shows that the flow rate changes between 470 m and 480 m, and geothermal fluid flows into the well through that section. The section corresponds to the depth of lost circulation while drilling (477 m).

Table 5.4-4 Progress of Well Logging of GTE-8 (Stage 3)

Logging Items	Temperature logging		Electrical logging	Pressure logging	Caliper logging	Flowmeter logging
	Date	Mar. 3, 1987	Mar. 5, 1987	Mar. 5, 1987	Mar. 5, 1987	Mar. 5, 1987
Drilling depth	499 m	501 m	501 m	501 m	501 m	501 m
Casing	(6") 421 m	(6") 421 m	(6") 421 m	(6") 421 m	(6") 421 m	(6") 421 m
Shut in	Mar. 2, 1987 22:00	Mar. 4, 1987 8:00	Mar. 4, 1987 8:00	Mar. 4, 1987 8:00	Mar. 4, 1987 8:00	Mar. 4, 1987 8:00
Standing time	15 hr	Blowing out	—	—	—	—
Time of measurement	13:18 ~ 14:06	15:25 ~ 16:15	19:04 ~ 19:10		11:38 ~ 11:44	18:00 ~ 22:00
Depth of measurement	0 ~ 499 m	0 ~ 500 m	420 ~ 500 m	0 ~ 500 m	410 ~ 500 m	400 ~ 500 m
Others	Max temperature 113.8°C (499 m)	Max temperature 117°C (500 m)	—	Max pressure 46 kg/cm <sup>2</sup> G (500 m)	—	—

4) The fourth well logging

When the well was drilled to depth of 755m, well logging was carried out (Fig. 5.4-12 and Table 5.4-5).

The results are as follows:

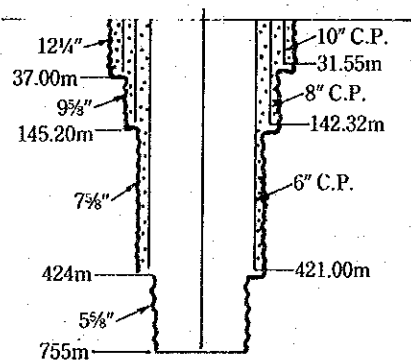


Fig. 5.4-12 Well State in Logging of GTE-8 (Stage 4)

- ① Because temperature logging was carried out immediately after producing geothermal fluid was stopped by mud, the temperature curve does not show the temperature of formations. Therefore temperature variation of formations is not known. The maximum temperature at 755 m (well bottom) is 121°C (Fig. 5.4-13).

Temperature measurement under producing conditions, just before stopping of flushing geothermal fluid, shows that temperature change occurs at around 710 m depth and



geothermal fluid flows into the well at that point. Temperature at 710 m is 119.6°C. Beyond 710 m, temperature decreases for a short distance, but shows an increasing trend thereafter, becoming 121.2°C at 755 m (well bottom) (Fig. 5.4-14).

- ② Resistivity distribution to 500 m depth is almost the same as the above-mentioned well logs. Low resistivity of 150 Ω-m is recorded between 620 m and 635 m, and around 750 m, and resistivity in other sections is high. Resistivity between 550 m and 580 m, and between 670 m and 745 m is over 1,000 Ω-m and that between 690 m and 700 m is very high 2,500 Ω-m (Fig. 5.4-13).

SP curve does not show any noticeable change.

- ③ Flow meter logging shows that fluid flows into the well at 706 m the same depth as indicated by the temperature logging.

Table 5.4-5 Progress of Well Logging of GTE-8 (Stage 4)

Logging Items	Temperature logging	Electrical logging	Pressure logging	Caliper logging	Flowmeter logging
Date	Jul. 18, 1987	Jul. 18, 1987	Jul. 18, 1987	Jul. 18, 1987	Jul. 18, 1987
Drilling depth	755 m	755 m	755 m	755 m	755 m
Casing	(6'') 421 m	(6'') 421 m	(6'') 421 m	(6'') 421 m	(6'') 421 m
Shut in	Jul. 18, 1987 14:15	Jul. 18, 1987 14:15	Jul. 18, 1987 14:15	Jul. 18, 1987 14:15	Jul. 18, 1987 14:15
Standing time	1 hr	—	—	—	—
Time of measurement	14:20 ~ 15:34	17:13 ~ 17:34	21:26 ~ 22:19	20:23 ~ 20:48	10:00 ~ 12:00
Depth of measurement	0 ~ 755 m	420 ~ 755 m	0 ~ 755 m	400 ~ 755 m	0 ~ 755 m
Others	Max temperature 121°C (755 m)	—	Max pressure 71.2 kg/cm <sup>2</sup> G (755 m)	—	—

5) The fifth well logging

Well logging was carried out at depth of 1,031 m, with casing pipe to 755 m. Geothermal fluid flushed fairly strongly into the well and it was very difficult to log the well under static conditions. (Fig. 5.4-16 and Table 5.4-6)

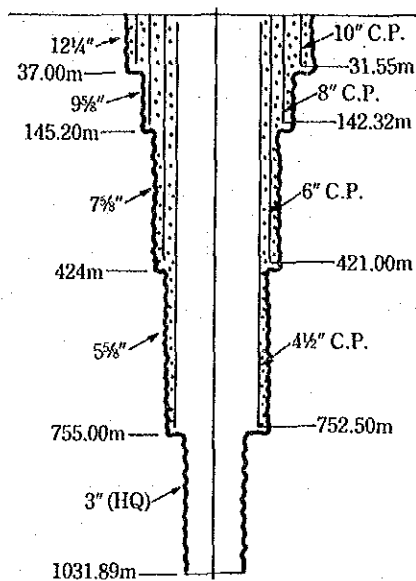


Fig. 5.4-16 Well State in Logging of GTE-8 (Stage 5)

The results are as follows:

- ① Temperature logging with standing time of 51 hours shows temperature increase to 20 m depth, decrease from 20 to 50 m, and gentle increase after 50 m to depth. The maximum temperature, 224°C, was recorded at 922 m. Temperature decreases after 922 m and is 120°C at the bottom of the well (1,031 m) (Fig. 5.4-17).
- ② High resistivity zones, over 500 Ω-m, are between 780 m and 800 m, around 830 m, around 880 m, and between 900 m and 925 m. Resistivity in other sections is below 500 Ωm, and a low resistivity zone is between 835 m and 850 m (Fig. 5.4-18).  
SP log does not show any remarked features.
- ③ Pressure logging shows that the pressure at the well bottom is 99.3 kg/cm<sup>2</sup> G while that at the well head is 3.1 kg/cm<sup>2</sup> G.

Table 5.4-6 Progress of Well Logging of GTE-8 (Stage 5)

Logging Items	Temperature logging	Electrical logging	Pressure logging	Caliper logging
Date	Dec. Oct. 9, 1987	Nov. 19, 1987	Oct. 9, 1987	Nov. 19, 1987
Drilling depth	1,031 m	1,031 m	1,031 m	1,031 m
Casing	(4½") 752 m	(4½") 752 m	(4½") 752 m	(4½") 752 m
Shut in	Oct. 7, 1987 8:40	—	Oct. 7, 1987 8:40	—
Standing time	51 hr	—	—	—
Time of measurement	9:54 ~ 11:34	10:04 ~ 10:16	13:55 ~ 14:49	11:50 ~ 12:00
Depth of measurement	0 ~ 1,031 m	750 ~ 930 m	0 ~ 1,031 m	750 ~ 930 m
Others	Max temperature 123.9°C (920 m)	—	Max 99.3 kg/cm <sup>2</sup> G (1,031 m)	—

#### 5.4.2 Production Logging

##### (1) Generalization

Drilling of this exploratory well encountered loss of circulation several times and some lost circulations accompanied water inflow and steam flushing. A large amount of drilling mud was lost beyond 900 m after casing pipe was set to 752.50 m. Geothermal water of temperature over 100°C flushed into the well when drilling was stopped. Drilling was continued with lost circulation to 1,031 m depth. Then, in order to get the characteristics of fractures through which geothermal fluid produced into the well and of producing geothermal fluid, well testing and various measurement in production were carried out.

Items of measurement are as follows:

- i) Measurement of characteristics of flow rate during producing:  
Flow rate vs. pressure at the wellhead.
- ii) Temperature in the well, pressure and flow rate during producing (production test):  
Flow rate is changed in three steps.
- iii) Flow rate-production logging:  
Measurement of flow rate and pressure at the wellhead with the progress of time.

In order to carry out these well tests, it was necessary to install a pipe line to measure flow rate

and a wellhead assembly to log the well while producing. The installation of equipment and measurement were carried out after consultation between the Thai team and the JICA team.

(2) Method of measurement

- 1) Down-hole measurement was carried out by logging equipment (temperature, pressure, flow meter) used for static measurement. A lubricator was installed at the wellhead to log the well while producing.

The following figure shows the measurement procedure.

Down-hole measurement is very useful because it can measure producing fluid and conditions of the ground directly.

Producing fluid was controlled to pre-set pressures and flow rates. After flow of flushing fluid became stable, probes of temperature, pressure and flow meters were lowered into the well to collect necessary information. After measurement was completed with one pre-determined flow rate, another measurement was carried out with different flow rate.

For this survey, three different flow rates were used.

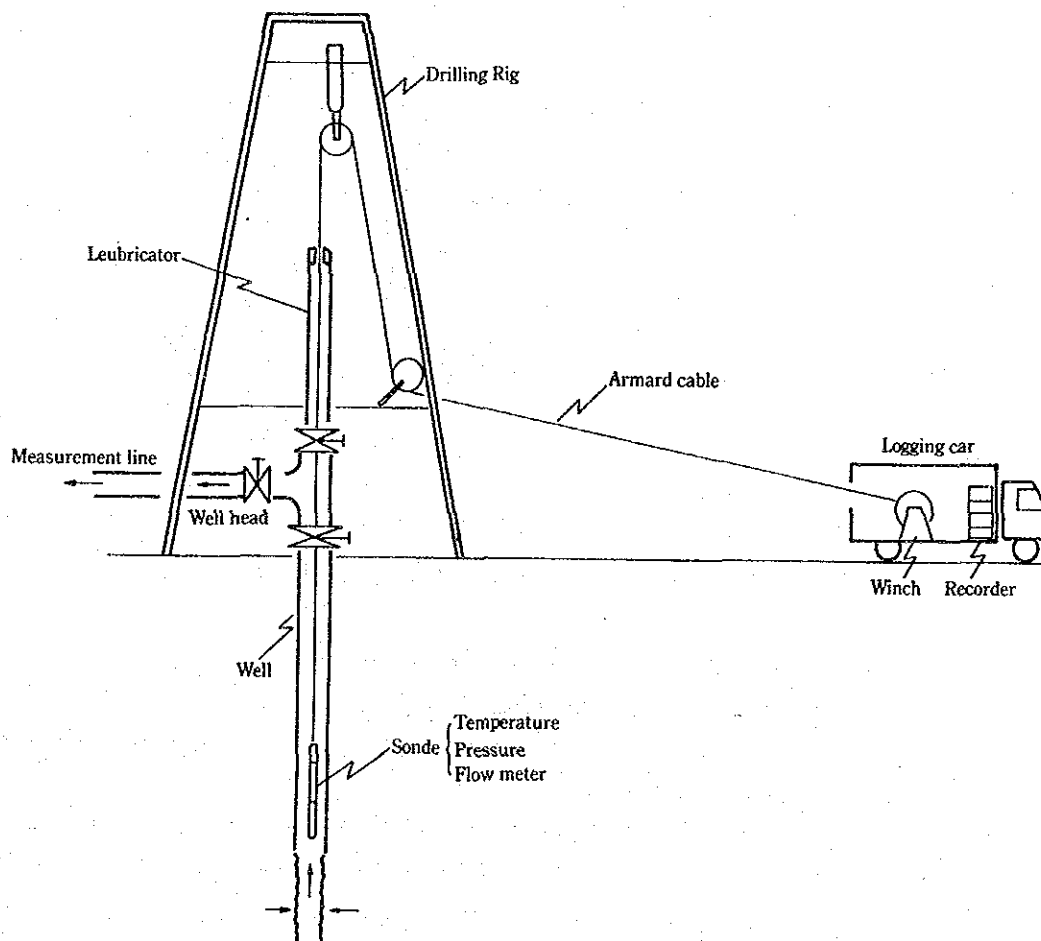


Fig. 5.4-19 Layout of Well Testing

2) Measurement of characteristics of flow rate

A pipe was installed from the wellhead to the measurement device to record pressure, temperature and flow rate of geothermal fluid (steam and geothermal water) flowing to the ground surface from the underground formation.

Piping for the measurement is as shown in Fig. 5.4-20 and Table 5.4-7.

Flow rate was controlled by a secondary valve and an adjustment valve on the measurement piping, and a flow rate characteristics curve was obtained by measuring amounts of steam and geothermal water against pressure at the wellhead.

Table 5.4-7 Items and Using Meters of Measurement for GTE-8

Measurement Item	Used Meter
1 Well head pressure	Bourdon tube pressure gauge
2 Steam pressure	Bourdon tube pressure gauge
3 Hot water pressure	Bourdon tube pressure gauge
4 Steam flow rate	Orifice, Mercury manometer
5 Water flow rate	Triangle dam

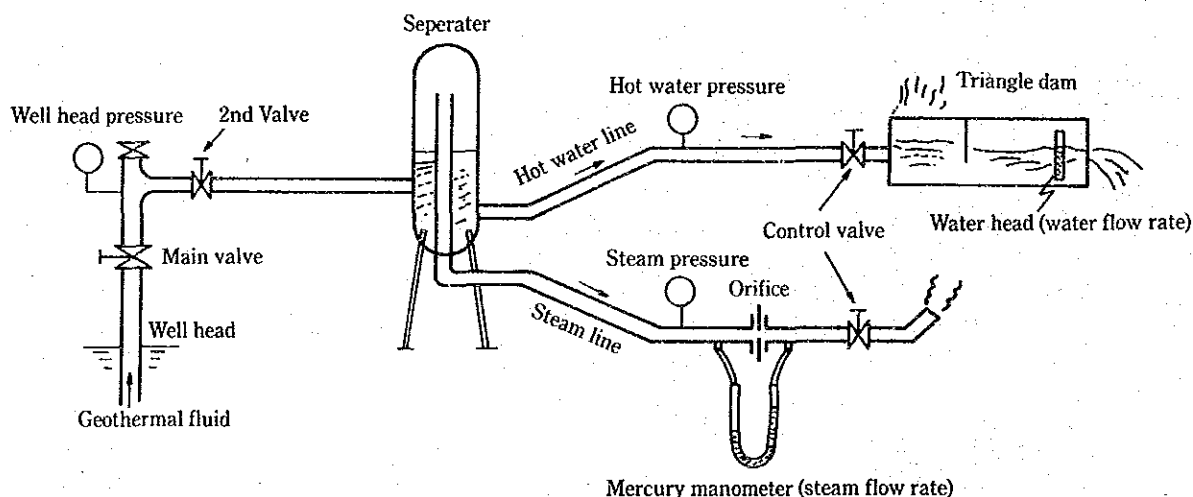


Fig. 5.4-20 Piping for Measuring Flow Rate of GTE-8

(3) Measurement and results of production test

1) Down-hole measurement during producing (Table 5.4-8)

For the production test, down-hole temperature, pressure and flow rate were measured by changing the flow rate in three stages.

Temperature and pressure for every ten meters are shown in Table 5.4-9 and Fig. 5.4-21. The table and figure also show temperature and pressure under static conditions at about the same time.

Table 5.4-8. Summary of Well Logging in Production Test of GTE-8

Item \ Stage	①	②	③
Date	Oct. 12, 1987	Oct. 13, 1987	Oct. 14, 1987
Drilling depth	1,031 m	1,031 m	1,031 m
Depth of measurement	0 ~ 1,031 m	0 ~ 1,031 m	0 ~ 1,031 m
Well head pressure	1.2 kg/cm <sup>2</sup> G (at full open)	2.2 kg/cm <sup>2</sup> G	3.1 kg/cm <sup>2</sup> G
Total flow rate	45.6 t/h	35.9 t/h	23.5 t/h
Steam flow rate	1.2 t/h (0.4 kg/cm <sup>2</sup> G)	1.1 t/h (0.35 kg/cm <sup>2</sup> G)	0.7 t/h (0.17 kg/cm <sup>2</sup> G)
Hot water flow rate	44.4 t/h (0.3 kg/cm <sup>2</sup> G)	34.8 t/h (0.3 kg/cm <sup>2</sup> G)	22.8 t/h (0.2 kg/cm <sup>2</sup> G)
Sorts of measurement	Temperature, Pressure Flow rate	Temperature, Pressure	Temperature, Pressure

The following are obtained from the results of measurement:

① Temperature of producing fluid

Temperature beyond about 920 m decreases drastically in all three stages while temperature in the zone shallower than 920 m is constant. Therefore, temperature of the producing fluid is estimated to be 124°C.

② Flow-in depth of producing fluid.

From the inflection point of the temperature logging and the measurement of the flow meter, flow-in depth of flushing is between 915 m and 930 m.

③ Productivity index

A productivity index which represents the capacity of producing fluid from a well is calculated from the total amount of flow and amount of pressure draw-down as follows:

For this survey, the productivity index is calculated from down-hole pressure measurement in the three stages as follows:

$$PI = G / (P_e - P_w)$$

PI : productivity index (t/h)/(kg/cm<sup>2</sup>)

G : total amount of flow (t/h)

P<sub>e</sub> : reservoir pressure at flow-in depth (kg/cm<sup>2</sup>)

P<sub>w</sub> : pressure in the well at flow-in depth (kg/cm<sup>2</sup>)

For this survey, the productivity index is calculated from down-hole pressure measurement in the three stages as follows:

$$PI = \Delta G / \Delta P$$

The pressures in the hole and the total amounts of flow at 920 m are as follows;

$$\begin{aligned} P_{w1} &= 86.9 \text{ kg/cm}^2 G & G_1 &= 45.6 \text{ t/h} \\ P_{w2} &= 88.4 \text{ kg/cm}^2 G & G_2 &= 35.9 \text{ t/h} \\ P_{w3} &= 88.8 \text{ kg/cm}^2 G & G_3 &= 23.5 \text{ t/h} \end{aligned}$$

From the values above

$$\begin{aligned} PI' &= (G_1 - G_3)/(P_{w3} - P_{w1}) \doteq 12 \text{ (t/h)/(kg/cm}^2) \\ PI'' &= (G_1 - G_2)/(P_{w2} - P_{w1}) \doteq 7 \text{ (t/h)/(kg/cm}^2) \\ PI''' &= (G_2 - G_3)/(P_{w3} - P_{w2}) \doteq 31 \text{ (t/h)/(kg/cm}^2) \end{aligned}$$

The average value of production indices is:

$$PI = 17 \text{ (t/h)/(kg/cm}^2)$$

④ Transmissivity

Transmissivity, which represents permeability of a reservoir, is calculated as follows by assuming single phase fluid flow;

$$G = \frac{2\pi khr}{\mu \ln(re/rw)} \cdot (P_e - P_w)$$

Therefore,

$$Kh = \frac{G}{P_e - P_w} \cdot \frac{\mu \ln(re/rw)}{2\pi r} = PI \cdot \frac{\mu \ln(re/rw)}{2\pi r}$$

where,

- Kh : transmissivity m<sup>3</sup>
- G : total amount of flow t/h
- K : permeability m<sup>2</sup>
- h : effective thickness of reservoir m
- r : specific gravity of fluid kg/m<sup>3</sup>
- μ : coefficient of viscosity of fluid kg.sec/m<sup>2</sup>
- re : radius of effective zone m
- rw : radius of well m
- Pe : reservoir pressure at flow-in depth kg/m<sup>2</sup>
- Pw : pressure in a well at flow-in depth kg/m<sup>2</sup>

As calculation condition,

$$\begin{aligned} \mu &= 0.238 \times 10^{-4} \text{ kg}\cdot\text{sec}/\text{m}^2 \\ r &= 947.2 \text{ kg}/\text{m}^3 \\ P_w &= 90 \text{ kg}/\text{cm}^2 \text{ abs, } T_w = 124^\circ\text{C} \\ \ln(re/rw) &= 5.0 \\ PI &= 17 \text{ (t/h)/(kg/cm}^2) = 4.7 \times 10^{-4} \text{ (kg/sec)/(kg/m}^2) \end{aligned}$$

Therefore,

$$Kh = \frac{0.238 \times 10^{-4} \times 5.0 \times 4.7 \times 10^{-4}}{2 \times 3.14 \times 947.2} = 9.4 \times 10^{-12} \text{ m}^3 = 9 \text{ darcy-m}$$

The productivity of GTE-8 and characteristics of the reservoir are as follows:

Temperature of flushing fluid: 124°C

Flow-in depth of fluid: around 915 m to 930 m

Productivity index: 17(t/h)/(kg/cm<sup>2</sup>)

Transmissivity:  $9.4 \times 10^{-12} \text{ m}^3 = 9 \text{ darcy-m}$

2) Characteristics of flow rate

A characteristic curve of the flow rate is illustrated from measurements of flow rate against change of well head pressure by using the pipe line for flow rate measurement.

The results are presented in Table 5.4-10 and Fig. 5.4-22.

The maximum flow, with valve being full open is 45.6 t/h at well head pressure of 1.2 kg/cm<sup>2</sup>G. The minimum is 16.7 t/h at wellhead pressure of 3.4 kg/cm<sup>2</sup>G. The minimum flow as value was gradually narrowed, is 16.7 t/h at well head pressure of 3.4 kg/cm<sup>2</sup>G.

3) Production test of flow rate

After measurements such as flow rate test were completed a production test was continued for 30 days with valve completely open to study the change of flow rate with the passage of time.

Well head pressure and flow rate of GTE-6 were recorded simultaneously to study the influence of producing on other wells.

The change of flow rate with the passage of time is illustrated in Fig. 5.4-23.

It can be seen that well head pressure of GTE-8 changed very little, and flow rate decreased from 46 t/h to 44 t/h during the approximately 30 days of continuous producing.

Wellhead pressure of GTE-6 decreased 0.1 kg/cm<sup>2</sup>G and its flow rate also decreased 1.7 t/h because GTE-6 was affected by the producing of GTE-8. However, wellhead pressure and flow rate returned to the original values after producing of GTE-8 was stopped.



**Table 5.4-10 Result of Characteristic of Flow Rate for GTE-8**

Date	Well head pressure (kg/cm <sup>2</sup> G)	Total flow rate (t/h)	Steam flow rate		Hot water flow rate		Remarks
			Flow rate (t/h)	Line pressure (kg/cm <sup>2</sup> G)	Flow rate (t/h)	Line pressure (kg/cm <sup>2</sup> G)	
Oct. 12, 1987	1.2	45.6	1.2	0.4	44.4	0.3	at full opened valve
Oct. 13, 1987	2.2	35.9	1.1	0.35	34.8	0.3	
Oct. 14, 1987	3.1	23.5	0.7	0.17	22.8	0.2	
Oct 16, 1987	3.4	16.7	0.5	0.05	16.2	0.05	
Oct 16, 1987	2.7	29.2	0.5	0.22	28.3	0.2	
Oct 16, 1987	1.8	39.8	1.1	0.36	38.7	0.35	

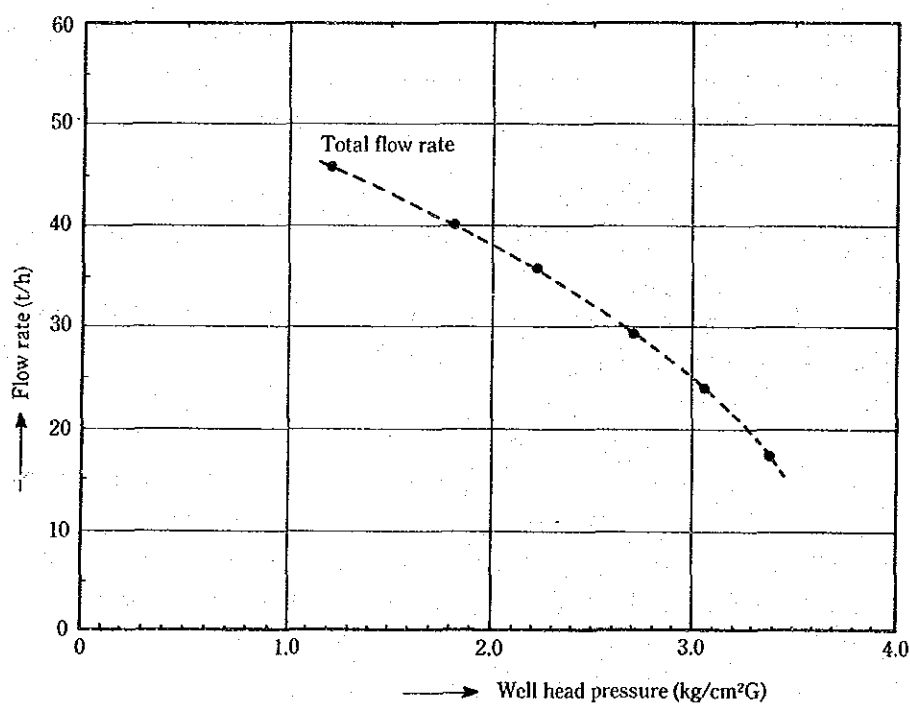


**Fig. 5.4-22 Characteristic Curve of Flow Rate of GTE-8**

## 5.5 Fluid Geochemistry

### 5.5.1 Objectives

To elucidate the chemical properties of the geothermal fluid ejected from the exploratory well GTE-8, analysis of the steam, water condensed, and the thermal water from GTE-8 were carried

out.

### 5.5.2 Result of Survey

The results of analysis of the steam, water condensed, and the thermal water from GTE-8 are shown from Table 5.5-1 to 5.5-3.

Samples of steam and water condensed are separated from the thermal water and taken by a small separator attached to the two phase flow line at GTE-8. The thermal water is sampled at atmospheric pressure. There are two wells, GTE-6 and EGAT-1, which are the only two survey wells ejecting fluid continuously in the San Kampaeng area. Periodical survey is conducted on these two wells by EGAT, and the results of this survey are shown in Table 5.5-3 as reference.

### 5.5.3 Characteristics of Chemical Property

#### (1) Steam

The composition of uncondensable gas consists of mostly  $\text{CO}_2$  at 90% of volume, and a small portion of  $\text{N}_2$  at 6.19% of volume. The result of the steam properties analysis at GTE-8 indicates presence of  $\text{H}_2$  -  $\text{N}_2$  -  $\text{CH}_4$ . The three component system is shown in Fig. 5.5-1 together with the results of hot spring gas analysis in the San Kampaeng area. The three component system is obtained only for the GTE-8, and as such the results can not be compared with the other survey wells. It is considered, nevertheless, that the  $\text{H}_2$  -  $\text{N}_2$  -  $\text{CO}_2$  composition is a common property of gas throughout the area.

In general, it is possible to study the genetics of gas and the genetic mechanism of a geothermal reservoir by analyzing the inert gas composition ( $\text{He}$ ,  $\text{Ar}$ ,  $\text{N}_2$ ) in the steam ejected.

On the other hand, the ratio of  $\text{He}/\text{Ar}$  in the steam from GTE-8 is found to be  $5.07 \times 10^{-2}$ , and this value is much larger than that of  $1.6 \times 10^{-4}$  in water under stable conditions in open air. This result suggests that steam from GTE-8 has accumulated helium generated from the earth crust.

#### (2) Water condensed from steam

The water condensed from the steam of GTE-8 shows weak acidic property of pH 5.50, and traces of As and Hg are detected.

Although the concentration of  $\text{SO}_4$  in the dissolved components is found to be a rather high value, a number of days elapsed from the sampling in the field to the time of analysis, and therefore, the high  $\text{SO}_4$  concentration is considered to have resulted from the oxidation of dissolved  $\text{H}_2\text{S}$ .

#### (3) Thermal water

The thermal water obtained from GTE-8 is alkaline with pH 9.36, and the suspended solid is low.

Judging from both the major cation composition (Fig. 5.5-2) and the major anion composition (Fig. 5.5-3) of the thermal water from GTE-8, it is found that the major chemical component is found to be  $\text{Na-HCO}_3\text{-SO}_4$ .

These characteristics of the thermal water obtained from GTE-8 are common as well to the hot

waters obtained from GTE-6 and EGAT-1, and the genesis mechanisms of these fluids is considered to be similar.

#### 5.5.4 Consideration on Geothermal Fluid from Geochemical View-Point

##### (1) Geochemically measured temperature

To estimate the maximum temperature which the geothermal fluid has experienced, geochemical temperature is calculated using the results of thermal water analyses. The geochemical thermometers used are shown in Table 5.5-4, and the calculated results are shown in Table 5.5-5 for GTE-8, GTE-6 and EGAT-1.

The five geochemical temperatures calculated for GTE-8 are scattered widely between 161~196°C.

In general, geochemical temperature is estimated by the temperature dependency of the ion exchange reaction between thermal water and wall rock, and the equilibrium constant of the quartz dissolving reaction. This estimation rests basically on the premise that chemical reaction occurs under stable conditions deep underground and the thermal water rises to the ground surface with the original stable environment remaining unchanged.

However, it is considered that there is a problem with the reliability of the geochemical temperature estimated from the water-rock reaction because the hot water obtained from the San Kampaeng area, such as that from GTE-8, has low dissolved chemical content.

However, the temperature estimated from the silica content and the Na/K ratio for thermal fluid from GTE-8 is found to be between 160~180°C. Subsequently, the temperature of the fluid which flows into the GTE-8 survey well drops to 120~130°C, during the ascension of the fluid from the geothermal reservoir by cooling due to the thermal conduction, as concluded from actual temperature measurement in the bore hole and from calculation of the vapor/liquid ratio. The same tendency as above is observed for the GTE-6 and EGAT-1 survey wells also.

##### (2) Genesis mechanism of geothermal reservoir estimated from chemical characteristics

Judging from the low dissolved chemical content, two possible mechanisms for genesis of the fluid obtained from the GTE-8 survey well are considered:

- ① The water penetrating underground from the ground surface is heated by contact with the geothermal reservoir host rock which exhibits low thermal activity.
- ② The water penetrating from the ground surface to deep underground is heated by geothermal vapor which has separated from the geothermal fluid.

To further consider the genetic mechanism, a B/C1 chart has been prepared (Fig. 5.5-4).

It is known that the B/C1 ratio reflects the chemical characteristics of the host rock of the geothermal reservoir, and is altered by the steam heating type geothermal reservoir mechanism. In general, the B/C1 ratio of the hot water in a volcanic rock zone and/or pyroclastic rock zone is usually 0.02~0.07. The B/C1 ratio of hot water from sedimentary rock as the geothermal reservoir host rock is usually around 1.0. On the other hand, a higher B/C1 ratio is generally observed in the steam from the geothermal area heated mainly by steam, than that of the water heated by the

host rock, because B is more concentrated in steam due to the difference in vapor pressure between B and Cl.

In Fig. 5.5-4, the B/Cl ratio of GTE-8 is found to be near the 1.0 line and that of GTE-6 and EGAT-1 is found to be near the 0.5 line.

Hence, the B/Cl ratio of the hot water obtained from the survey well in this area seems to be almost the same as that of thermal water from sedimentary rock as the geothermal host rock. This result agrees with the actual geologic condition; however, there is some possibility of a steam heating mechanism because of the low dissolved chemical content. In addition to the comparison of B/Cl ratio and geologic conditions of the various survey wells in the San Kampaeng area. It is also necessary to analyse  $\text{HCO}_3$  and its carbon isotope concentration, as these are major components of hot water and steam. The origin of  $\text{CO}_2$  in the thermal water and the steam a resulting from organic substances in the sedimentary rock, or as resulting from volcanic gas must be subsequently determined.

Further, judging from the  $\text{N}_2/\text{Ar}$  gas component ratio, the effect of groundwater seems to be large on the temperature of thermal water in the survey wells. However, the  $\text{He}/\text{Ar}$  ratio is much larger than the predicted value from the dissolved air in the groundwater.

Hence, the origin of helium is estimated as resulting from the accumulation of He from radioactive elements. The origin of He from radioactive elements can be confirmed by the  $^3\text{He}/^4\text{He}$  ratio, and this analysis is important to determine whether the geothermal system in this survey area possesses a structure capable of accumulating gas originated from the earth's crust.

### 5.5.5 Summary

The following are concluded from the results of GTE-8 field survey and the results of chemical survey of existing geothermal wells and hot springs in the San Kampaeng area.

- ① The chemical character of the thermal water and hot spring water is similar throughout the area, i.e., the major chemical components are Na,  $\text{SO}_4$  and  $\text{HCO}_3$ , and the concentration of dissolved chemical components is found to be low.
- ② The gas component from the geothermal wells and hot springs in the area is similar i.e., the major components are  $\text{CO}_2$  and  $\text{N}_2$ .
- ③ Judging from the  $\text{N}_2/\text{Ar}$  ratio of gas, the geothermal fluid in this area is greatly influenced by surface water.
- ④ The  $\text{He}/\text{Ar}$  ratio of the gas is larger than that of the air dissolved in the groundwater.  
There is a possibility of the He accumulation being sourced from radio active elements.
- ⑤ The geochemical temperature is about  $200^\circ\text{C}$  at its maximum.
- ⑥ The B/Cl ratio of thermal water shows a value for hot water emanating from sedimentary rock as the geothermal reservoir host rock. It is not clear whether the water is heated by steam or not, because of the limited amount of data obtained.

To clarify the heating mechanism of the fluid and its behavior further, additional geochemical survey on the following items would be considered effective.

- ① To estimate the origin of water and the duration time for the reaction with a host rock qualitatively, it is effective to analyse the isotopic ratio of the hydrogen and oxygen in the thermal water underground.

- ② To confirm the correspondence between the geothermal reservoir host rock and the B/Cl ratio of the hot spring water, it would be effective to measure the B/Cl ratio of hot spring water throughout the area and its environs.
- ③ To clarify the gas source, it would be effective to analyse the  $^3\text{He}/^4\text{He}$  ratio in the gas.

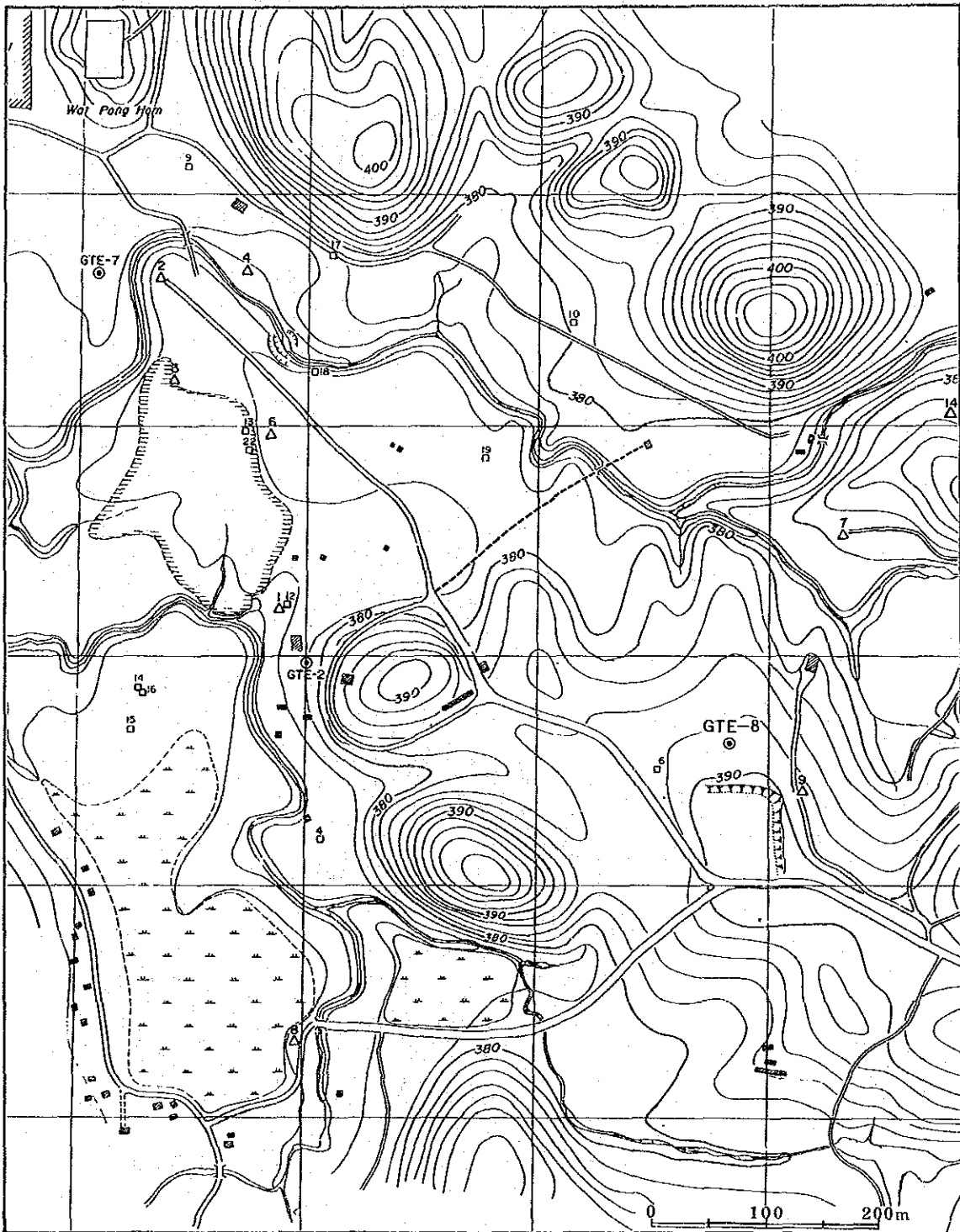


Fig. 5.2-1 Location of GTE-8









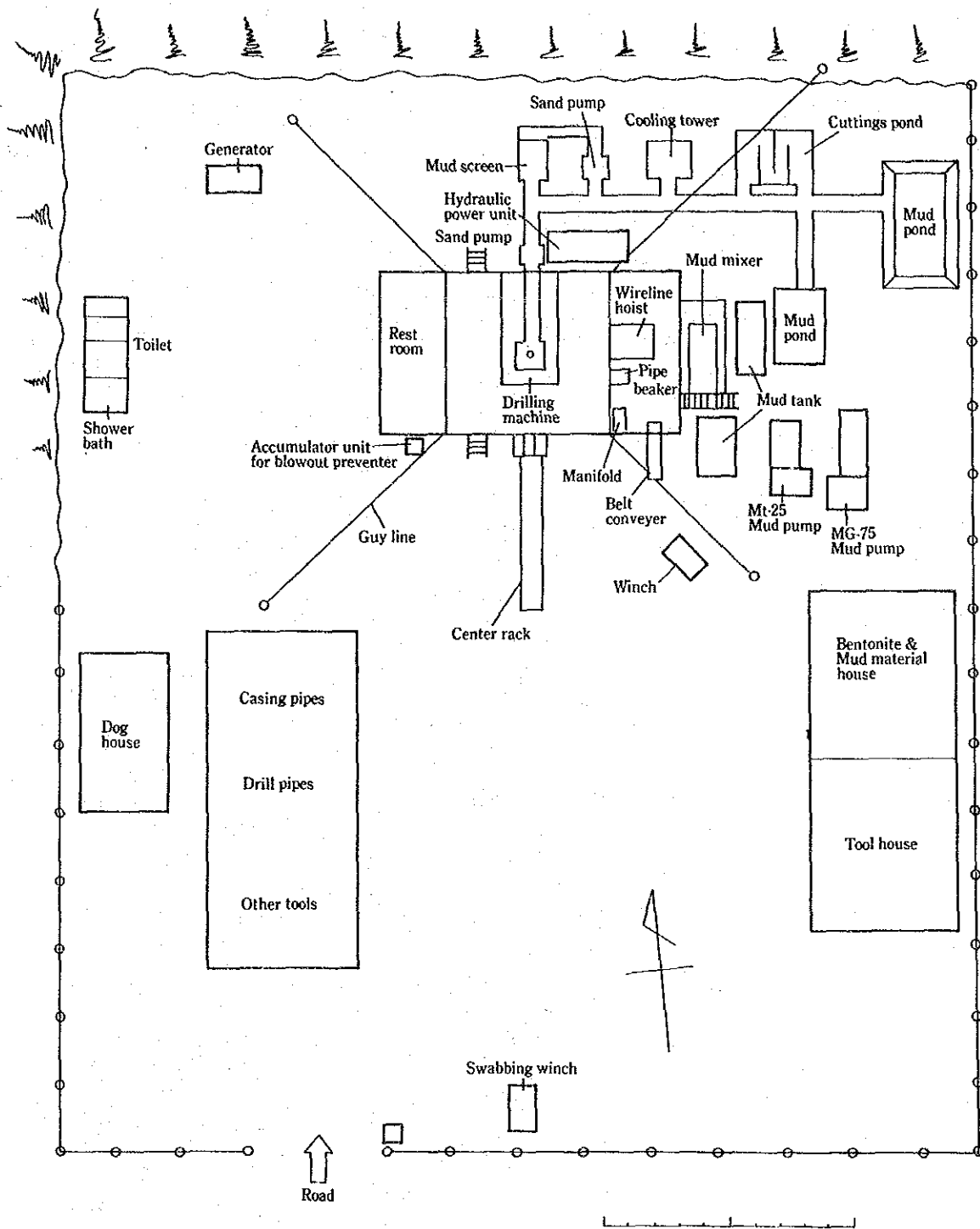


Fig. 5.2-3 Layout of Drilling site of GTE-8

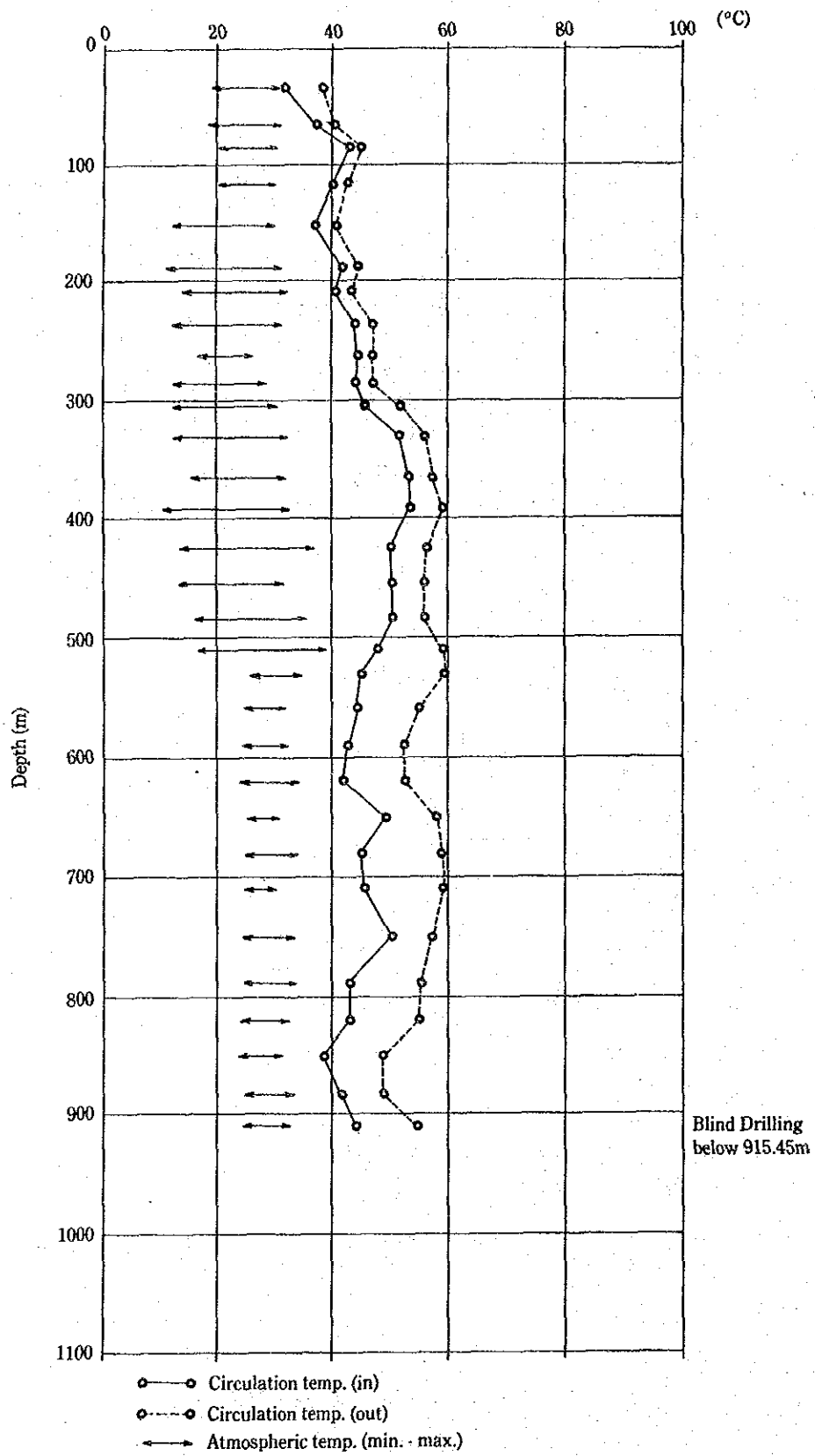


Fig. 5.2-4 Circulation Temperature of GTE-8

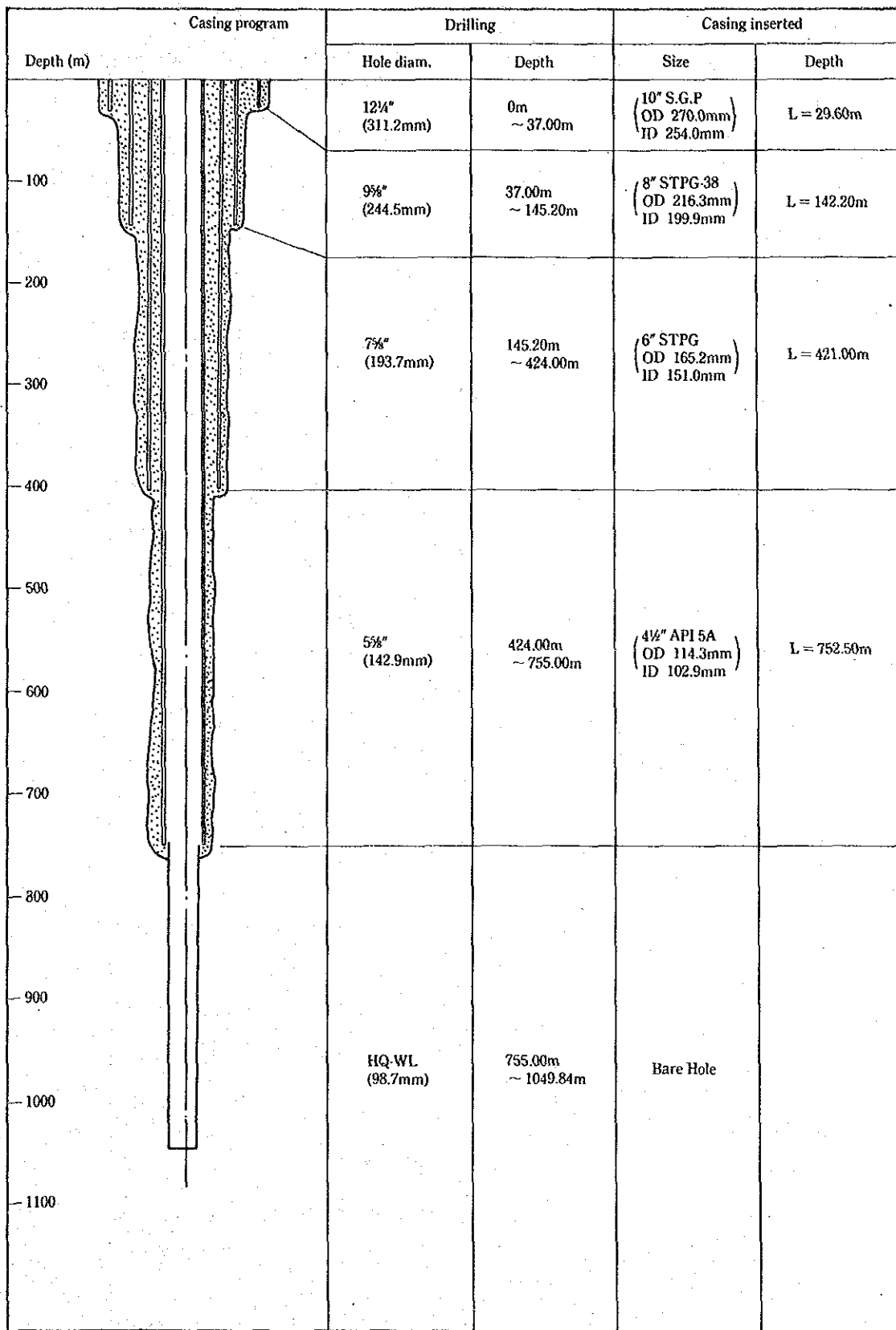


Fig. 5.2-5 Casing Program of GTE-8

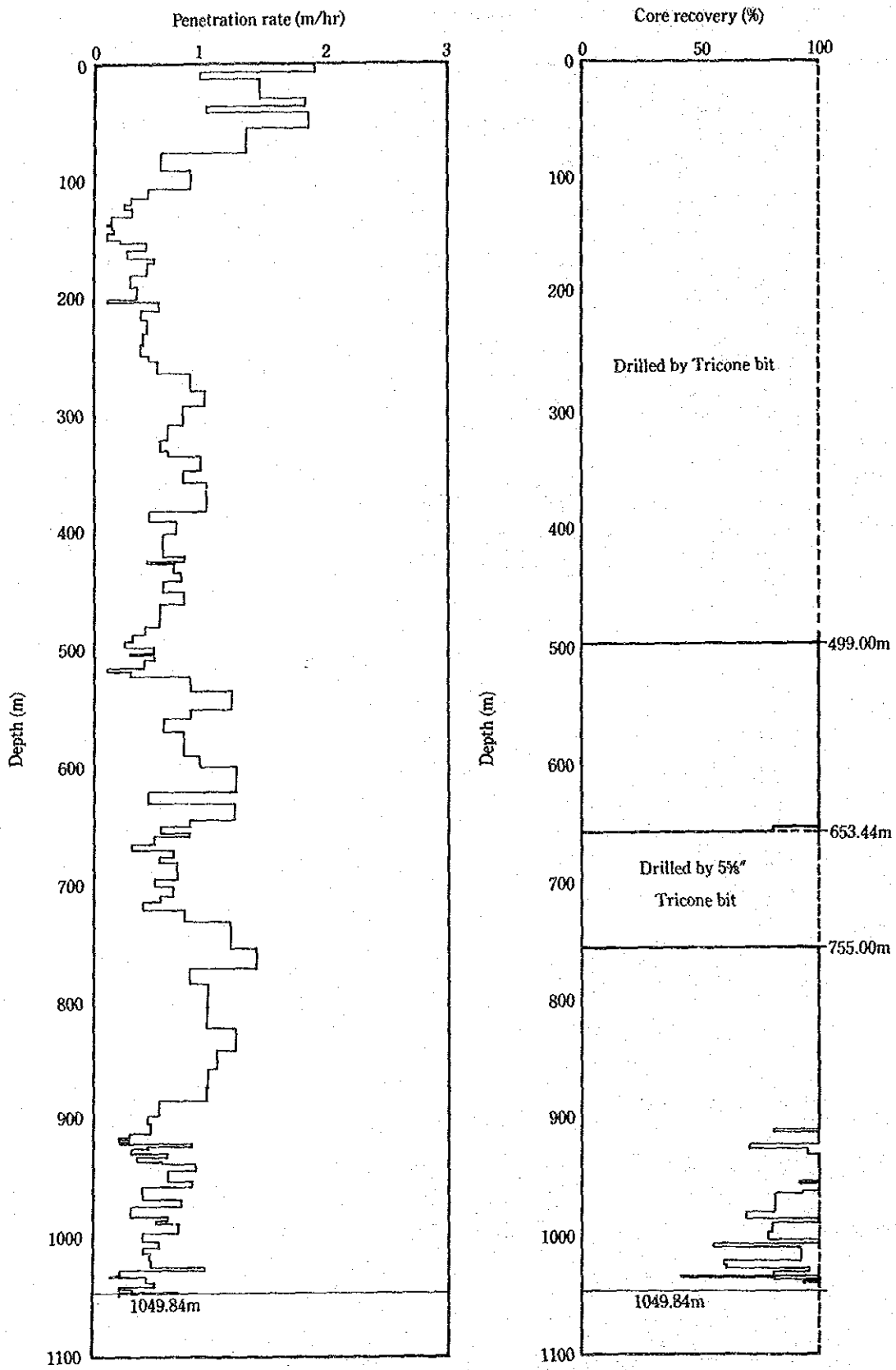


Fig. 5.2-6 Penetration Rate and Core Recovery of GTE-8

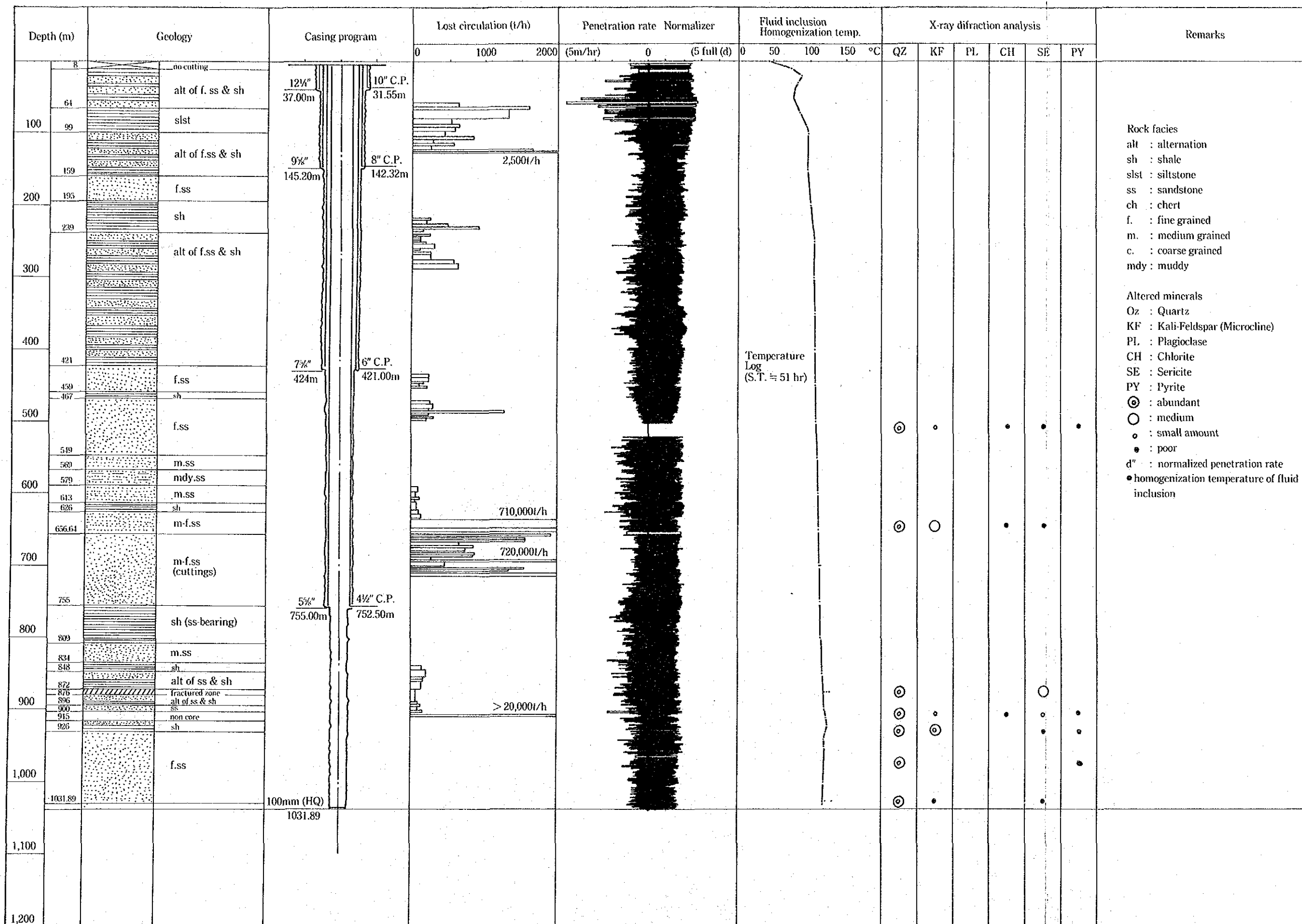


Fig. 5.3-1 Geological Column of GTE-8



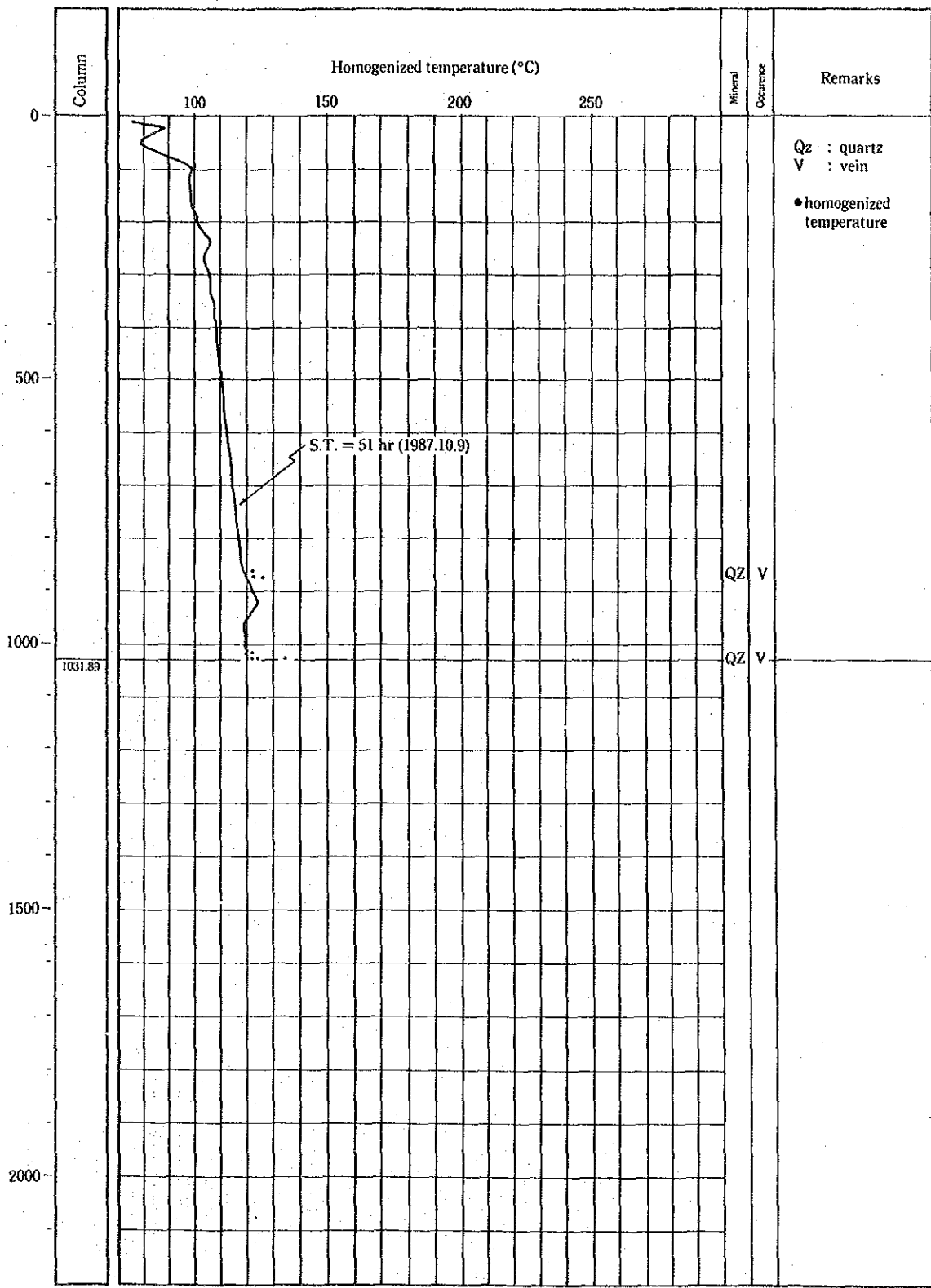


Fig. 5.3-2 Homogenized Temperature of GTE-8



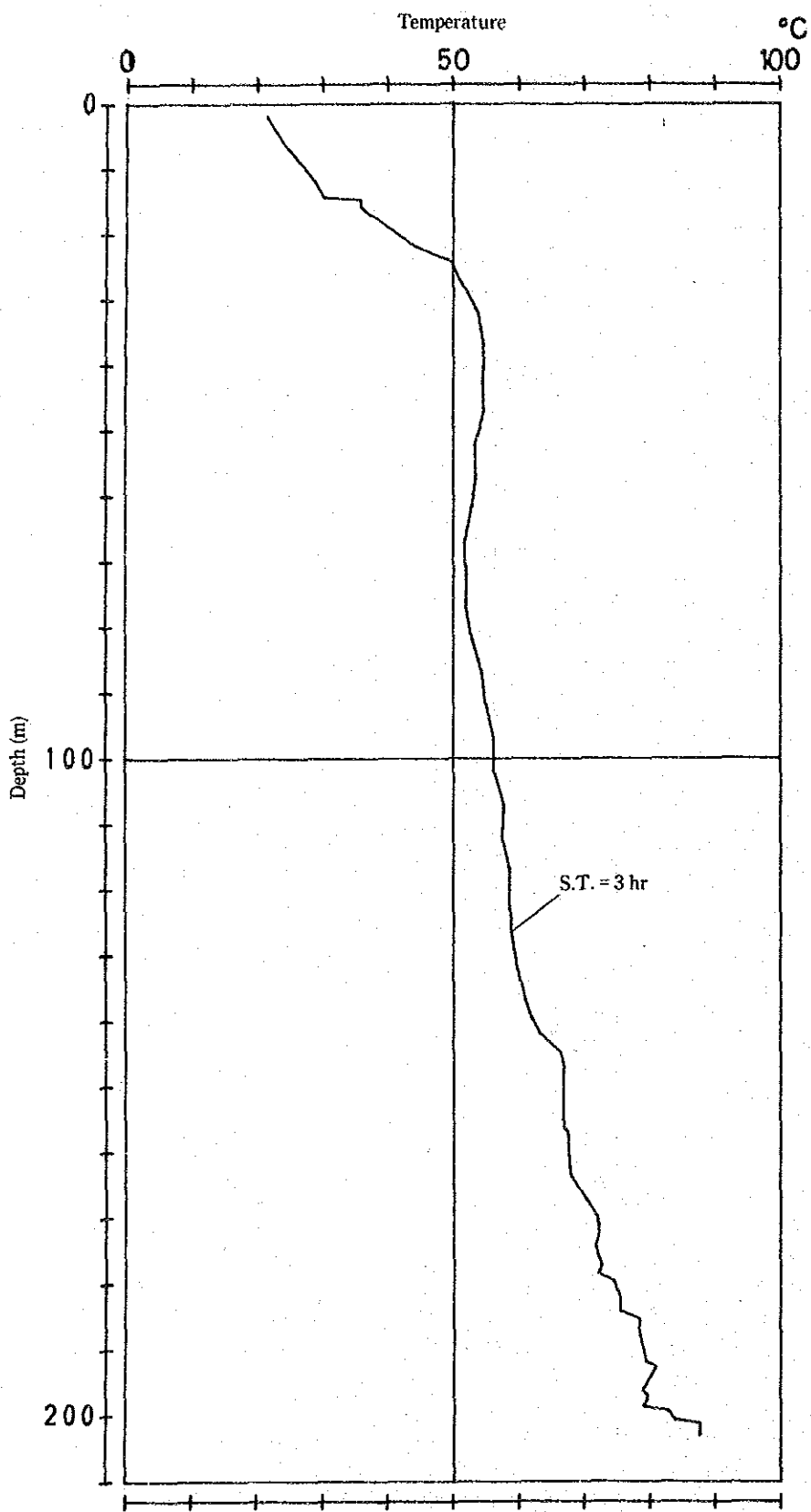


Fig. 5.4-2 Temperature Logging Chart of GTE-8 (Depth 0~203m)

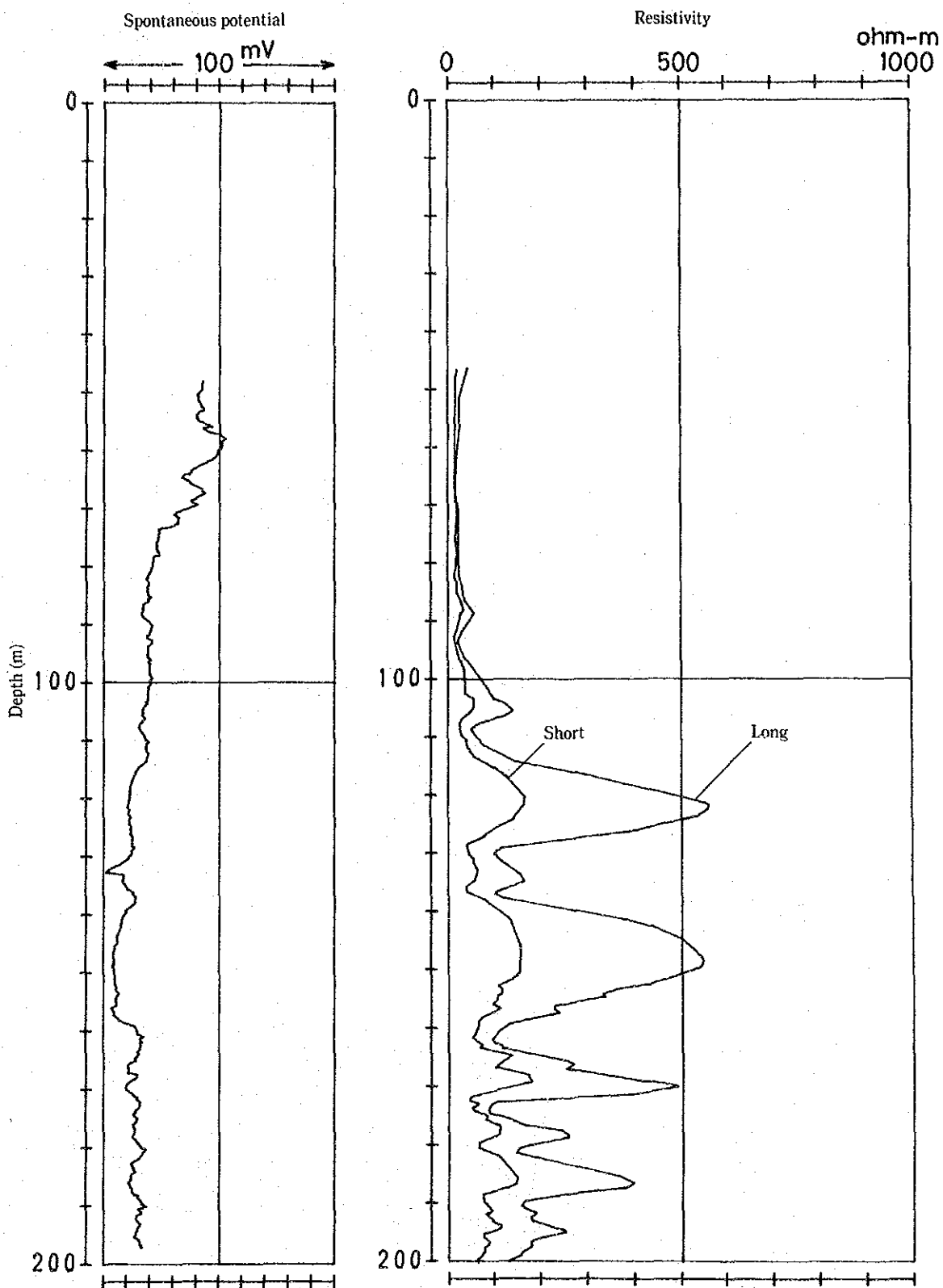


Fig. 5.4-3: Electrical Logging Chart of GTE-8 (Depth 30~200m)

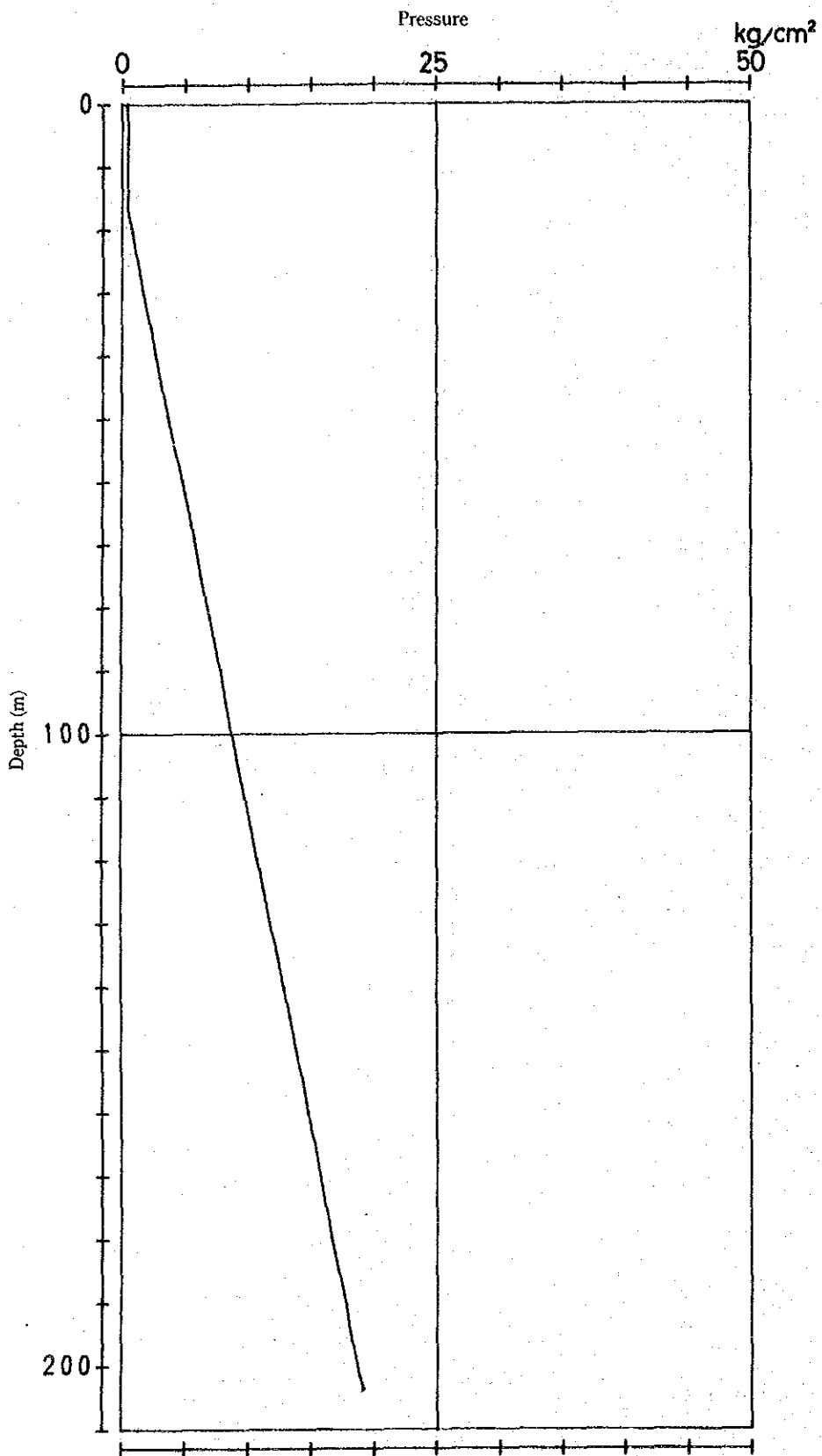


Fig. 5.4-4 Pressure Logging Chart of GTE-8 (Depth 0~203m)

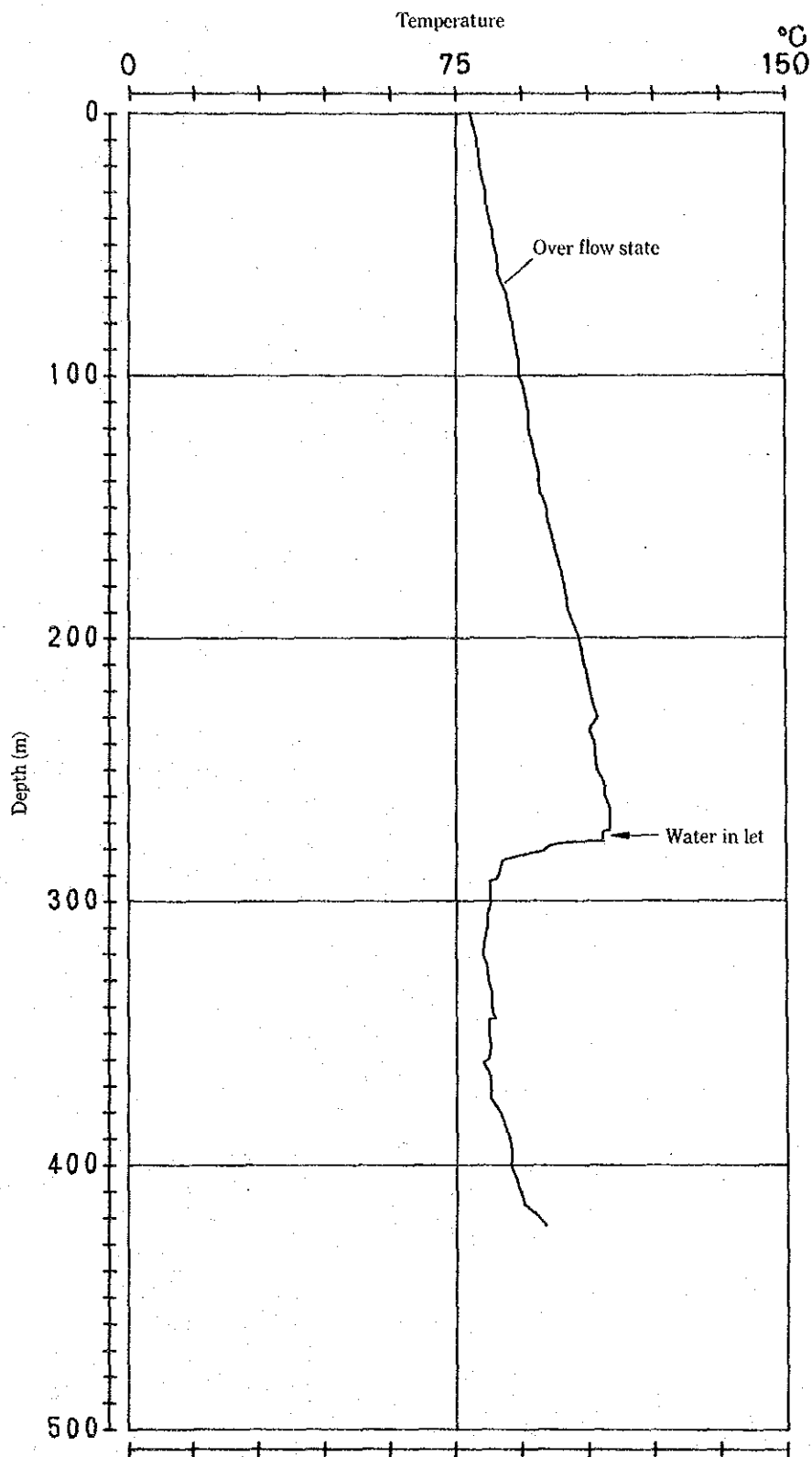


Fig. 5.4-6 Temperature Logging Chart of GTE-8 (Depth 0~424m)

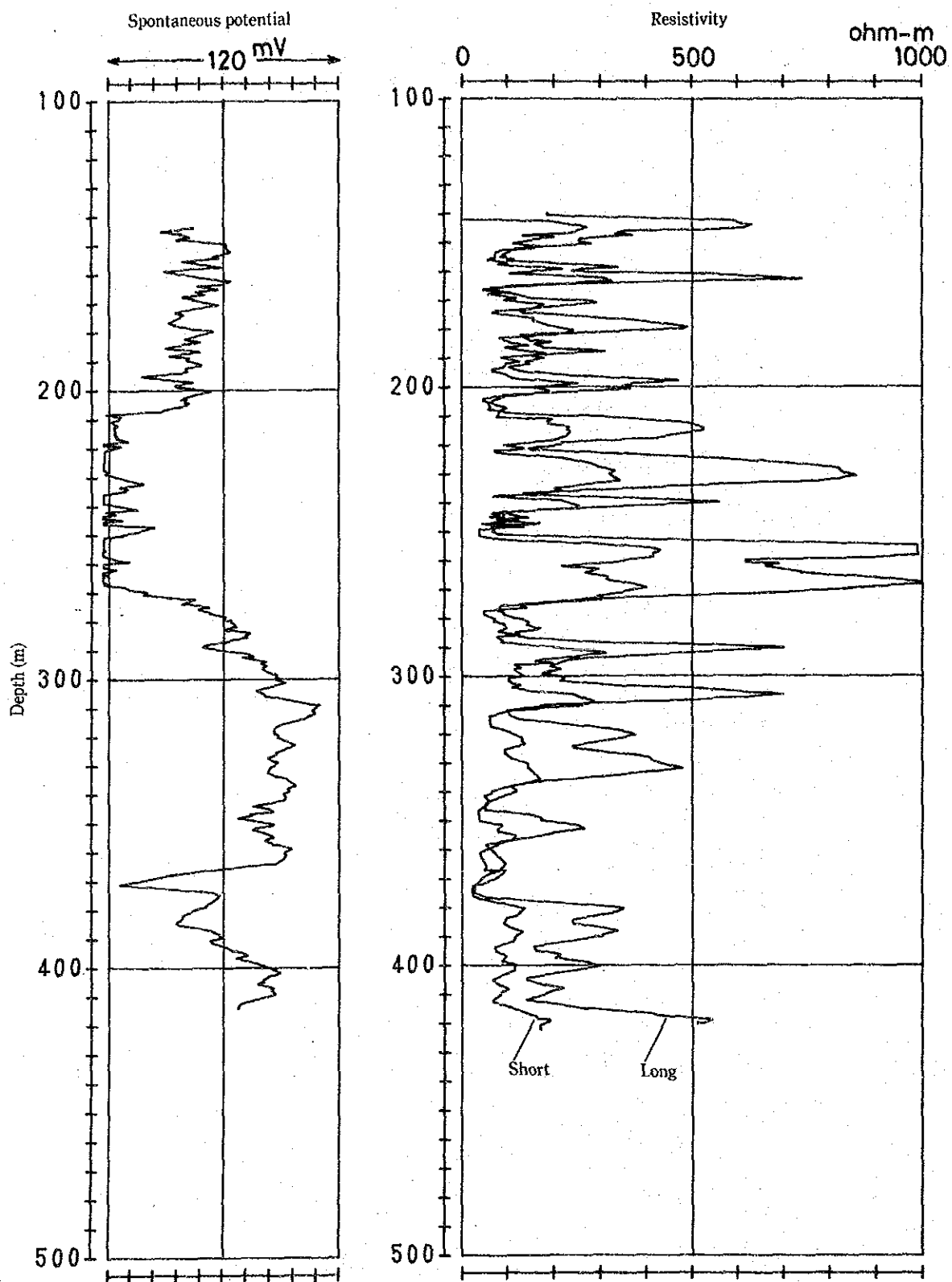


Fig. 5.4-7 Electrical Logging Chart of GTE-8 (Depth 140~420m)

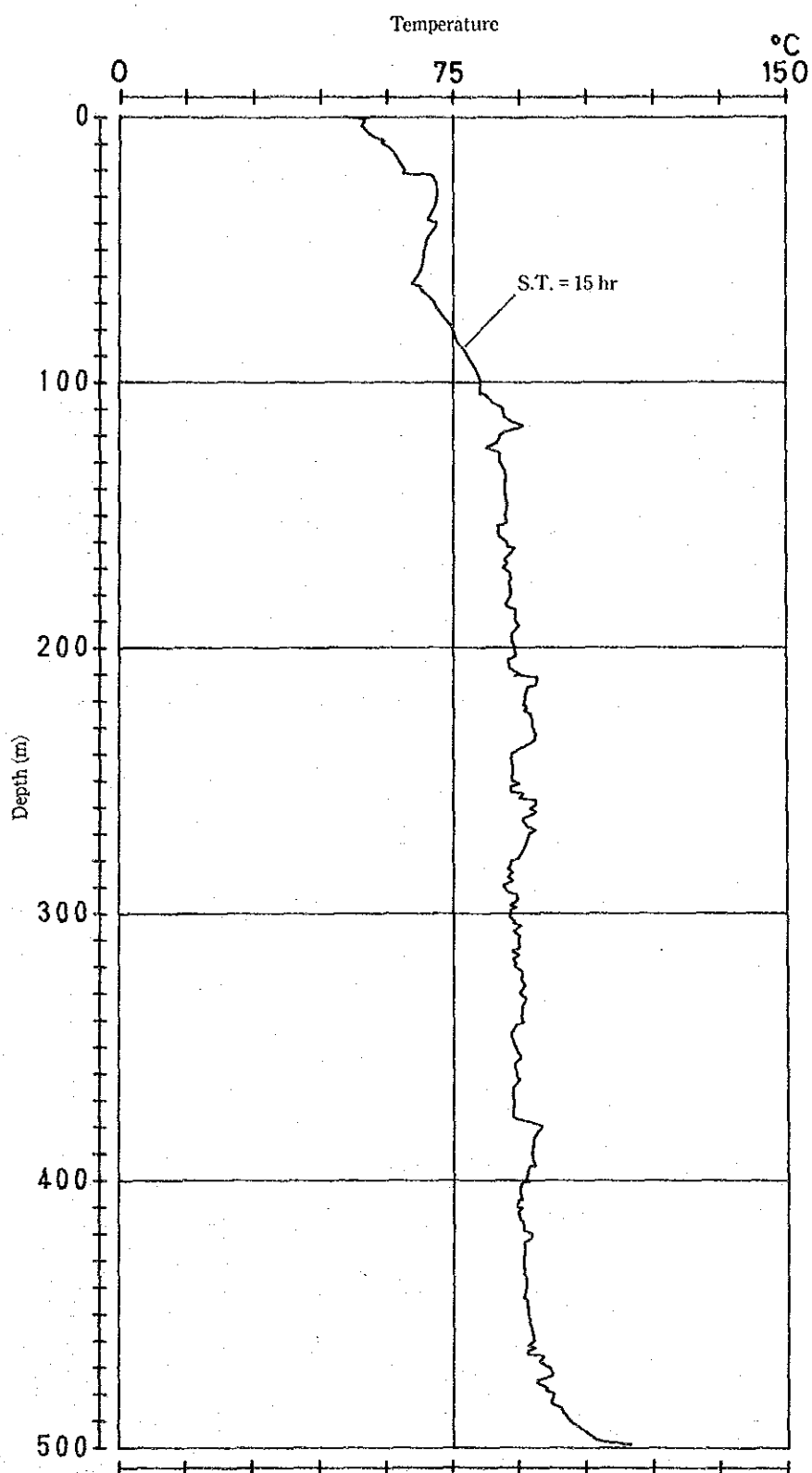


Fig. 5.4-9 Temperature Logging Chart of GTE-8 (Depth 0~499m)

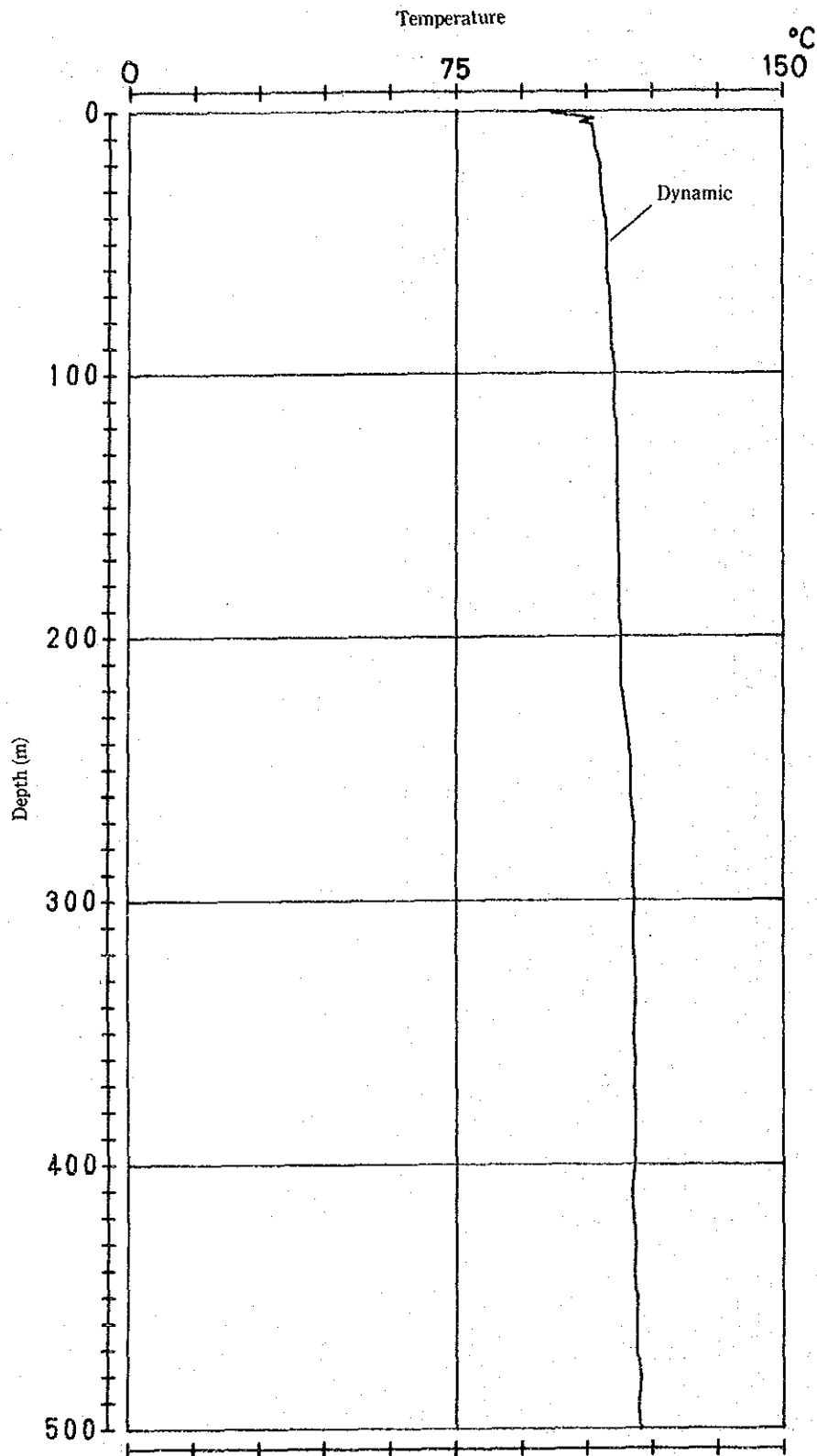


Fig. 5.4-10 Temperature Logging Chart of GTE-8 (Depth 0-500m)

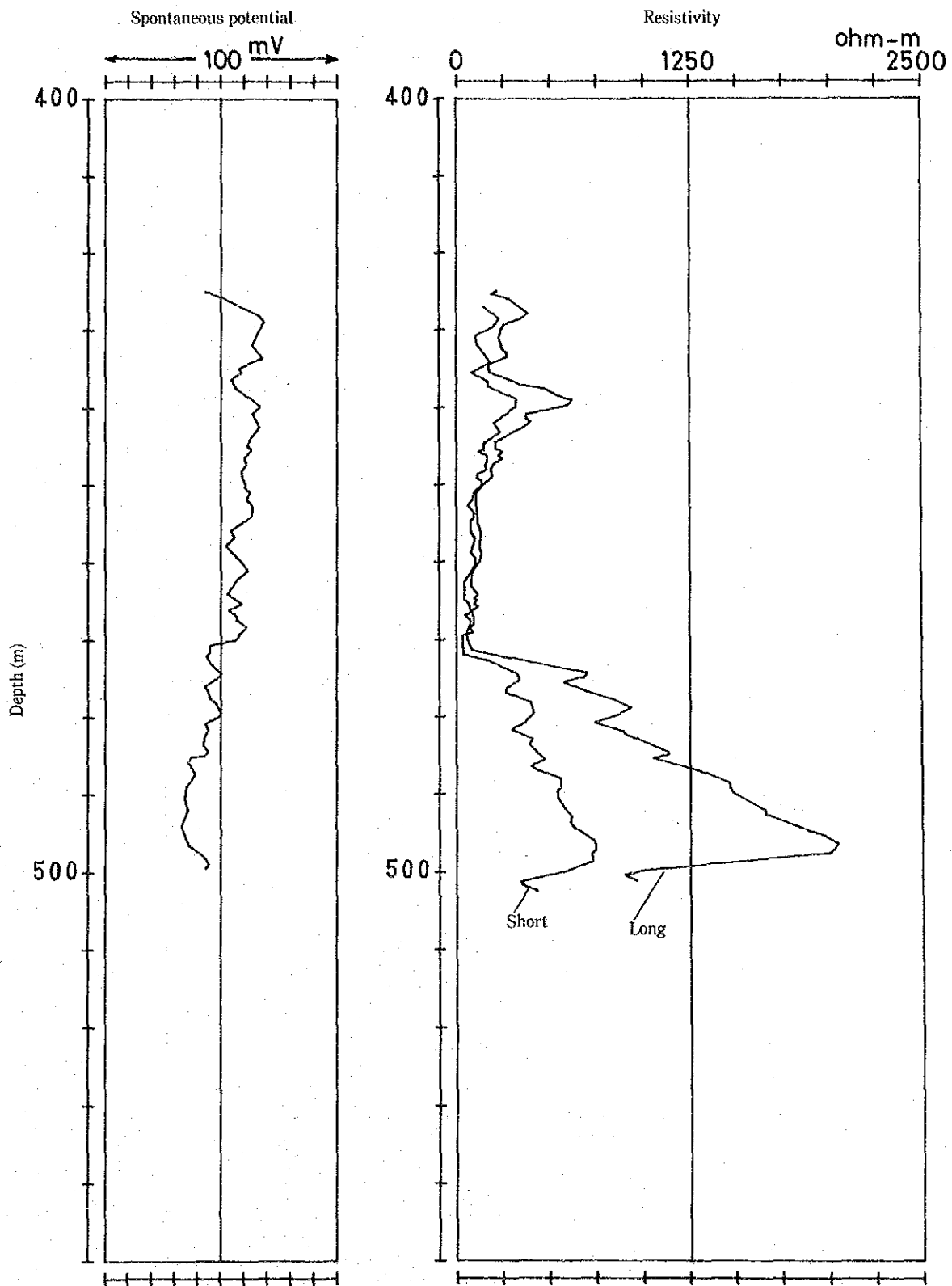


Fig. 5.4-11 Electrical Logging Chart of GTE-8 (Depth 420~550m)



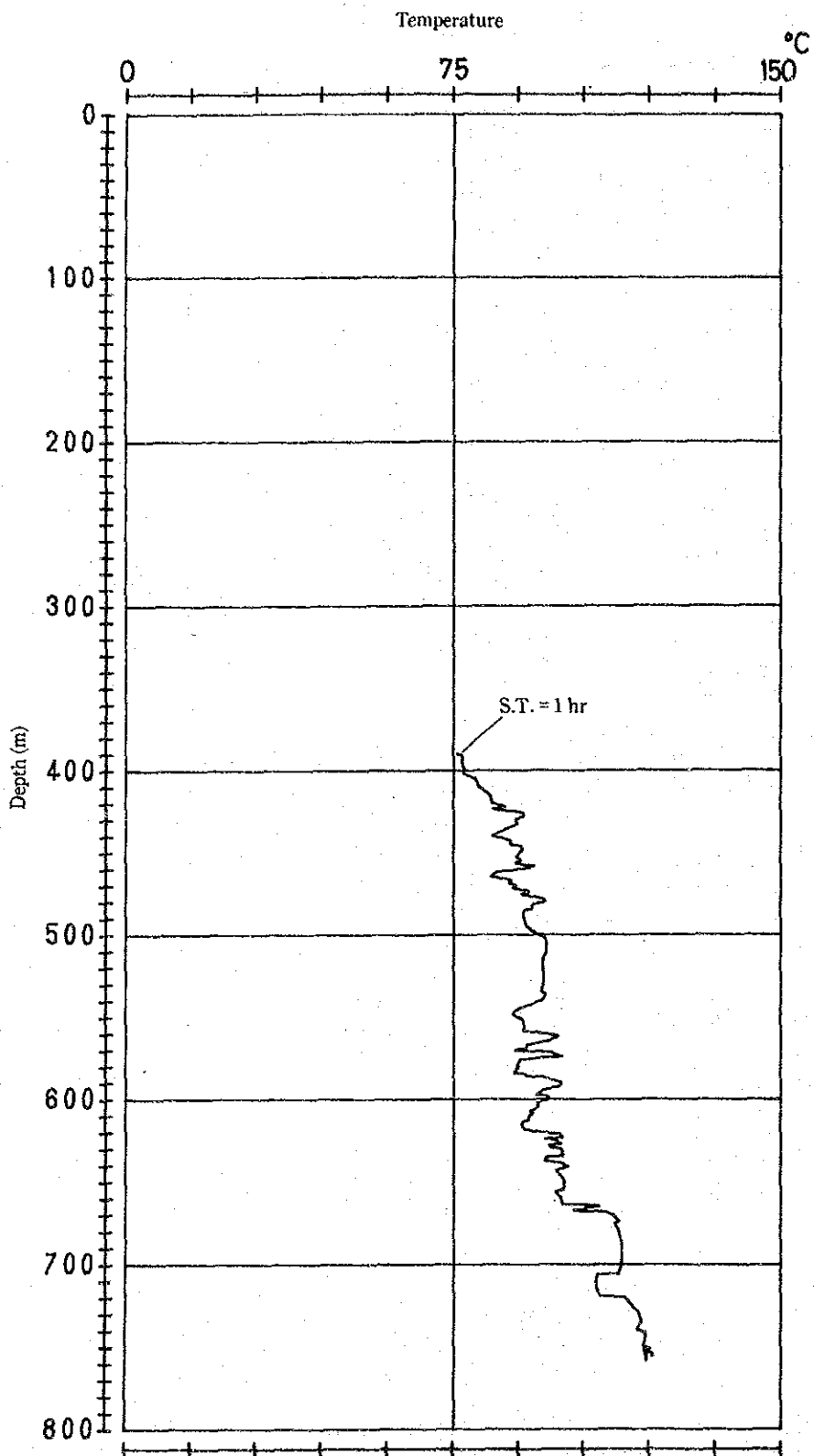


Fig. 5.4-13. Temperature Logging Chart of GTE-8 (Depth 390~755m)

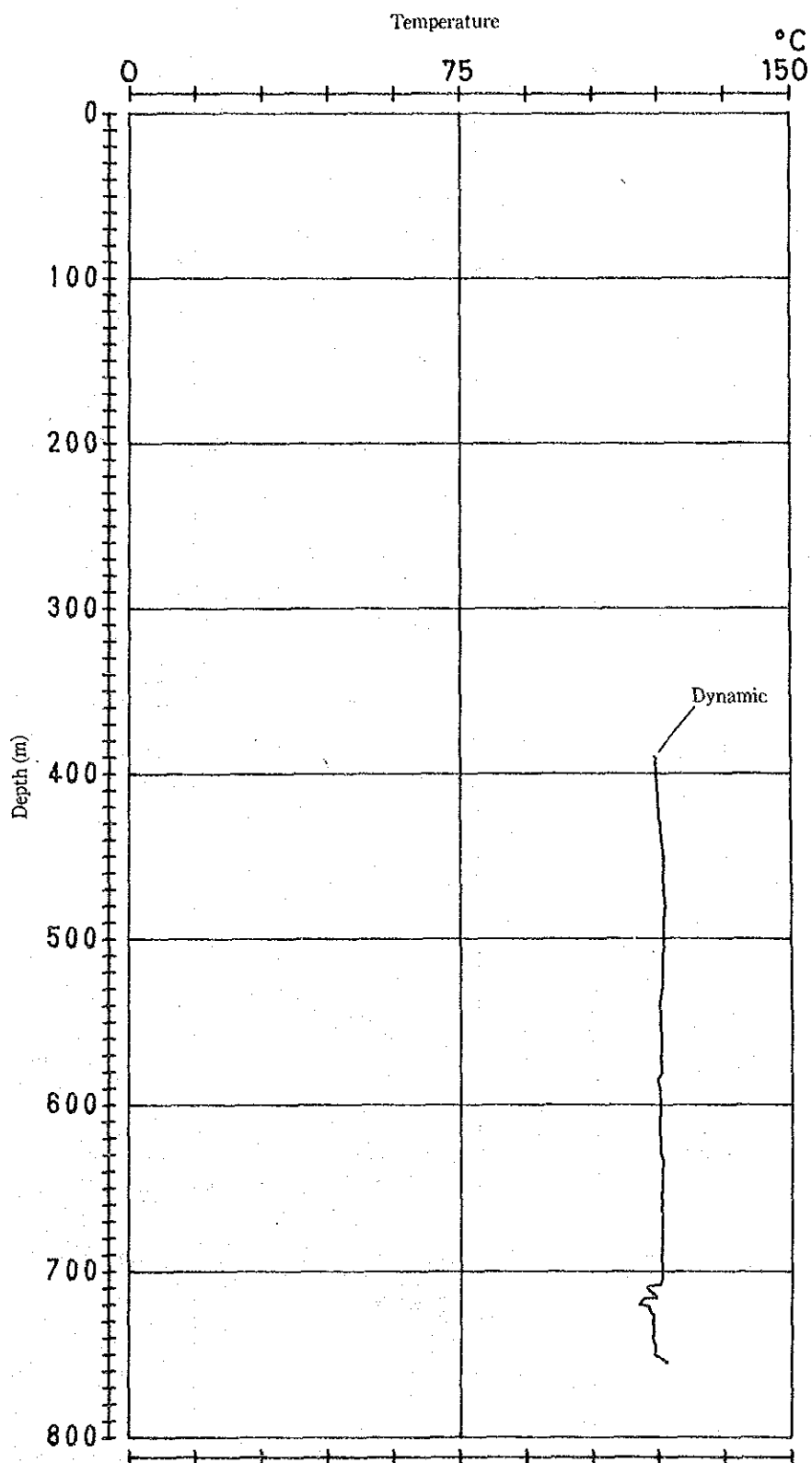


Fig. 5.4-14 Temperature Logging Chart of GTE-8 (Depth 390~755m)

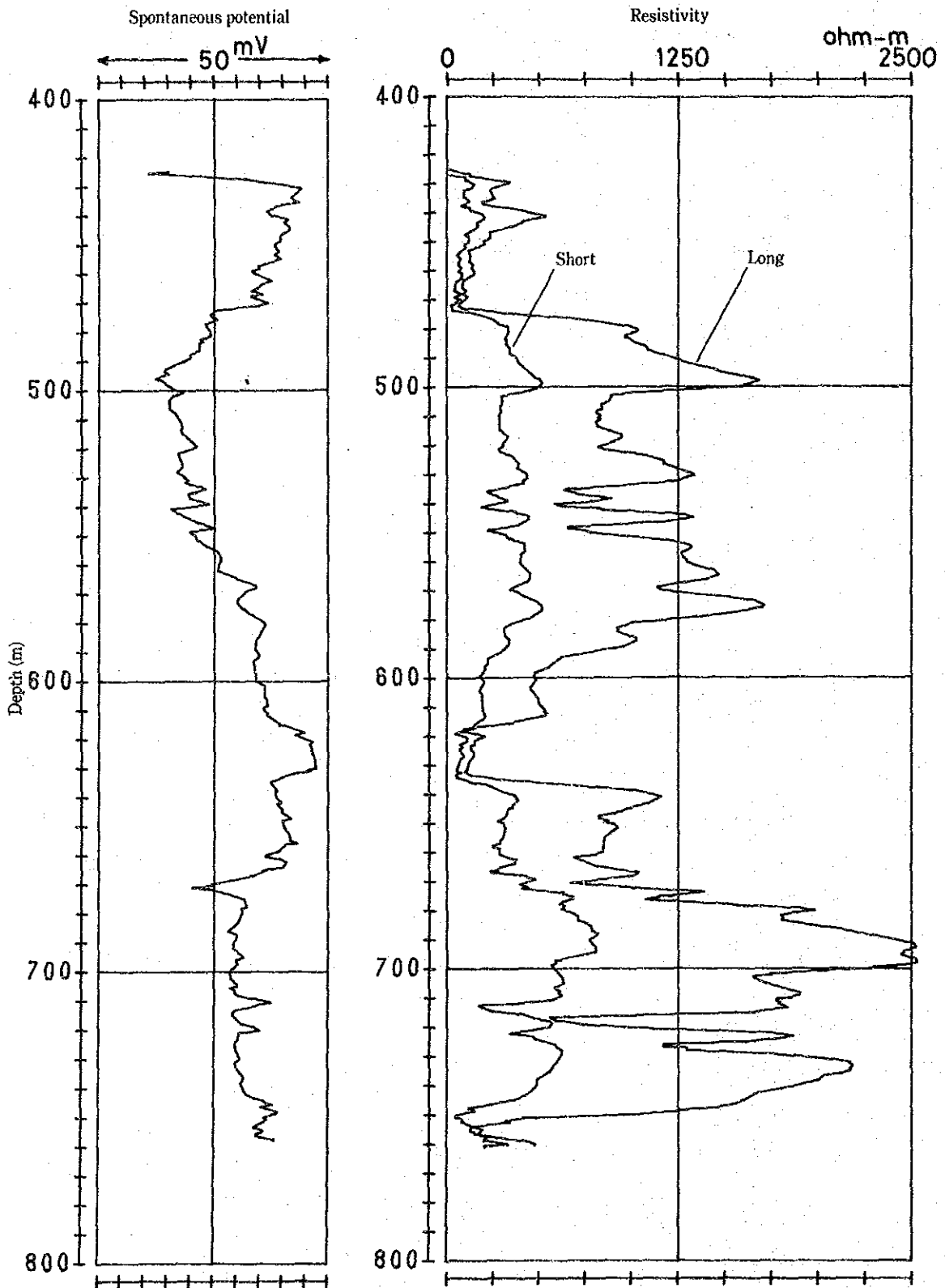


Fig. 5.4-15 Electrical Logging Chart of GTE-8 (Depth 420~755m)

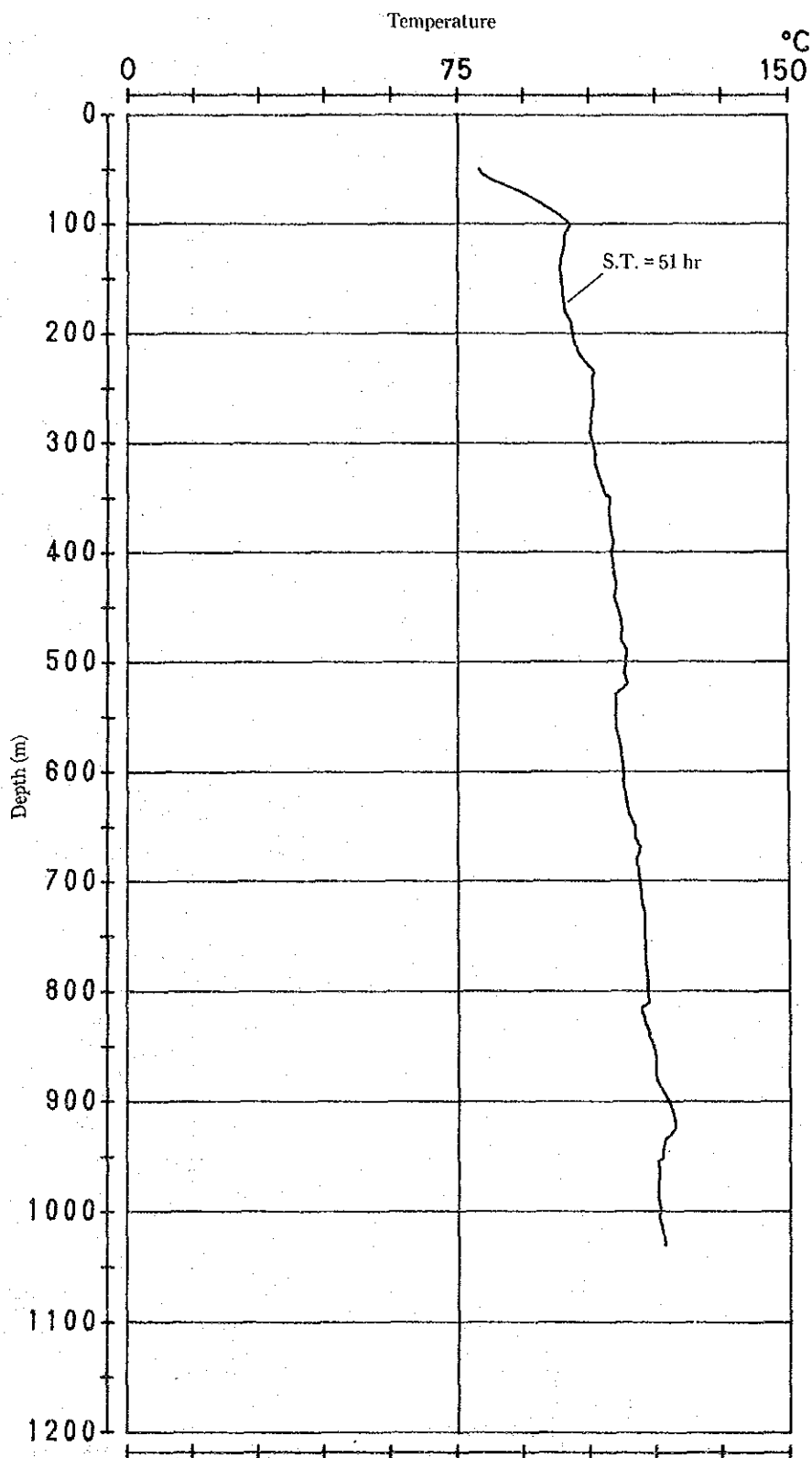


Fig. 5.4-17 Temperature Logging Chart of GTE-8 (Depth 0~1,031m)

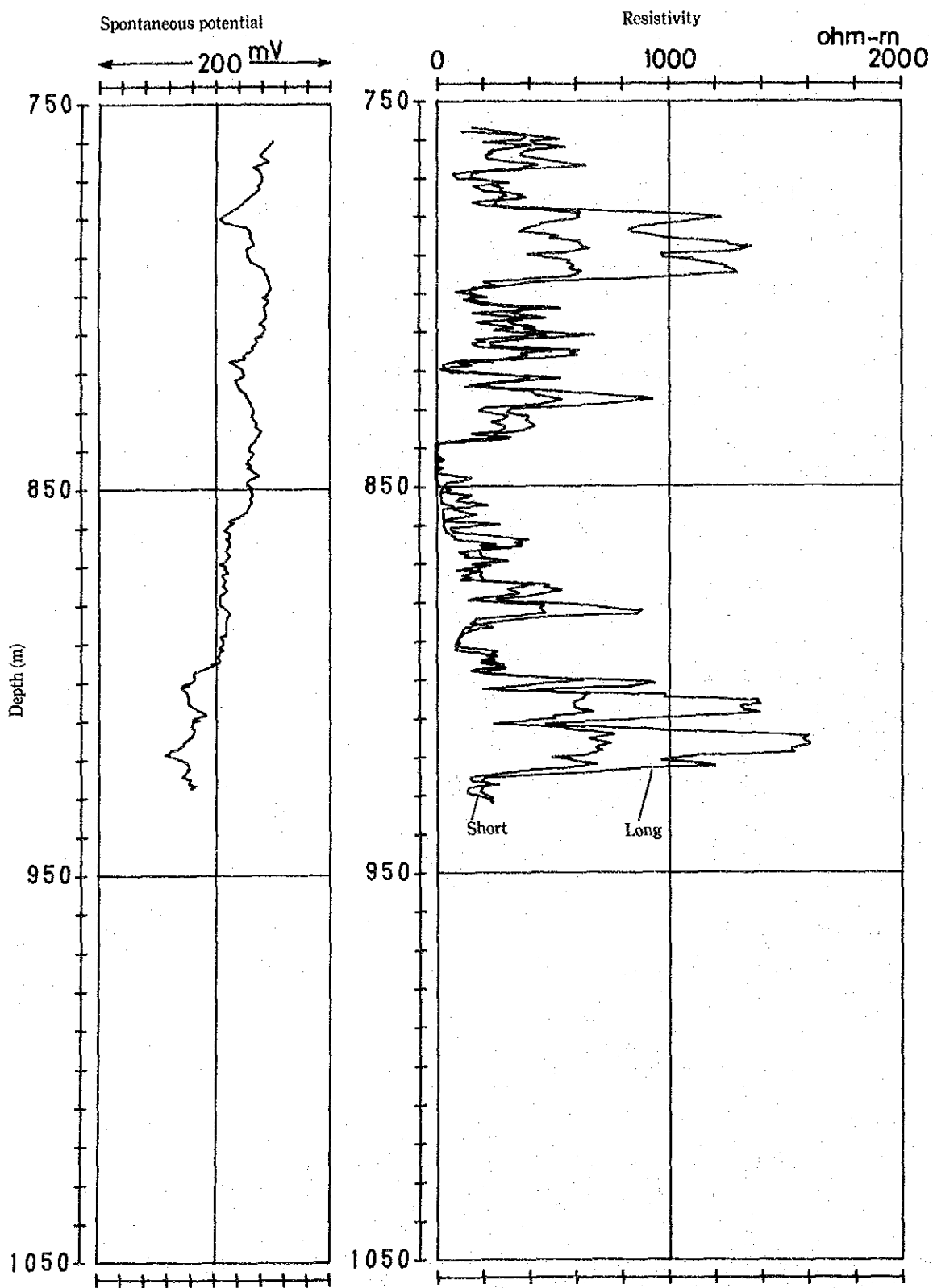


Fig. 5.4-18 Electrical Logging Chart of GTE-8 (Depth 750~930m)

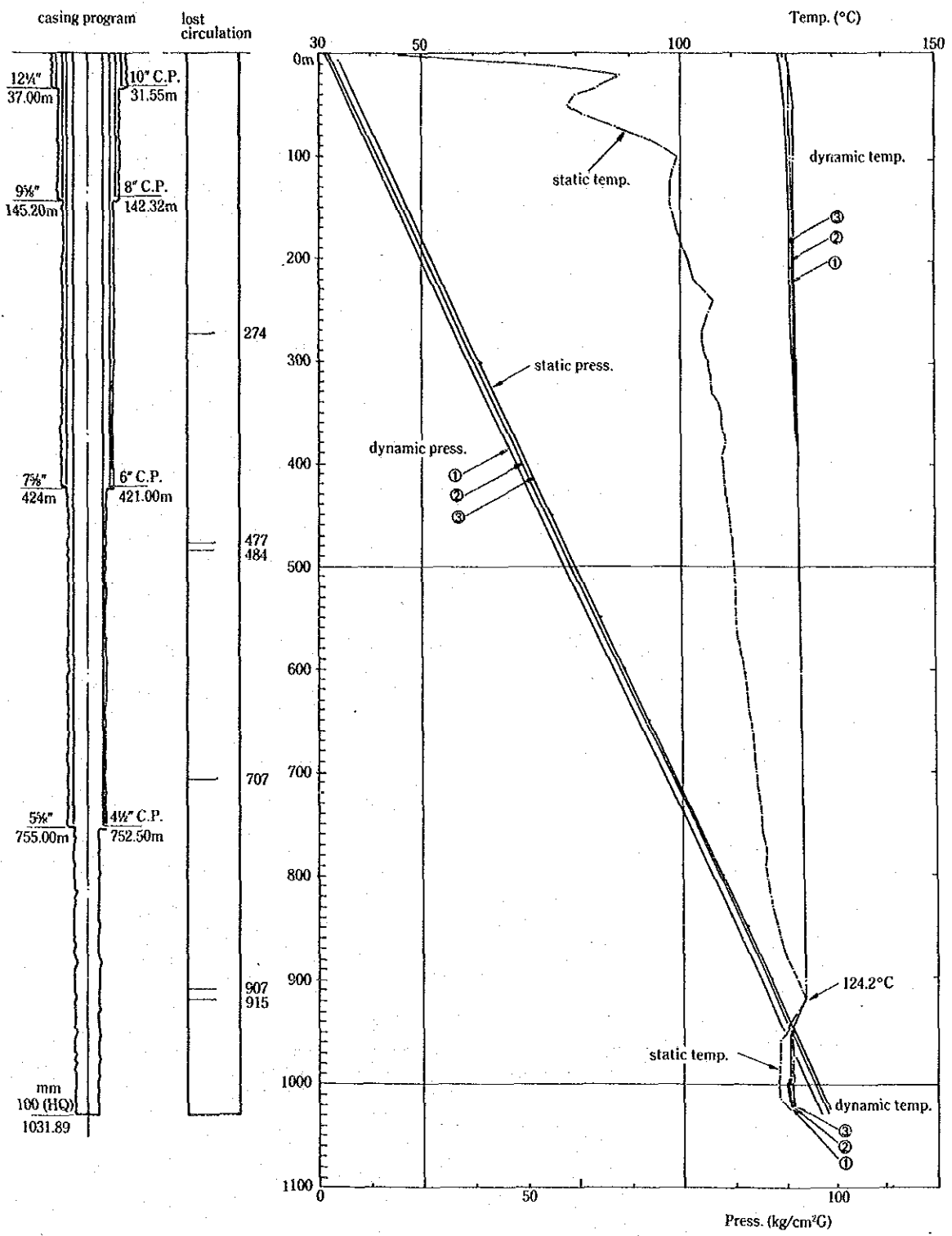


Fig. 5.4-21 GTE-8 Well Logging (Temperature, Pressure)

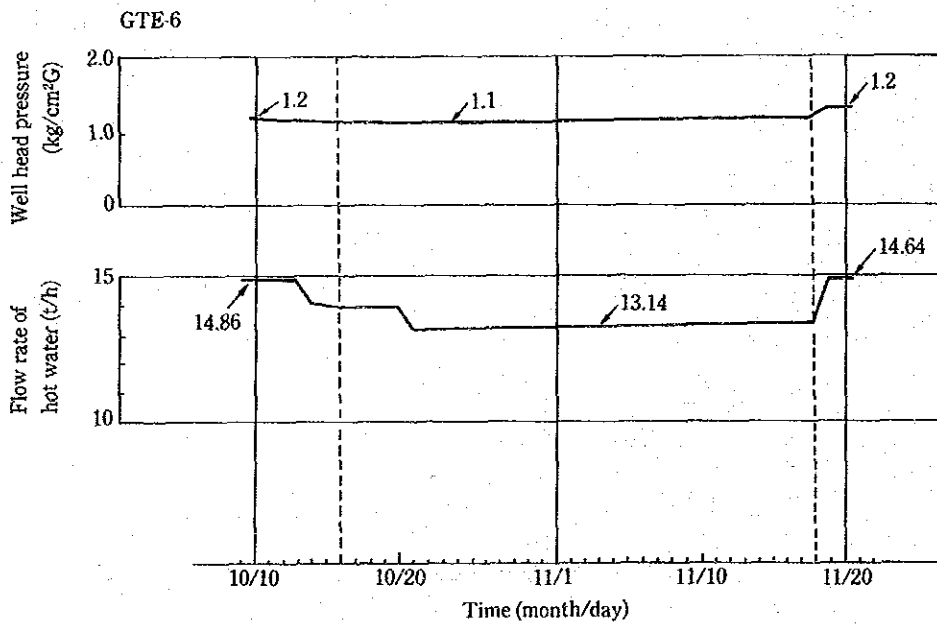
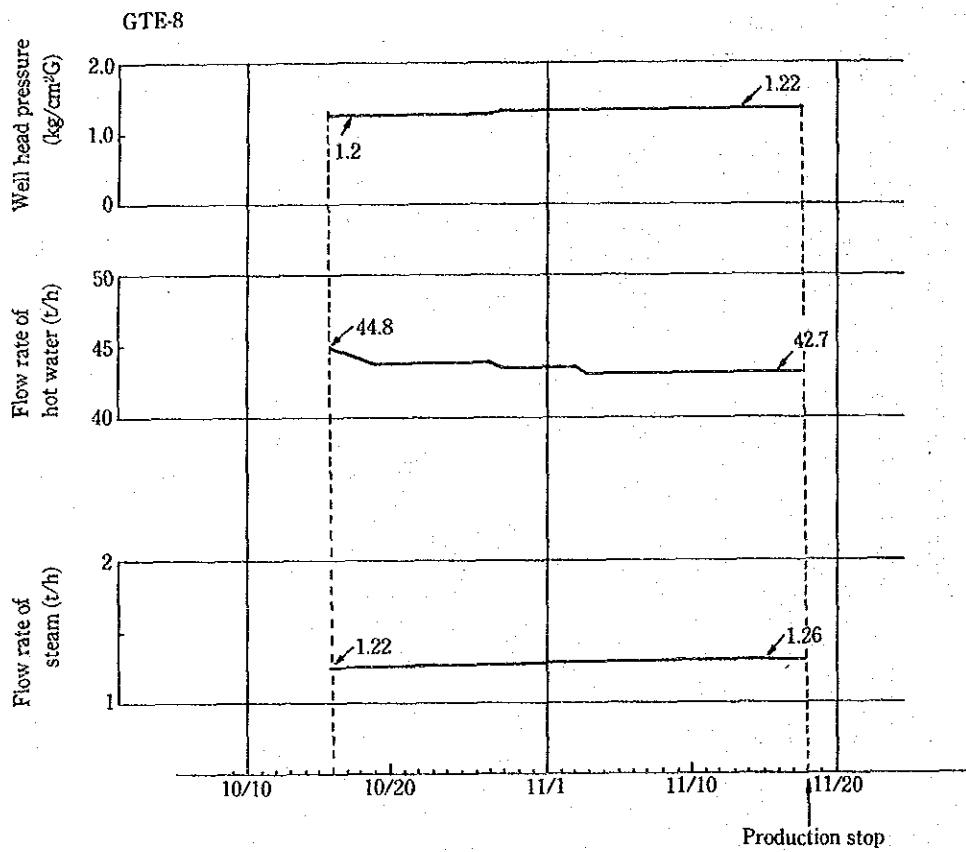


Fig. 5.4-23 Change of Production on GTE-8 and GTE-6

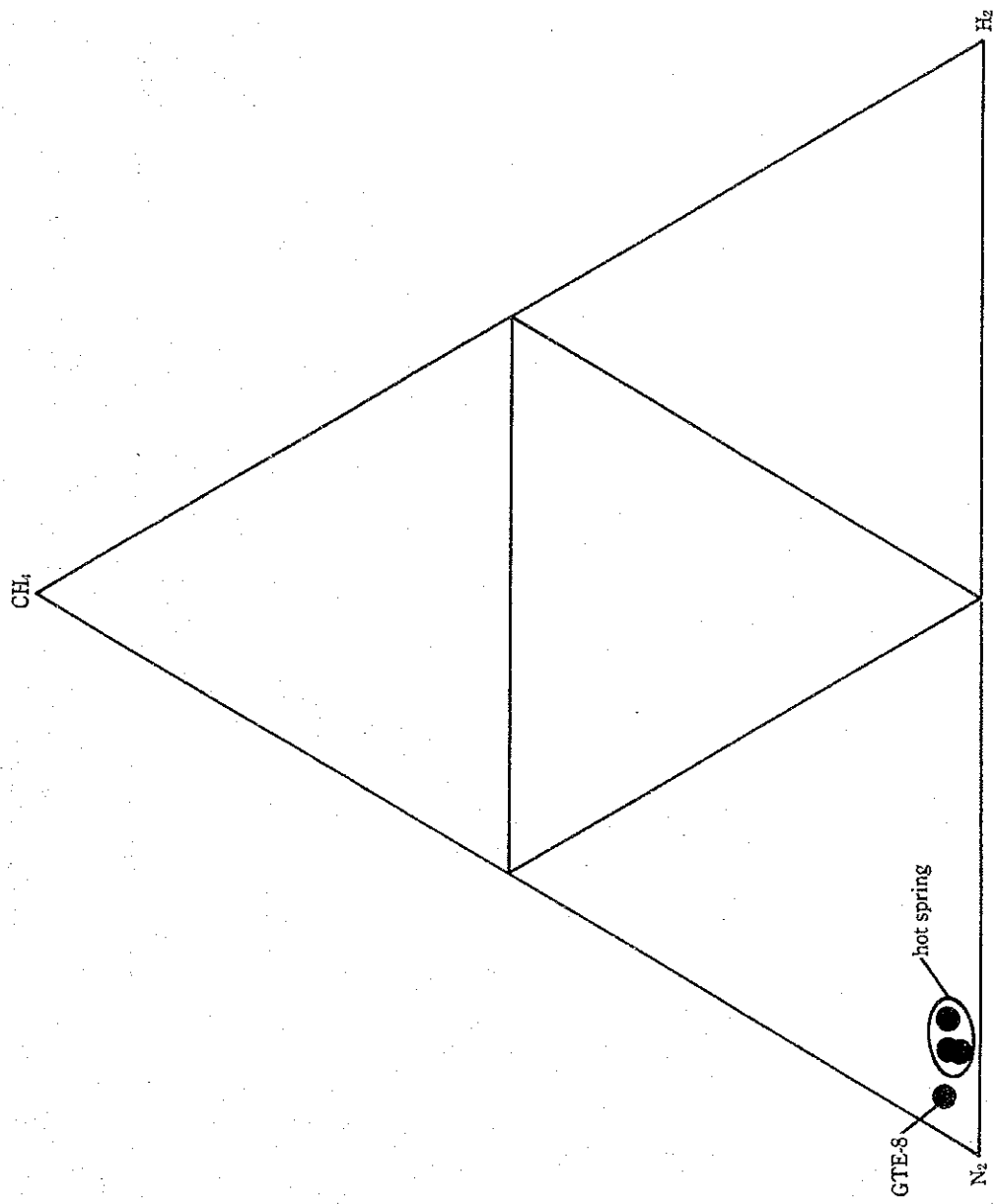


Fig. 5.5-1 Relationship among  $\text{H}_2$ ,  $\text{N}_2$  and  $\text{CH}_4$  in Geothermal Gases from GTE-8 and Hot Springs in and around San Kampaeng



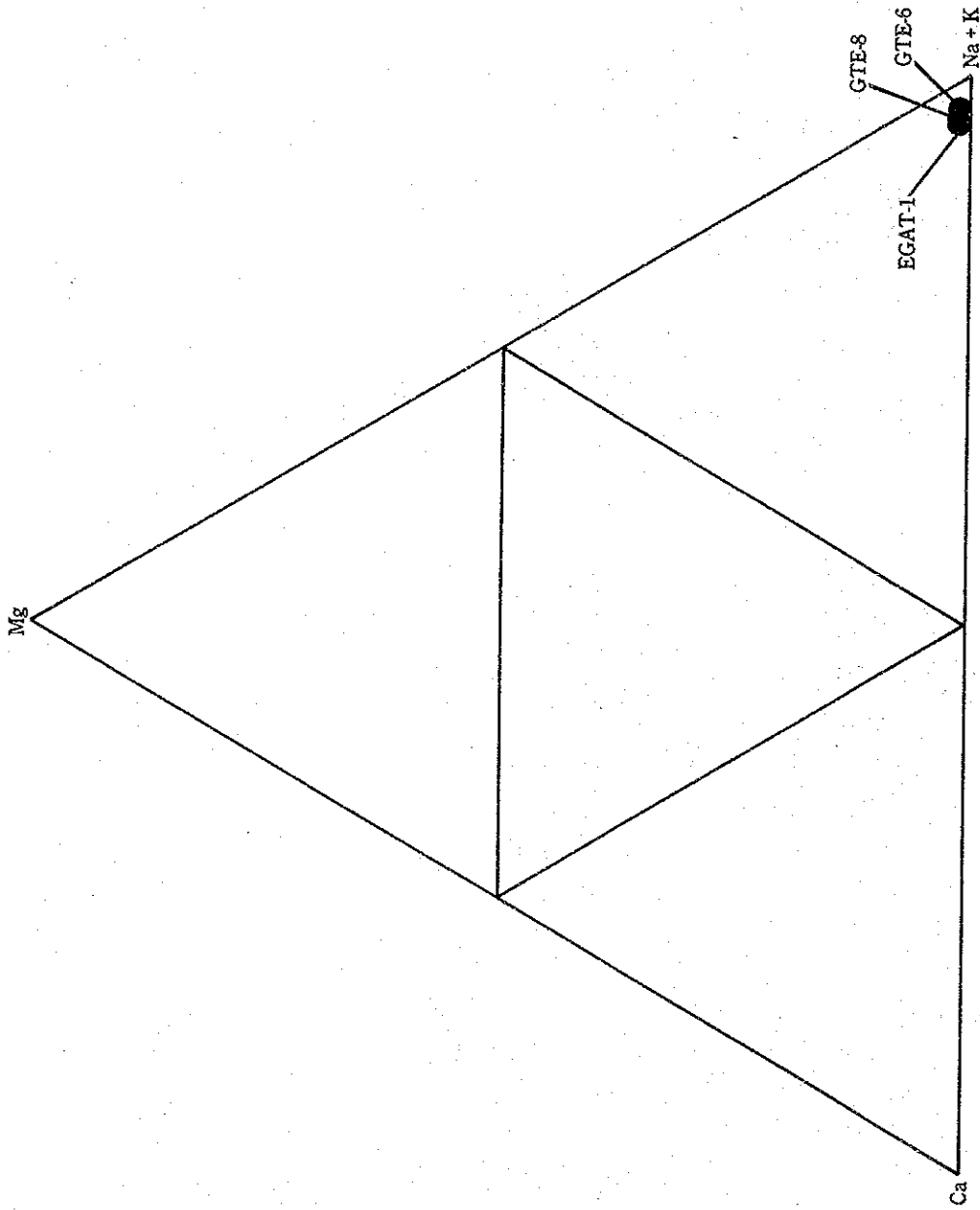


Fig. 5.5-2 Relationship among Molal Concentrations of (Na+K), Ca and Mg in Well Waters from GTE-8, GTE-6 and EGAT-1

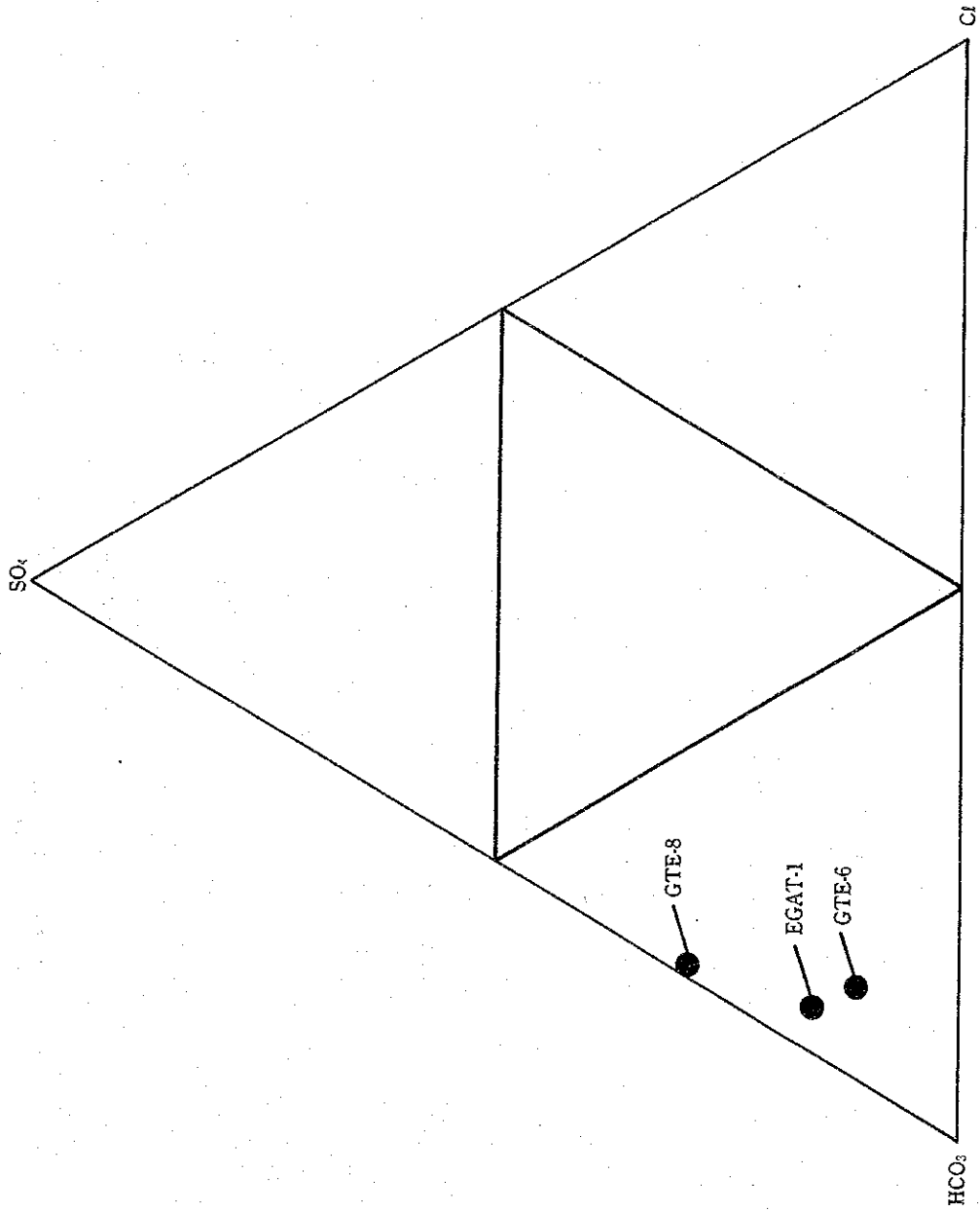


Fig. 5.5-3 Relationship among Molal Concentrations of  $\text{Cl}$ ,  $\text{HCO}_3$  and  $\text{SO}_4$  in Well Waters from GTE-8, GTE-6 and EGAT-1

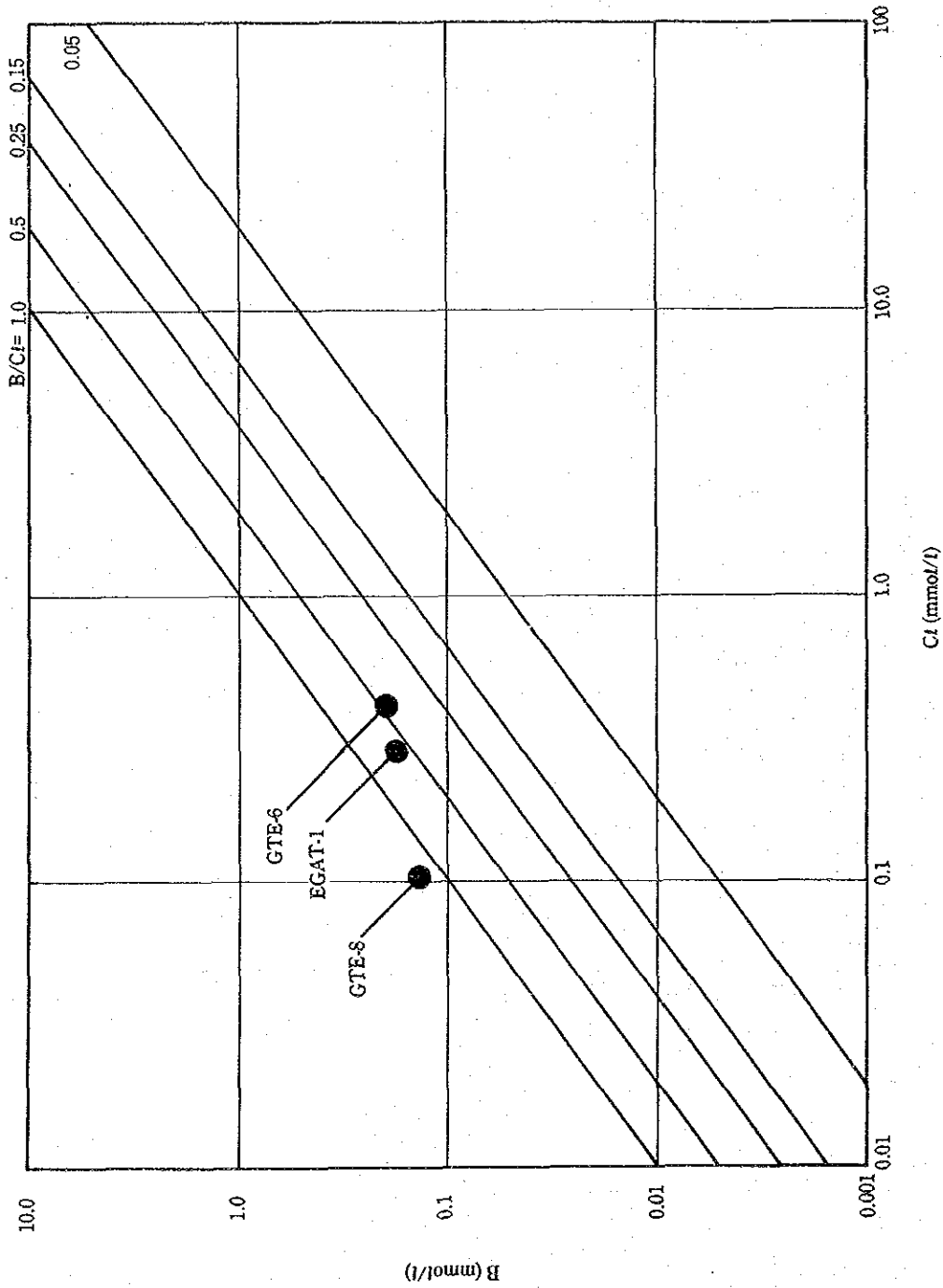


Fig. 5.5-4 Relationship between Molal Concentrations of B and Cl in Well Waters from GTE-8, GTE-6 and EGAT-1

Table 5.2-1 Summary of Drilling Work of GTE-8

Depth (m)	Well Diameter (mm)	Bit			Drilling Mud			Casing		Lithology	Drilling activities		
		Type	Size	Pressure (kg)	Revolutions (rpm)	Temperature in/out (°C)	Mud Supplied (ℓ/min)	Type	Lost Circulation			Size	Depth inserted (m)
0.00~ 37.00	311.20	Tricone	12-1/4"	1000~ 1300	20~ 30		780	Bentonite	None	10"	29.60	Non Coring 10" CP cementation	
37.00~ 203.00	244.50	Tricone	9-5/8"	3000~ 5000	25~ 40	32.0/39.6	780		40~60ℓ/min			Non Coring	
	193.60	Tricone	7-5/8"	3000~ 5000	35~ 45		780	Bentonite		8"	14.220	8" CP cementation	
		Tricone	5-5/8"	2000~ 3500	35~ 45	42.3/44.9	600						
203.00~ 424.00	193.65	Tricone	7-5/8"	3000~ 5000	40~ 45	41.6/43.8	660	Bentonite	40ℓ/min at 274.00m	6"	421.00	Non Coring 6" CP cementation	
		Tricone	5-5/8"	2500~ 3500	40~ 45	52.5/60.4	550						
424.00~ 755.00	142.90	Tricone	5-5/8"	2500~ 4000	40~ 45	49.9/55.9	380		6ℓ/min at 435.94m 110ℓ/min at 480.00m 110ℓ/min at 643.24m 110ℓ/min at 706.92m				
		Diamond	HQ-WL	1,500	100~150	46.2/60.3	110	Bentonite		4-1/2"	752.50	To 499M Non Coring From 499M Coring	
755.00~ 1049.84	98.7	Diamond	HQ-WL	1,500~ 2,500	100~200		100~ 250	Water	110ℓ/min at 907.00m 150ℓ/min at 915.45m	Bare hole		Fine sandstone	



Table 5.2-3 Breakdown of Drilling Work of GTE-8 (1)

Depth	Work Items	Period	No. of Calendar days	No. of Working days	Other days
0.00 m ~ 37.00 m	12-1/4" T.B (0.00 m ~ 37.00 m)	1986 Nov. 13 ~ Nov. 16	4	4	0
	10" C.P insertion	Nov. 17	1	1	0
	Wait on cement	Nov. 18	1	1	1
	<b>Total</b>		<b>6</b>	<b>5</b>	<b>1</b>
37.00 m ~ 203.00 m	9-5/8" T.B (37.00 m ~ 56.04 m)	Nov. 19 ~ Nov. 20	2	2	0
	Cementing, Drilling out cement	Nov. 21	1	1	0
	9-5/8" T.B (56.04 m ~ 121.50 m)	Nov. 22 ~ Nov. 27	6	6	0
	Cementing, Waiting on-cement, Drilling out cement	Nov. 28 ~ Nov. 30	3	3	0
	9-5/8" T.B (121.50 m ~ 137.51 m)	Dec. 1 ~ Dec. 4	4	4	0
	Cementing, Wait on cement, Drilling out cement	Dec. 5 ~ Dec. 8	4	4	0
	9-5/8" T.B (137.51 m ~ 139.22 m)	Dec. 9	1	1	0
	7-5/8" T.B (139.22 m ~ 144.47 m)	Dec. 10 ~ Dec. 11	2	2	0
	Fishing T.B cone	Dec. 12	1	1	0
	7-5/8" T.B (144.47 m ~ 150.40 m)	Dec. 13 ~ Dec. 15	3	3	0
	5-5/8" T.B (150.40 m ~ 203.00 m)	Dec. 16 ~ Dec. 22	7	7	0
	Well logging	Dec. 23	1	1	0
	9-5/8" T.B reaming (139.22 m ~ 145.20 m)	Dec. 24 ~ Dec. 26	3	3	0
	Cementing (145.20 m ~ 203.00 m)	Dec. 27	1	1	0
	Material procurement and machine maintenance	1987 Dec. 28 ~ Jan. 10	14	11	3
	Preparation of 8" C.P Insertion	Jan. 11 ~ Jan. 12	2	2	0
	8" C.P Insertion, Cementing	Jan. 13	1	1	0
	Wait on cement	Jan. 14	1	1	0
<b>Total</b>		<b>57</b>	<b>54</b>	<b>3</b>	
203.00 m ~ 424.00 m	7-5/8" T.B Drilling out cement and reaming (145.20 m ~ 203.00 m)	Jan. 15 ~ Jan. 20	6	6	0
	7-5/8" T.B (203.00 m ~ 235.44 m)	Jan. 21 ~ Jan. 24	4	4	0
	5-5/8" T.B (235.44 m ~ 337.45 m)	Jan. 25 ~ Feb. 2	9	9	0
	Well logging, Cementing	Feb. 3	1	1	0
	Wait on cement	Feb. 4	1	1	0
	7-5/8" T.B Drilling out cement and reaming (235.44 m ~ 337.45 m)	Feb. 5 ~ Feb. 10	6	6	0
	7-5/8" T.B (337.45 m ~ 424.00 m)	Feb. 11 ~ Feb. 15	5	5	0
	Well logging	Feb. 16	1	1	0
	6" C.P Insertion, Cementing	Feb. 17	1	1	0
	Wait on cement	Feb. 18 ~ Feb. 19	2	2	0
<b>Total</b>		<b>36</b>	<b>36</b>	<b>0</b>	
424.00 m ~ 518.07 m	B.O.P. Installation, 5-5/8" T.B Drilling out cement	Feb. 20	1	1	0
	5-5/8" T.B (424.00 m ~ 435.94 m)	Feb. 21	1	1	0
	Cementing	Feb. 22	1	1	0

Table 5.2-3 Breakdown of Drilling Work of GTE-8 (2)

Depth	Work Items	Period	No. of Calendar days	No. of Working days	Other days
424.00 m ~ 518.07 m	Drilling out cement	Feb. 23	1	0	1
	5-5/8" T.B (435.94 m ~ 499.00 m)	Feb. 24 ~ Mar. 2	7	7	0
	Machine repairs	Mar. 3	1	1	0
	HQ-WL Coring (499.00 m ~ 501.69 m)	Mar. 4	1	1	0
	Well logging	Mar. 5 ~ Mar. 7	3	3	0
	Cementing	Mar. 8	1	1	0
	Measurement of hole deviation	Mar. 9	1	1	0
	Drilling out cement	Mar. 10	1	1	0
	HQ-WL Coring (501.69 m ~ 518.07 m)	Mar. 11 ~ Mar. 14	4	4	0
	Cementing, Wait on cement	Mar. 15 ~ Mar. 17	3	3	0
	<b>Total</b>		<b>26</b>	<b>25</b>	<b>1</b>
518.07 m ~ 755.00 m	Preparation of Drilling	May 27 ~ May 28	2	2	0
	5-5/8" T.B Drilling out cement	May 29 ~ May 31	3	3	0
	HQ-WL Coring (518.07 m ~ 653.44 m)	Jun. 1 ~ Jun. 11	11	11	0
	5-5/8" T.B Reaming (to 654.00 m)	Jun. 12 ~ Jun. 22	11	11	0
	Well logging	Jun. 23 ~ Jun. 25	3	3	0
	Cementing	Jun. 26	1	1	0
	Wait on cement, Drilling out cement	Jun. 27 ~ Jun. 29	3	3	0
	HQ-WL Coring (654.00 m ~ 656.64 m)	Jun. 30	1	1	0
	Cementing, Wait on cement, Drilling out cement	Jun. 1 ~ Jul. 2	2	2	0
	5-5/8" T.B (654.00 m ~ 755.00 m)	Jul. 3 ~ Jul. 16	14	14	0
	Well logging	Jul. 17 ~ Jul. 19	3	3	0
	Cementing, Wait on cement, Drilling out cement	Jul. 20 ~ Jul. 24	5	5	0
	4-1/2" C.P Insertion, Cementing, Wait on cement	Jul. 25 ~ Jul. 28	4	4	0
	<b>Total</b>		<b>63</b>	<b>63</b>	<b>0</b>
755.00 m ~ 1049.00 m	HQ-WL Coring (755.00 m ~ 914.59 m)	Jul. 29 ~ Aug. 11	14	14	0
	Well logging, Flow test	Aug. 12 ~ Aug. 19	8	8	0
	Cementing, Wait on cement, Drilling out cement	Aug. 20 ~ Sep. 5	17	17	0
	HQ-WL Coring (914.59 m ~ 1031.89 m)	Sep. 6 ~ Oct. 3	28	28	0
	Preparation of Production test	Oct. 4 ~ Oct. 8	5	5	0
	Well logging, Production test	Oct. 9 ~ Oct. 17	9	9	0
	Flow test, Machine maintenance	Oct. 18 ~ Nov. 17	31	31	0
	Well logging	Nov. 18 ~ Nov. 19	2	2	0
	Preparation of Drilling	Nov. 20 ~ Nov. 24	5	5	0
	HQ-WL Coring (1031.89 m ~ 1049.84 m)	Nov. 25 ~ Dec. 4	10	10	0
	Miscellaneous work	Dec. 5 ~ Dec. 7	3	3	0
	Repairs of Brak drum, Inspection of Drilling tools	Dec. 8 ~ Dec. 16	9	9	0
	Well logging	Dec. 17 ~ Dec. 19	3	3	0
	<b>Total</b>		<b>144</b>	<b>144</b>	<b>0</b>
	<b>Grand Total</b>		<b>332</b>	<b>327</b>	<b>5</b>

Table 5.2.4 Details of Cementing of GTE-8

(1) Casing Pipe Cementing

Casing Step	1st step	2nd step	3rd step	4th step	Remarks
Nominal dia. x depth	10B x 29.60 m	8B x 142.20 m	6B x 421.00 m	4B x 752.50 m	
Volume of clearance between well wall and casing	1,174 L	1,919 L	3,796 L	5,241 L	
Q'ty of slurry pressed in	1,760 L	2,552 L	4,942 L	7,196 L	
Q'ty of cement used	2,217 kg	2,302 kg	4,007 kg	4,092 kg	API class G cement containing Silica four
Specific gravity	1.80	1.80	1.80	1.50	
Setting time	48 hr	40 hr	65 hr	64 hr	
Method	one-plug method	two-plug method	two-plug method	two-plug method	

(2) Plug Back Cementing

Depth of well bottom (m)	Purpose	Q'ty injected (kg)	Method	Cement head (m)	Result
56.00	Preventing cave-in	2,850	Squeezed through HQ rod	24.60	Success
121.50	Preventing lost circulation	2,180	Squeezed through HQ rod	88.00	Failure
137.51	Preventing lost circulation	4,800	Squeezed through HQ rod (2 times)	90.00	Success
203.00	Preventing lost circulation	1,200	Squeezed through HQ rod	145.20	Success
337.00	Preventing blow-out	2,800	Squeezed through HQ rod (2 times)	203.00	Success
435.94	Preventing lost circulation	1,279	Squeezed through HQ rod	361.54	Success
499.00	Preventing blow-out	2,132	Squeezed through HQ rod	445.24	Success
518.07	Preventing blow-out	1,535	Squeezed through HQ rod	420.00	Success
643.00	Preventing blow-out	7,103	Squeezed through BQ rod (2 times)	630.00	Success
706.92	Preventing blow-out	9,720	Squeezed through BQ rod (3 times)	650.00	Success
907.00	Preventing blow-out	13,211	Squeezed through BQ rod (4 times)	870.00	Success
907.00	Preventing blow-out	9,600	Plug method (2 times)	530.00	Success



Table 5.2-5 Lost Circulation and Drilling Mud of GTE-8

Depth of Lost circulation	Water level	Rocks	Mud circulation in/out (lost (-) or over (+) flow) (ℓ/min)	Drilling mud used
8.00 m		Siltstone	700/683 (-17)	Tel-stop (grain) 5 kg
61.80 m ~ 79.60 m	17 m	Shale & Siltstone	780/720 (-40 ~ -60)	Tel-stop (powder) 25 kg
119.22 m ~ 121.50 m	8 m	Shale & Fine sandstone	780/730 (-40 ~ -50)	Tel-stop (grain) 134 kg Tel-stop (powder) 100 kg Cement slurry 2400 ℓ
137.51 m		Fine sandstone	780/730 (-50)	Cement slurry 4090 ℓ
272.80 m ~ 279.34 m		Shale & Fine sandstone	660/677 (+8 ~ +17)	Tel-stop (powder) 4 kg Cement slurry 2051 ℓ
435.94 m		Fine sandstone	380/374 (-6)	Tel-stop (powder) 2 kg Cement slurry 1485 ℓ
472.94 m ~ 484.00 m		Fine sandstone	380/385 (+5)	Tel-stop (powder) 2 kg Cement slurry 2502 kg
484.00 m		Fine sandstone	380/0 (-380) Recovered by supplementing mud	Tel-stop (grain) 16 kg
484.00 m ~ 499.00 m		Fine sandstone	380/385 (+5)	Tel-stop (grain) 29 kg
501.69 m		Fine sandstone	120/370 (-250)	Cement slurry 2361 ℓ
518.07 m		Fine sandstone	110/260 (-150)	Cement slurry 2833 ℓ
643.24 m		Fine sandstone	110/0 (-110)	Cement slurry 7962 ℓ
706.92 m		Fine sandstone	350/0 (-350)	Cement slurry 10284 ℓ
907.00 m		Fine sandstone	110/0 (-110)	Cement slurry 26063 ℓ
915.45 m		Fine sandstone	150/0 (-150)	

Table 5.3-1 X-ray Diffraction Data of Altered Rock of GTE-8

Depth	Constituent Mineral	Quartz	K-feldspar		Chlorite	Sericite	Pyrite					Remark
	Rock											
506.90	Quartzose sand stone	⊙	Δ		●	●	●					○ Much ○ Common Δ Few ● Very rare
643.24	Quartzose sand stone	⊙	⊙		●	●						
872.10	Beccia	⊙				○						
906.49	Quartzose sand stone	⊙	Δ		●	Δ	●					
907.00	Quartzose sand stone	⊙	Δ		●	●						
928.00	Quartzose sand stone	⊙	⊙			●	●					
972.90	Quartzose sand stone	⊙					●					
1,023.59	Quartzose sand stone	⊙	●			●						

Table 5.3-2 Homegenized Temperature of Fluid Inclusion of GTE-8

Depth	Mineral	Homegenized Temperature (°C)
872.10 m	Vein quartz	121, 121, 126
1,023.59 m	Vein quartz	119, 119, 122, 122, 12.4, 13.4

Table 5.4-9 GTE-8 Well Logging (1)

(Drilling Depth 1,031.89 m, Casing Depth 752.50 m)

State	Static		Dynamic 1		Dynamic 2		Dynamic 3	
Date	Oct. 9, 1987		Oct. 12, 1987		Oct. 13, 1987		Oct. 14, 1987	
	Blow out stop Oct. 7 8:40 a.t. = 51 hr Well head press. 3.1 kg/cm <sup>2</sup> G		Well head press. 1.2 kg/cm <sup>2</sup> G Total flow-rate 45.6 t/h Steam flow-rate 1.2 t/h (at 0.4 kg/cm <sup>2</sup> G) Hot water flow-rate 44.4 t/h (at 0.3 kg/cm <sup>2</sup> G)		Well head press. 2.2 kg/cm <sup>2</sup> G Total flow-rate 35.9 t/h Steam flow-rate 1.1 t/h (at 0.35 kg/cm <sup>2</sup> G) Hot water flow-rate 34.8 t/h (at 0.3 kg/cm <sup>2</sup> G)		Well head press. 3.1 kg/cm <sup>2</sup> G Total flow-rate 23.5 t/h Steam flow-rate 0.7 t/h (at 0.17 kg/cm <sup>2</sup> G) Hot water flow-rate 22.8 t/h (at 0.2 kg/cm <sup>2</sup> G)	
Depth (m)	T (°C)	P (kg/cm <sup>2</sup> G)	T (°C)	P (kg/cm <sup>2</sup> G)	T (°C)	P (kg/cm <sup>2</sup> G)	T (°C)	P (kg/cm <sup>2</sup> G)
0	44.7	3.1	120.6	1.1	120.8	1.9	119.4	3.0
10	75.7	4.0	121.5	2.0	121.1	2.8	119.9	3.9
20	88.3	5.0	121.6	2.9	121.2	3.8	120.1	4.9
30	84.2	6.0	121.7	3.8	121.3	4.7	120.2	5.8
40	79.6	6.9	121.8	4.8	121.4	5.7	120.4	6.7
50	78.5	7.9	121.9	5.7	121.5	6.6	120.5	7.6
60	81.9	8.9	122.0	6.6	121.6	7.6	120.6	8.6
70	87.5	9.8	122.0	7.6	121.6	8.5	120.8	9.6
80	92.6	10.8	122.1	8.5	121.7	9.5	120.9	10.5
90	96.7	11.7	122.1	9.4	121.8	10.4	121.0	11.5
100	99.2	12.6	122.2	10.3	121.8	11.4	121.1	12.4
10	98.5	13.6	122.2	11.3	121.9	12.3	121.2	13.3
20	98.1	14.5	122.2	12.3	121.9	13.3	121.2	14.3
30	97.9	15.5	122.3	13.2	122.0	14.2	121.3	15.2
40	98.0	16.4	122.3	14.1	122.1	15.2	121.3	16.2
50	98.2	17.3	122.4	15.0	122.1	16.1	121.4	17.1
60	98.7	18.3	122.4	16.0	122.1	17.0	121.5	18.0
70	99.2	19.2	122.5	16.9	122.2	18.0	121.5	18.9
80	99.9	20.1	122.5	17.9	122.2	18.9	121.6	19.9
90	100.8	21.1	122.6	18.8	122.3	19.9	121.6	20.8
200	101.5	22.0	122.6	19.7	122.3	20.8	121.5	21.7
10	101.9	22.9	122.6	20.6	122.4	21.7	121.7	22.7
20	102.5	23.8	122.7	21.6	122.4	22.7	121.8	23.6
30	104.7	24.8	122.7	22.5	122.4	23.7	121.9	24.6
40	106.0	25.7	122.7	23.5	122.5	24.6	121.9	25.5
50	105.4	26.6	122.8	24.4	122.5	25.5	122.0	26.4
60	104.8	27.6	122.8	25.3	122.6	26.4	122.0	27.4
70	104.2	28.5	122.8	26.2	122.6	27.4	122.1	28.3
80	104.1	29.4	122.8	27.2	122.6	28.3	122.1	29.2
90	104.7	30.3	122.9	28.1	122.7	29.3	122.2	30.2
300	105.2	31.3	122.9	29.0	122.7	30.2	122.2	31.1

Table 5.4-9 GTE-8 Well Logging (2)

Depth (m)	Static		Dynamic 1		Dynamic 2		Dynamic 3	
	T (°C)	P (kg/cm <sup>2</sup> G)	T (°C)	P (kg/cm <sup>2</sup> G)	T (°C)	P (kg/cm <sup>2</sup> G)	T (°C)	P (kg/cm <sup>2</sup> G)
10	105.5	32.2	123.0	29.9	122.8	31.1	122.3	32.0
20	105.7	33.1	123.0	30.9	122.8	32.1	122.3	32.9
30	106.2	34.0	123.0	31.8	122.8	33.0	122.4	33.8
40	107.2	35.0	123.0	32.7	122.9	33.9	122.4	34.8
50	107.7	35.9	123.1	33.7	122.9	34.9	122.4	35.7
60	107.9	36.8	123.1	34.6	122.9	35.8	122.5	36.6
70	108.1	37.8	123.1	35.5	123.0	36.8	122.3	37.6
80	108.3	38.7	123.2	36.5	123.0	37.7	122.5	38.5
90	107.9	39.6	123.2	37.4	123.0	38.7	122.6	39.4
400	108.0	40.5	123.2	38.3	123.0	39.6	122.6	40.3
10	108.2	41.5	123.3	39.3	123.1	40.5	122.7	41.3
20	108.4	42.4	123.3	40.2	123.1	41.5	122.7	42.2
30	108.6	43.3	123.3	41.2	123.1	42.5	122.8	43.1
40	108.9	44.3	123.3	42.1	123.2	43.4	122.8	44.1
50	109.2	45.2	123.4	43.0	123.2	44.3	122.9	45.0
60	109.4	46.2	123.4	43.9	123.3	45.3	122.9	46.0
70	109.7	47.1	123.4	44.9	123.3	46.2	122.9	46.9
80	109.9	48.0	123.4	45.8	123.3	47.1	123.0	47.8
90	110.1	49.0	123.5	46.8	123.3	48.1	123.0	48.8
500	110.2	49.9	123.5	47.7	123.4	49.0	123.1	49.7
10	110.3	50.8	123.5	48.6	123.4	50.0	123.1	50.7
20	110.3	51.7	123.6	49.5	123.5	50.9	123.1	51.6
30	110.4	52.7	123.6	50.5	123.5	51.8	123.2	52.5
40	110.4	53.6	123.6	51.4	123.5	52.8	123.3	53.4
50	110.6	54.5	123.7	52.3	123.6	53.7	123.3	54.3
60	110.7	55.5	123.7	53.2	123.6	54.7	123.3	55.2
70	110.9	56.4	123.7	54.2	123.6	55.6	123.4	56.2
80	111.2	57.3	123.7	55.1	123.6	56.6	123.4	57.1
90	111.6	58.3	123.7	56.1	123.7	57.5	123.5	58.0
600	111.9	59.2	123.8	57.0	123.7	58.4	123.5	58.9
10	112.2	60.2	123.8	58.0	123.7	59.4	123.5	59.9
20	112.5	61.1	123.8	58.9	123.8	60.3	123.6	60.8
30	112.8	62.0	123.9	59.8	123.8	61.3	123.6	61.7
40	113.0	63.0	123.9	60.8	123.8	62.2	123.6	62.7
50	113.2	63.9	123.9	61.7	123.9	63.2	123.7	63.6
60	113.5	64.9	123.9	62.7	123.9	64.1	123.7	64.6
70	113.7	65.8	123.9	63.6	123.9	65.1	123.8	65.5
80	113.8	66.7	123.9	64.5	123.9	66.0	123.8	66.4
90	114.0	67.6	124.0	65.5	124.0	67.0	123.8	67.3
700	114.2	68.6	124.0	66.4	124.0	67.9	123.9	68.3

Table 5.4-9 GTE-8 Well Logging (3)

Depth (m)	Static		Dynamic 1			Dynamic 2			Dynamic 3		
	T (°C)	P (kg/cm <sup>2</sup> G)	T (°C)	P (kg/cm <sup>2</sup> G)		T (°C)	P (kg/cm <sup>2</sup> G)		T (°C)	P (kg/cm <sup>2</sup> G)	
10	114.6	69.5	124.0	67.3		124.0	68.8		123.9	69.2	
20	114.9	70.4	124.0	68.3		124.1	69.8		123.9	70.1	
30	115.2	71.4	124.0	69.3		124.1	70.7		123.9	71.1	
40	115.4	72.3	124.1	70.1		124.1	71.6		124.0	72.0	
50	115.5	73.2	124.1	71.0		124.1	72.5		124.0	72.9	
60	115.7	74.2	124.1	72.0		124.1	73.5		124.0	73.9	
70	116.0	75.1	124.1	72.9		124.1	74.4		124.1	74.8	
80	116.3	76.0	124.1	73.9		124.1	75.4		124.1	75.8	
90	116.2	76.9	124.2	74.8		124.2	76.3		124.1	76.7	
800	116.4	77.9	124.2	75.7		124.2	77.3		124.1	77.6	
10	116.7	78.8	124.2	76.7		124.2	78.2		124.1	78.6	
20	117.1	79.7	124.2	77.6		124.2	79.1		124.2	79.5	
30	117.6	80.7	124.2	78.5		124.2	80.1		124.2	80.5	
40	118.1	81.6	124.2	79.4		124.3	81.0		124.2	81.5	
50	118.6	82.5	124.2	80.4		124.3	81.9		124.2	82.4	
60	119.2	83.5	124.2	81.3		124.2	82.9		124.1	83.3	
70	119.8	84.4	124.2	82.2		124.2	83.8		124.1	84.2	
80	120.5	85.3	124.2	83.1		124.2	84.7		124.1	85.1	
90	121.3	86.2	124.2	84.0		124.2	85.6		124.1	86.0	
900	122.1	87.2	124.1	85.0		124.2	86.6		124.1	87.0	
10	123.1	88.1	124.0	86.0		124.2	87.5		124.2	87.9	
20	123.9	89.0	123.1	86.9		124.2	88.4		123.2	88.8	
30	122.6	89.9	122.3	87.8		123.1	89.3		120.9	89.7	
40	121.0	90.8	120.9	88.7		121.0	90.2		121.0	90.6	
50	120.2	91.7	120.9	89.6		121.0	91.1		121.3	91.5	
60	118.8	92.7	121.0	90.6		121.1	92.1		121.4	92.4	
70	118.8	93.6	121.0	91.5		121.2	93.0		121.5	93.3	
80	118.8	94.5	121.0	92.4		121.2	94.0		121.5	94.2	
90	118.8	95.5	121.0	93.3		121.3	94.9		121.5	95.2	
1000	118.6	96.4	120.2	94.2		121.4	95.8		121.2	96.1	
10	118.9	97.3	120.7	95.1		120.6	96.7		121.5	97.0	
20	120.0	98.2	120.6	96.0		121.1	97.6		121.4	97.9	
30	120.3	99.2	120.6	97.0		121.1	98.6		121.5	98.9	
31	120.3	99.3	120.6	97.1		121.1	98.7		121.5	99.0	

**Table 5.5-1 Analytical Result of Water Steam of GTE-8**

Well (Sampling date)		GTE-8 (Oct. 17, '87)
Liquid-vapour separate pressure (kg/cm <sup>2</sup> G)		0.2
Total gas in steam (vol %)		0.83
Gas composition	H <sub>2</sub> S (vol %)	2.60
	CO <sub>2</sub> (vol %)	90.6
	N <sub>2</sub> (vol %)	6.19
	H <sub>2</sub> (ppm)	2230
	CH <sub>4</sub> (ppm)	2540
	He (ppm)	63.9
	Ar (ppm)	1260

**Table 5.5-2 Analytical Result of Condensed Water of GTE-8**

Component		GET-8 (Oct. 15, '87)
Electrical conductivity	μS/cm	97.4
pH		5.50
SiO <sub>2</sub>	mg/l	0.07
Cl	mg/l	0.02
SO <sub>4</sub>	mg/l	11.3
Na	mg/l	0.03
K	mg/l	0.04
Ca	mg/l	<0.01
Mg	mg/l	<0.01
Fe	mg/l	<0.01
Al	mg/l	<0.01
As	mg/l	0.015
Hg	mg/l	1.1
total-CO <sub>2</sub>	mg/l	164
H <sub>2</sub> S	mg/l	51

Table 5.5-3 Analytical Result of Hot Water of GTE-8, GTE-6 and EGAT-1

Component		GET-8 (Oct. 15, '87)	GET-6 (May 18, '87)	EGAT-1 (May 18, '87)
Electrical conductivity	$\mu\text{S}/\text{cm}$	710	742	740
pH		9.36	9.3	9.2
SiO <sub>2</sub>	mg/l	173	158	144
Cl	mg/l	4.28	16.9	12.0
SO <sub>4</sub>	mg/l	76.7	24.8	44.2
H <sub>2</sub> CO <sub>3</sub>	mg/l	0.24		
HCO <sub>3</sub>	mg/l	233	236	289
CO <sub>3</sub>	mg/l	40.5	54	168
Na	mg/l	148	146	146
K	mg/l	14.2	15.8	14.0
Li	mg/l	0.37	0.32	0.32
Ca	mg/l	2.28	1.71	2.86
Mg	mg/l	0.06	0.16	0.22
Fe	mg/l	0.03	<0.13	<0.13
Al	mg/l	0.24	<1.1	<1.1
Mn	mg/l	0.03	<0.03	<0.03
B	mg/l	1.45	2.07	1.84
H <sub>2</sub> S	mg/l	4.8	28.5	25.5
TDS	mg/l	599	590	575
As	ng/l	9	33	24
Hg	ng/l	<0.5		

Table 5.5-4 Used Geothermometer

Geothermometer	Formula	Remarks
T SiO <sub>2</sub> (adia)	$t (^{\circ}\text{C}) = \frac{1533.5}{5.768 - \log \text{SiO}_2} - 273.15$	±2°C, 125°C ~ 275°C SiO <sub>2</sub> Concentration: mg/l
T SiO <sub>2</sub> (cond)	$t (^{\circ}\text{C}) = \frac{1315}{5.205 - \log \text{SiO}_2} - 273.15$	±0.5°C, 125°C ~ 250°C SiO <sub>2</sub> Concentration: mg/l
T Na-K (Truesdell, 1975)	$t (^{\circ}\text{C}) = \frac{855.6}{\log (\text{Na}/\text{K}) + 0.8573} - 273.15$	±2°C, 100°C ~ 275°C Na, K Concentration: mg/l
T Na-K (Fournier & Truesdell, 1973)	$t (^{\circ}\text{C}) = \frac{777}{\log (\text{Na}/\text{K}) + 0.70} - 273.15$	Na, K Concentration: mg/l
T Na-K-Ca (Fournier & Truesdell, 1973, 1974)	$t (^{\circ}\text{C}) = \frac{1647}{\log (\text{Na}/\text{K}) + \beta \log (\sqrt{\text{Ca}/\text{Na}}) + 2.24} - 273.15$	$\beta = 4/3$ for $\sqrt{\text{Ca}/\text{Na}} > 1$ and $t < 100^{\circ}\text{C}$ $\beta = 1/3$ for $\sqrt{\text{Ca}/\text{Na}} < 1$ or $t 4/3 > 100^{\circ}\text{C}$ Na, K, Ca Concentration: mol/l



Table 5.5-5 Geochemical Temperature of GTE-8, GTE-6 and EGAT-1

WELL	GTE-8 Oct. 15, '87	GTE-6 May 18, '87	EGAT-1 May 18, '87
T-SiO <sub>2</sub> (adia.)	161	157	152
T-SiO <sub>2</sub> (cond.)	170	164	159
T-Na/K (Truesdell)	183	196	183
T-Na/K (Fournier & Truesdell)	179	193	179
T-Na, K, Ca (Fournier & Truesdell)	196	206	193
Steam-Water ratio*	123 – 124	—	—
Downhole temperature	124	—	—

(Unit: °C)

\* Data of under 30 t/h of total flow rate was excluded.

## 6. Reservoir Evaluation

### 6.1 Method of Evaluation

In order to know the shape, extent, and structure of the reservoir, characteristics of fractures, and characteristics of geothermal fluid contained in the geothermal reservoir in the area, many surveys were carried out in the area and fruitful results were obtained. One such fruitful result was producing of geothermal fluid from the exploratory well GTE-8. Many kinds of well measurement and tests at the well, during producing of geothermal fluid, provided very important information for analyzing behavior of the reservoir.

Here, data collected from all the surveys and tests conducted are examined in an integrated manner and the reservoir is evaluated by computer simulation in terms of change of temperature and pressure in the reservoir if geothermal fluid is pumped from the well.

The procedure of analysis is as shown in the following Fig. 6.1-1.

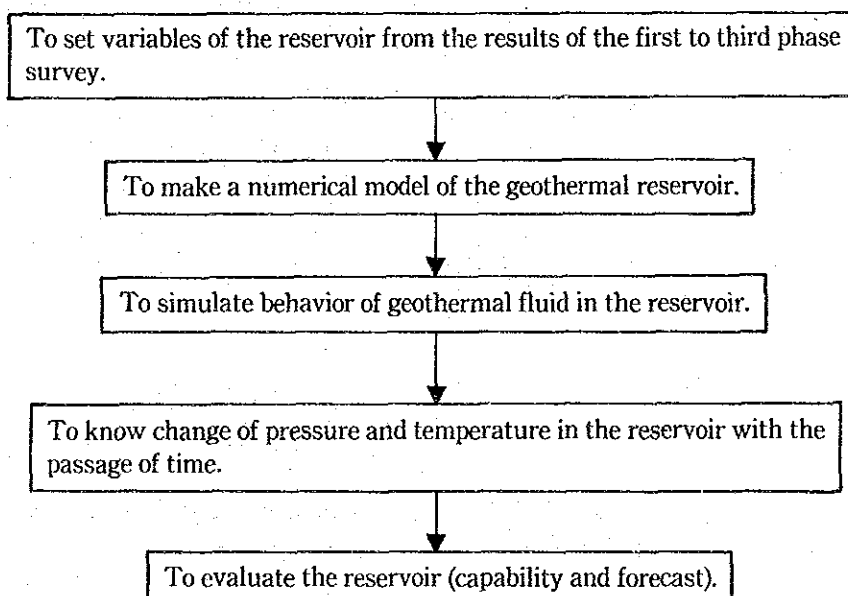


Fig. 6.1-1 Flow Chart of Reservoir Analysis

#### (1) Setting variables of the geothermal reservoir and making a numerical model of the reservoir

In order to determine the extent of the geothermal reservoir, shape, scale (vertical and horizontal), and geological structure of the reservoir are examined. As a result, the area with high temperature and bounded by faults is assumed to be the extent of the reservoir which is horizontally 3 km by 1.5 km and centered on GTE-8 (Fig. 6.1-2).

Its vertical extent is assumed to be to about 2 km depth based on results of drilling GTE-7 and GTE-8, although data obtained there is insufficient for precise estimation.

The numerical model of the reservoir consists of three by three grids horizontally and two layers vertically (Fig. 6.1-3).

In order to determine values for all variables of the numerical model of the reservoir reference

was made to results of all geophysical survey, well logs and production tests.

1) Characteristics of the reservoir

① Porosity

Porosity is set to a larger value than given by the core test because core samples are solid rock and lost circulation was not stopped easily.

The porosities of each layer are as follows:

Layer 1 : 7%  
Layer 2 : 10%

② Permeability

The results of production test at GTE-8 and conditions of lost circulation of the wells were examined to determine permeability. Permeability varies depending on cells and is between 3 and 20 m darcy. Permeability at the center of the reservoir is large and that at its fringe is small.

③ Heat conductivity, density and specific heat of rocks

Heat conductivity, density and specific heat of rocks do not vary much with type of lithology and lithofacies. Therefore, these are set to constant values in all cells as follows:

Heat conductivity:  $10 \times 10^{-3}$  cal/cm sec $^{\circ}$ C  
Density: 2.67 g/cm $^3$   
Specific heat: 0.25 kcal/kg $^{\circ}$ C

2) Characteristics of geothermal fluid

Characteristics of geothermal fluid in the reservoir are set similar to those of fluid from GTE-8.

Temperature of fluid is set to 125 $^{\circ}$ C. Viscosity and density of fluid are set by assuming chemical content to be similar to that of geothermal fluid from GTE-8.

3) Initial condition

Initial temperature and pressure distribution are set for each cell. Initial pressure is set to a constant value for each layer (Figs. 6.1-5~6).

4) Boundary conditions

A closed condition for the upper boundary and open conditions for other boundaries are adopted for simulation.

(2) Analysis of fluid behavior in the reservoir

Assuming conservation of mass and energy, the basic equations explaining movement of geothermal fluid in a reservoir are as follows:

Equation of mass conservation

$$\nabla \cdot \frac{k \rho}{\mu} \nabla P - G = \phi \frac{\partial \rho}{\partial t}$$

Equation of energy conservation

$$\nabla \cdot \frac{k \rho h}{\mu} \nabla P + \nabla \cdot \lambda \nabla T - q_L - G \cdot h = \frac{\partial}{\partial t} (\phi \rho h + (1 - \phi) \rho_r C_r T)$$

where

- k : permeability (m<sup>2</sup>)
- ρ : density of fluid (kg/m<sup>3</sup>)
- μ : viscosity of fluid (kg·sec/cm<sup>2</sup>)
- P : pressure (kg/cm<sup>2</sup>)
- G : production rate (t/h)
- φ : porosity
- t : time (sec)
- q<sub>L</sub> : heat loss (k cal)
- h : specific enthalpy (kcal/kg)
- ρ<sub>r</sub> : density of rock (kg/m<sup>3</sup>)
- Gr : specific heat of rock (kcal/kg°C)
- T : temperature (°C)
- λ : thermal conductivity (kcal/m·h·°C)

The equation of mass conservation signifies the following:

$$GW_{acc} = GWin - (GW_{out} + GW_{prod})$$

where,

- GW<sub>acc</sub> : geothermal water accumulated in a grid cell)
- GWin : geothermal water following into a grid cell
- GW<sub>out</sub> : geothermal water following out of a grid cell
- GW<sub>prod</sub> : production of geothermal water out of a cell

The equation of energy conservation signifies the following:

$$(\text{Energy change}) = (\text{Enthalpy in}) - (\text{Heat out by production})$$

where,

- (Energy change) : change of energy in a cell
- (Enthalpy in) : enthalpy flowing into and conducted into a cell
- (Heat out by production) : loss of heat by fluid production and flowing out of a cell

The simulation calculation was performed on the three dimensional reservoir model by applying these equations in computer analysis.

### (3) Calculation

The condition of production from the reservoir are as follows:

The production zone is at the center (i-2, j-2) of layer 2. Geothermal fluid with temperature of 125°C is produced continuously without reinjection of fluid. Pressure and temperature in the reservoir are calculated for ten years.

Production rates are set at seven stages: 75, 250, 500, 1,000, 1,250, and 1,500 t/h.

## 6.2 Flow Analysis by Computer Simulation

The results of simulation show that the production zone receives the greatest influence of production. Therefore, behavior of geothermal fluid at the production zone was given focus.

Initial temperature distribution is shown in Fig. 6.2-1 and the calculated results of temperature and pressure of each layer after ten years of production at 75, 750, 1,500 t/h are shown in Fig. 6.2-2 to Fig. 6.2-7.

Change of temperature and pressure with the passage of time is shown in Fig. 6.2-8.

The following are found from the results:

- ① Temperature distribution after ten years of production is the same regardless of production rate. Even if production rate is high, temperature drop in the production zone is as small as about 3°C from the initial temperature.
- ② Pressure distribution after ten years of production shows pressure drop at the center of the production zone regardless of production rate. The larger the production rate is, the more pressure drops. Pressure drop is not only inside of the production zone but also in the surrounding area.
- ③ Temperature and pressure change similarly with the passage of time regardless of production rate.

Temperature decreases linearly with time, and pressure drops very quickly after starting production and becomes stable after a short period of production.

## 6.3 Result of Analysis

Computer simulation of fluid behavior in the reservoir analyzed quantitative change of temperature and pressure during ten years of production.

Because simulation shows that temperature drop is small, but pressure drop is large, with a large amount of production, the production rate from the reservoir is governed by the pressure factor in the reservoir at the production zone.

Fig. 6.3-1 shows the relation between the production rate and pressure drop in the reservoir at the production zone. Production rate is linearly proportional to pressure drop.

Therefore, it is very important to control adequately the pressure drop in the reservoir for continuous production of geothermal fluid.

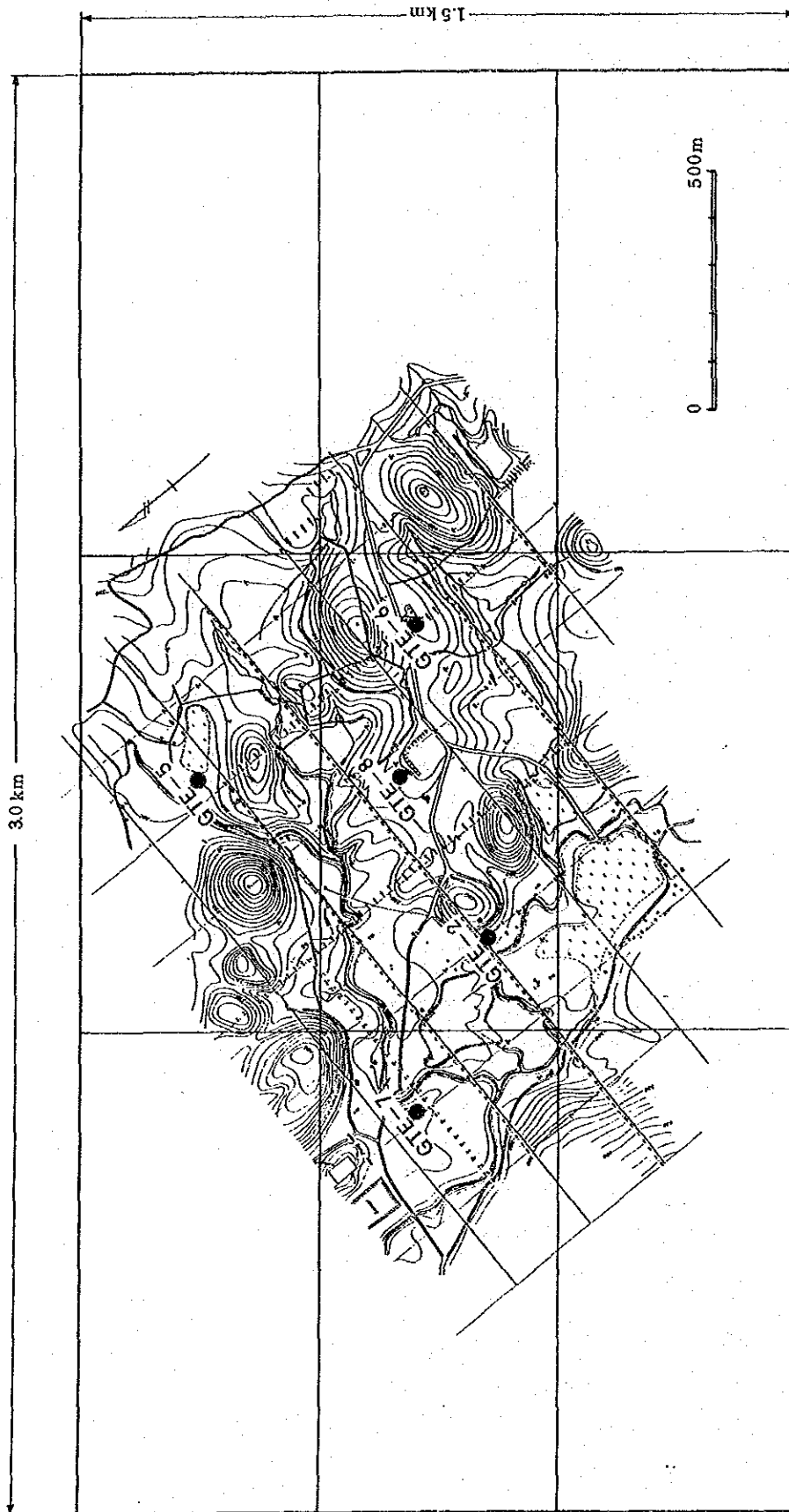
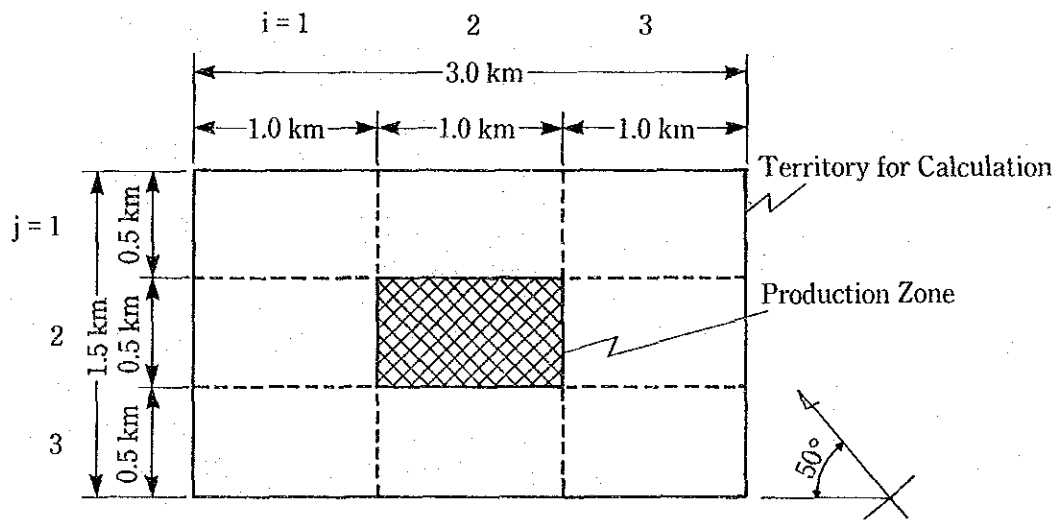


Fig. 6.1-2 Area of Reservoir Analysis

- Territory for Calculation { Horizontal: 1.5 km x 3.0 km  
Vertical: 2.0 km
- Number of Grid { Horizontal: 3 x 3  
Vertical: 2 Layer

- Horizontal Grid



- Vertical Grid

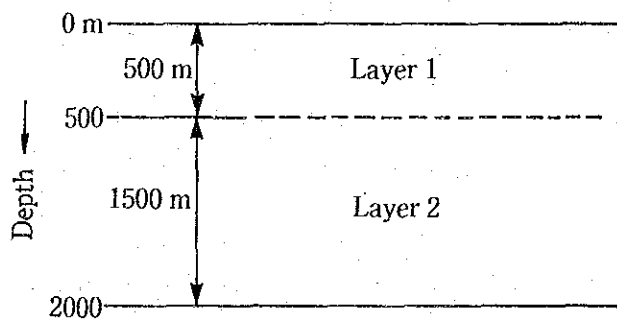


Fig. 6.1-3 Conceptual Reservoir Model



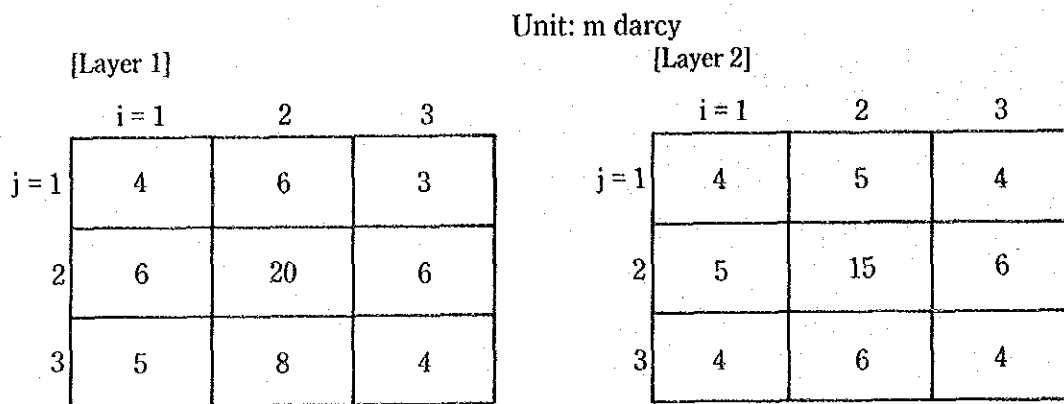


Fig. 6.1-4 Distribution of Permeability

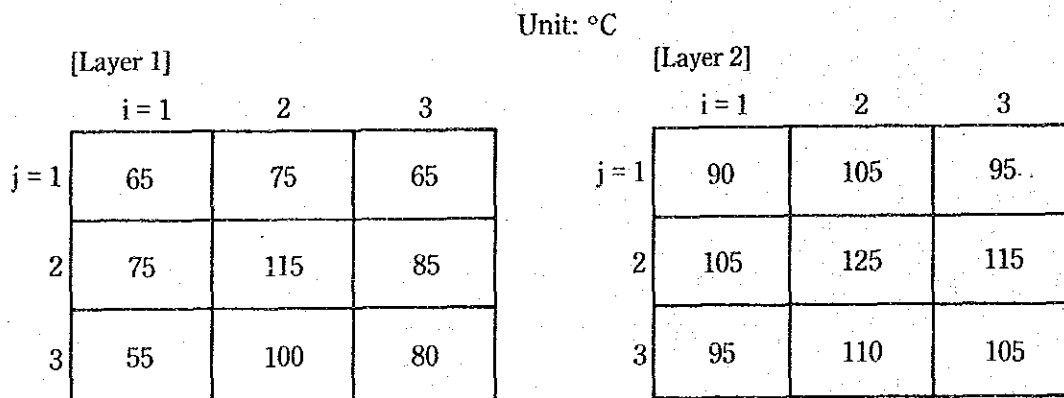


Fig. 6.1-5 Distribution of Initial Temperature

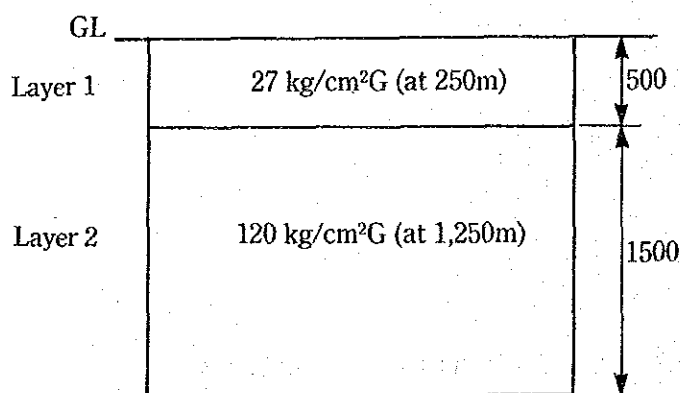


Fig. 6.1-6 Distribution of Initial Pressure

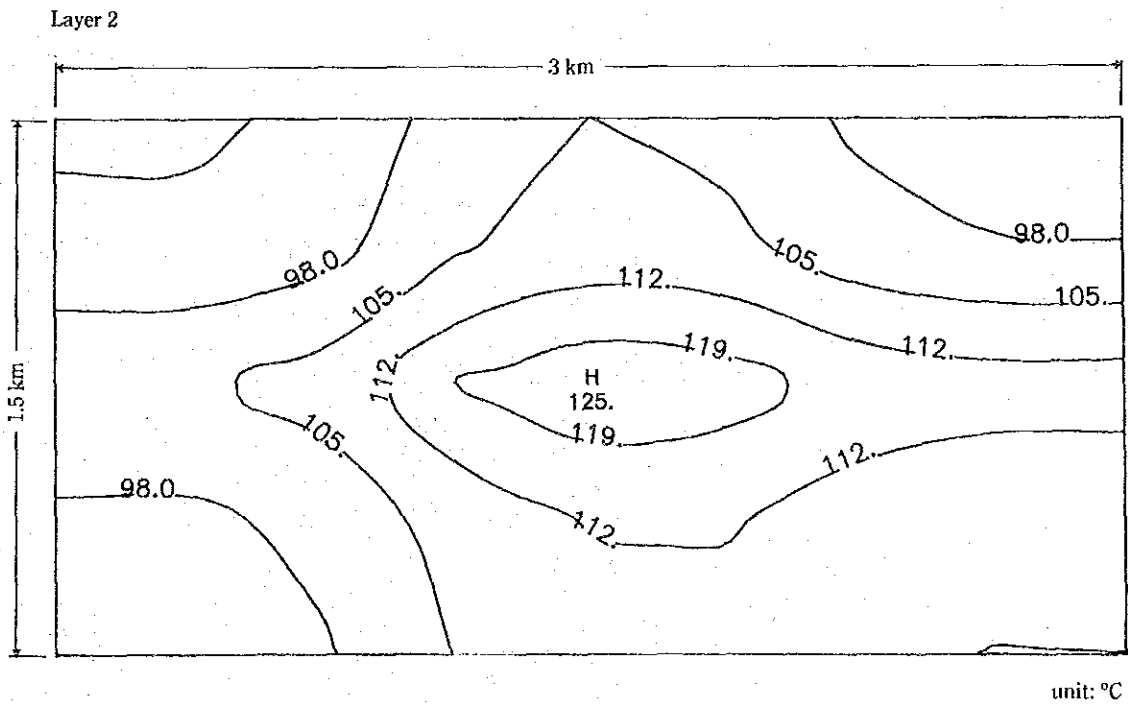
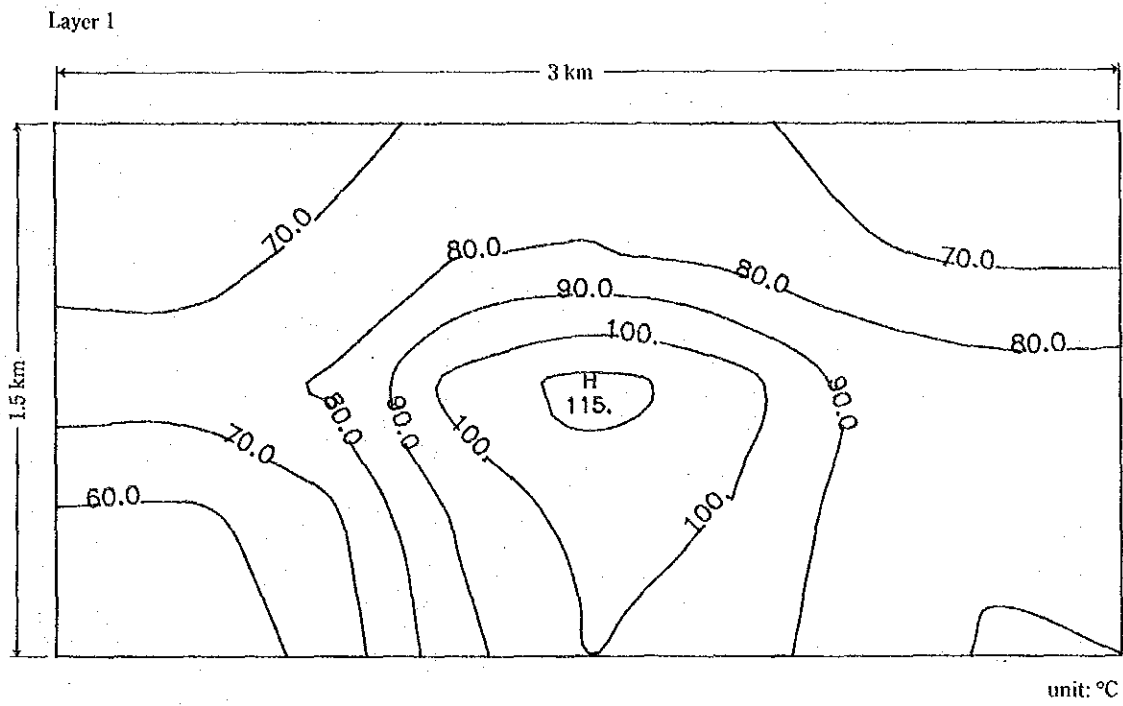


Fig. 6.2-1 Distribution of Initial Temperature

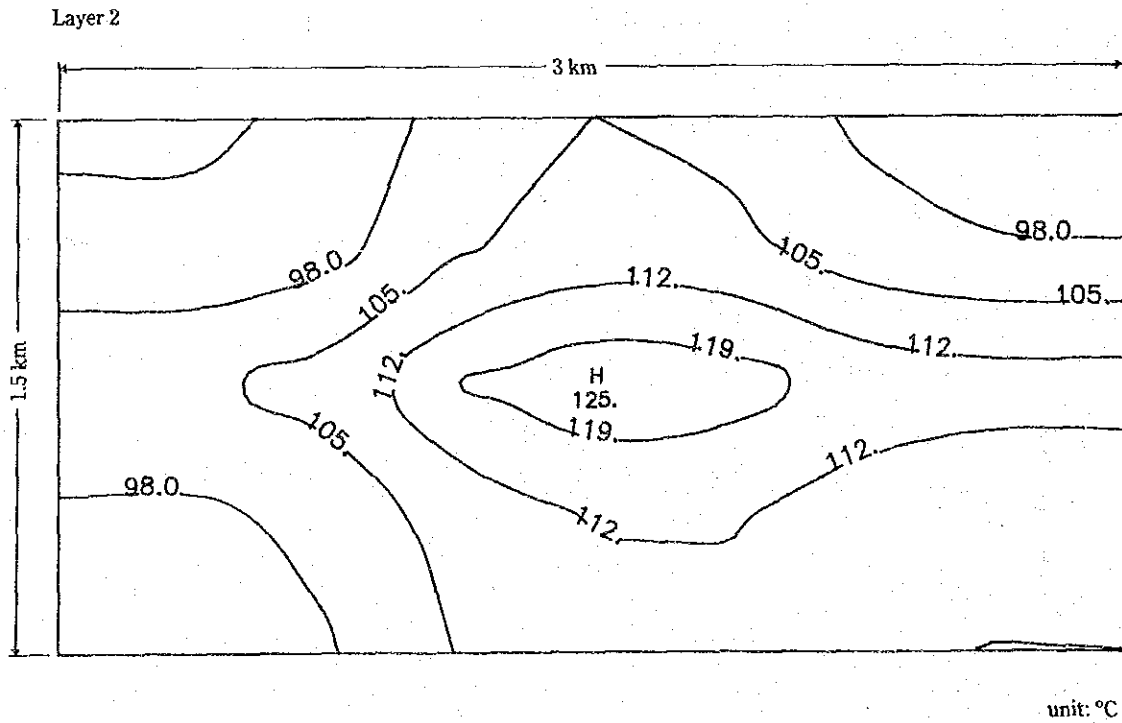
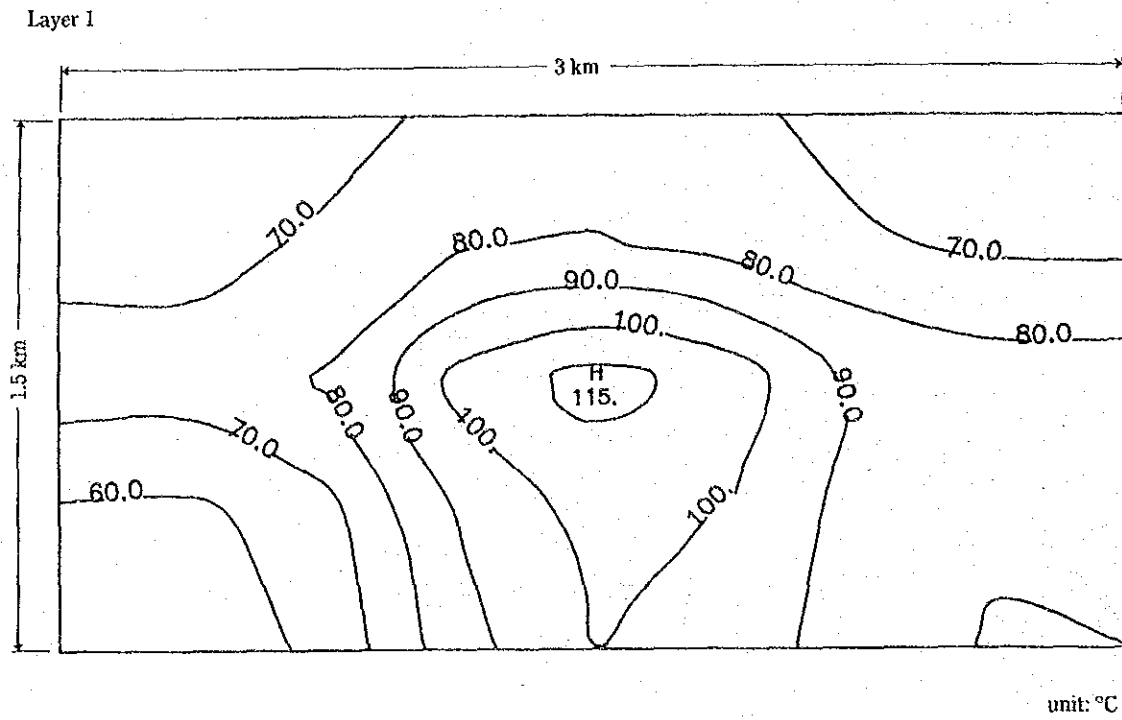
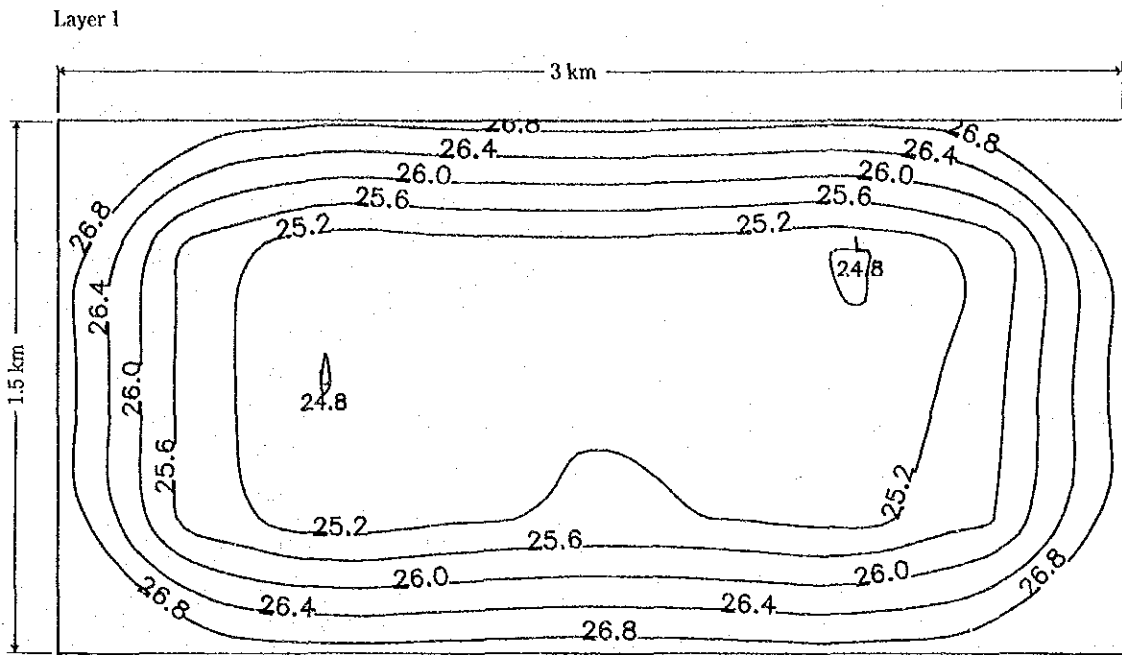
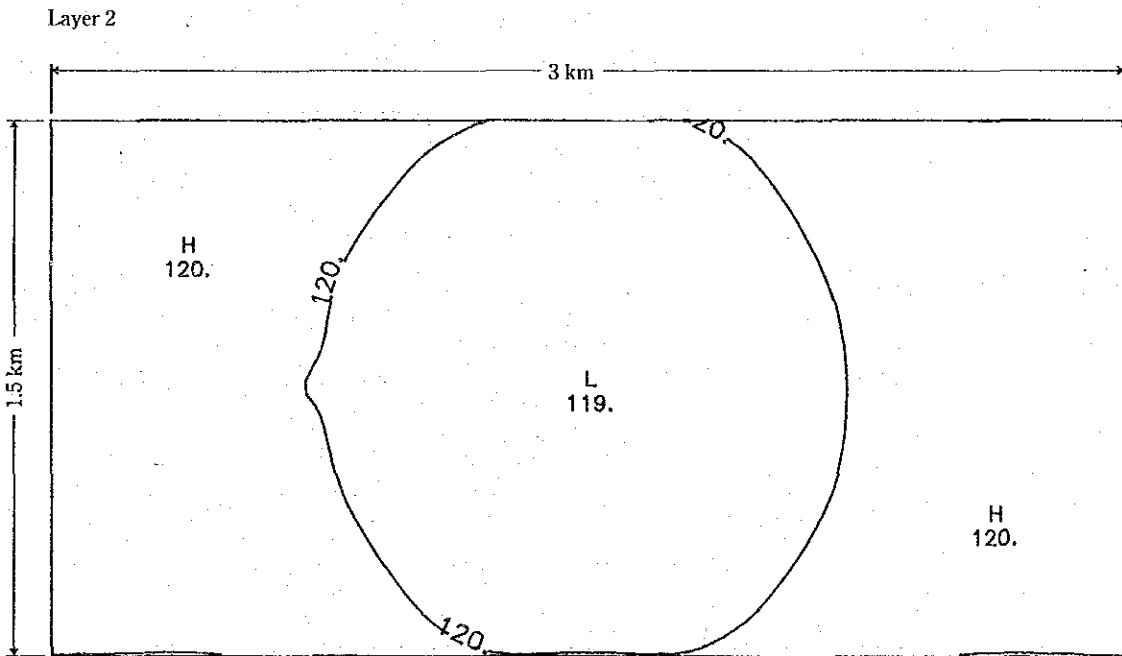


Fig. 6.2-2. Distribution of Temperature after 10 years — Rate of Production 75 t/h



unit: kg/cm<sup>2</sup>



unit: kg/cm<sup>2</sup>

Fig. 6.2-3 Distribution of Pressure after 10 years — Rate of Production 75 t/h

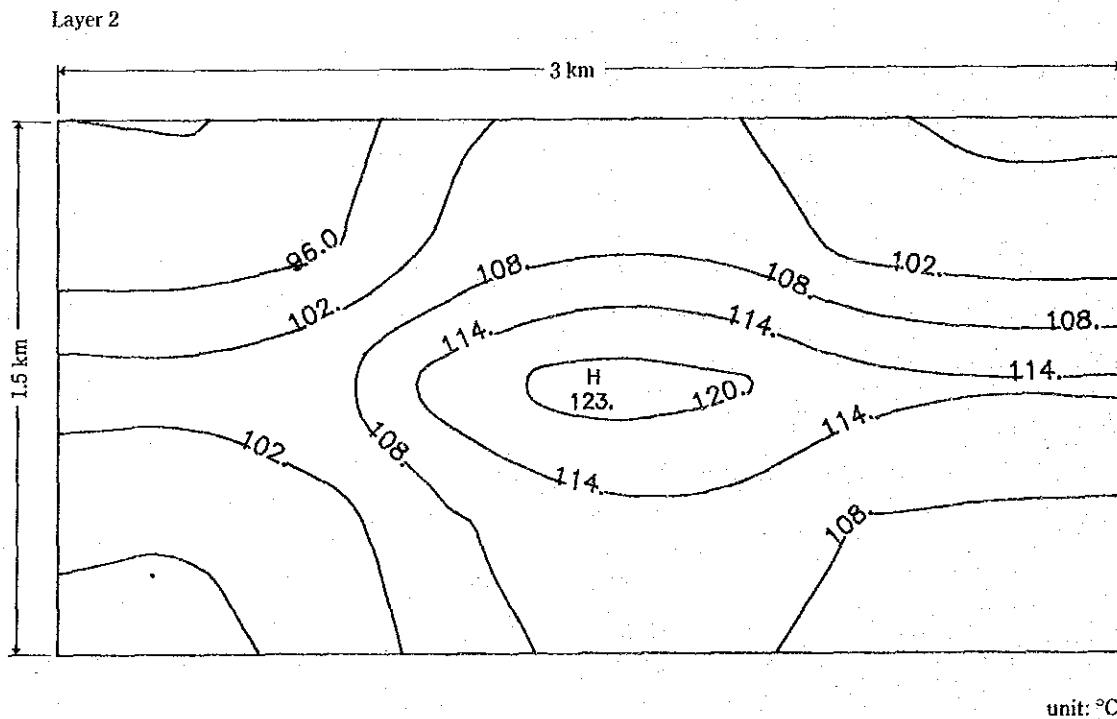
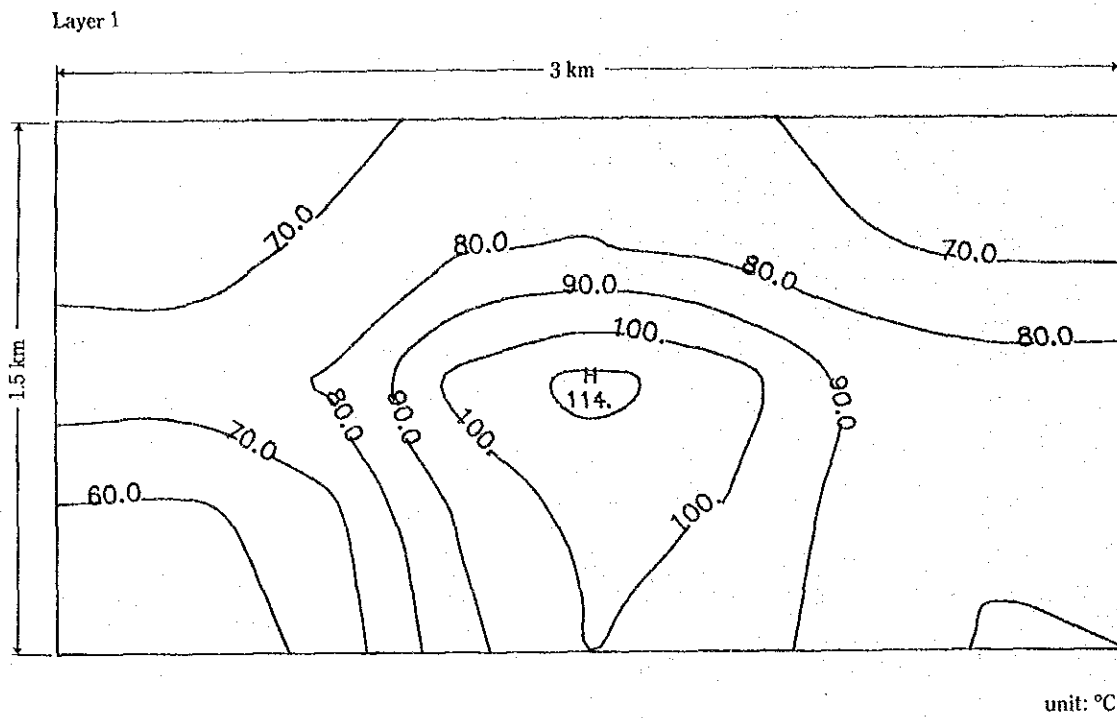


Fig. 6.2-4 Distribution of Temperature after 10 years — Rate of Production 750 t/h

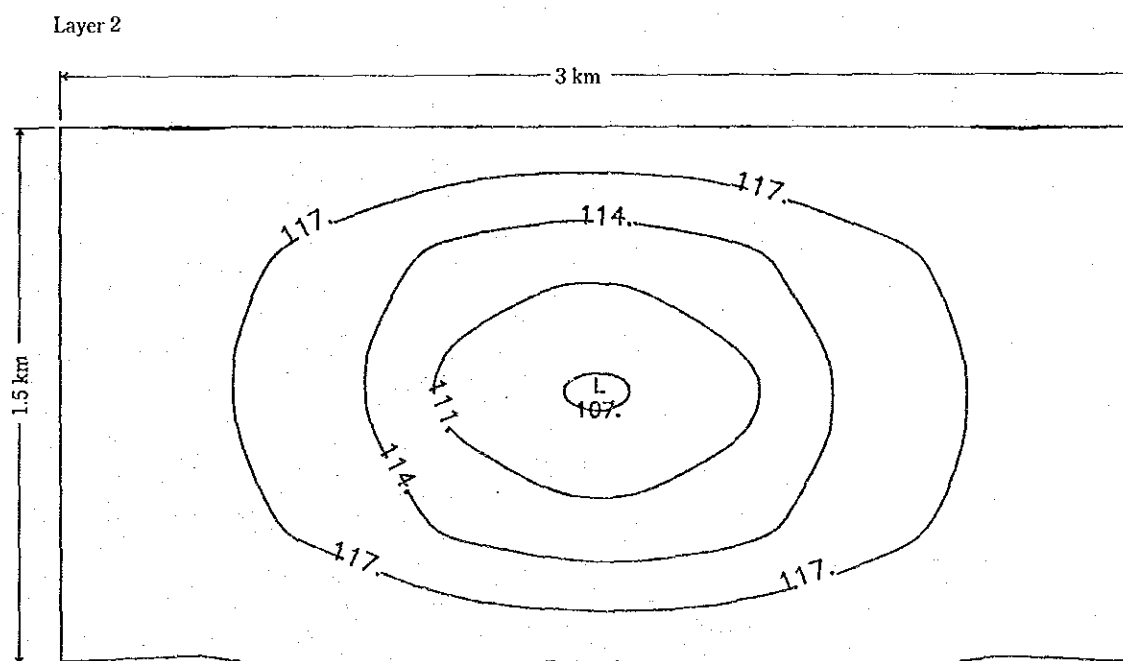
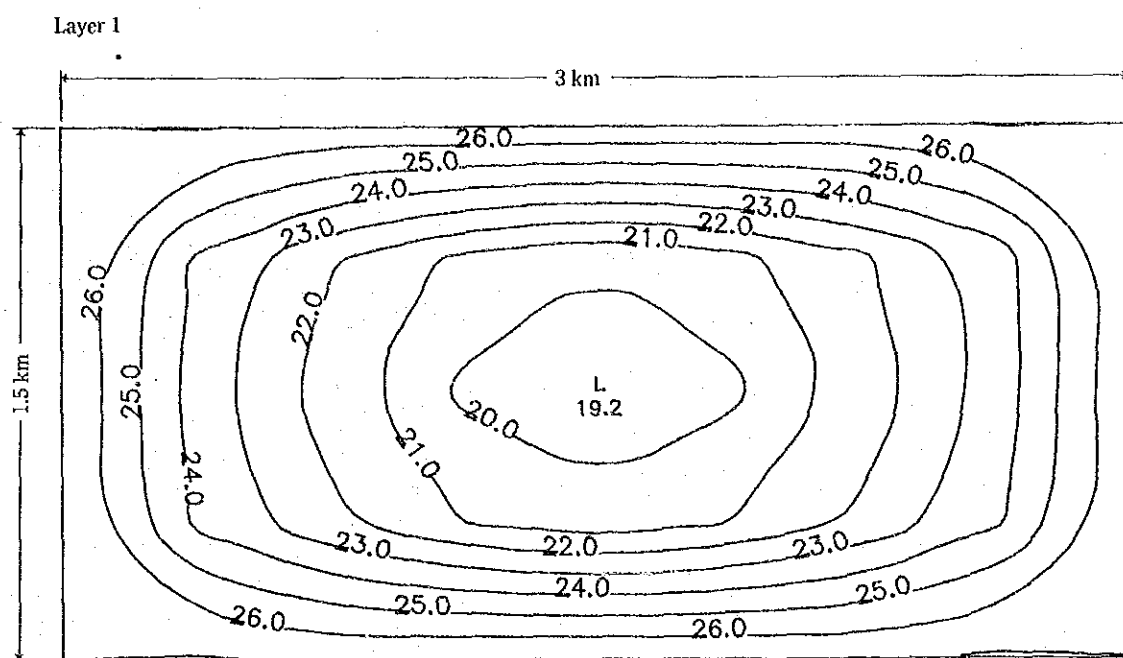


Fig. 6.2-5 Distribution of Pressure after 10 years — Rate of Production 750 t/h

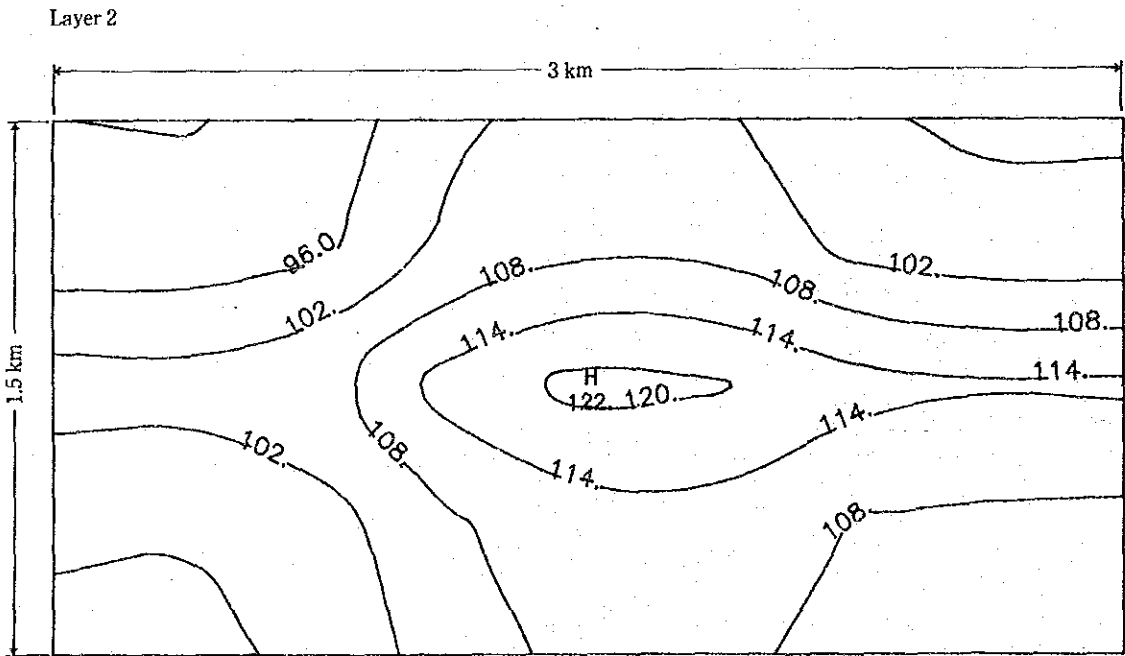
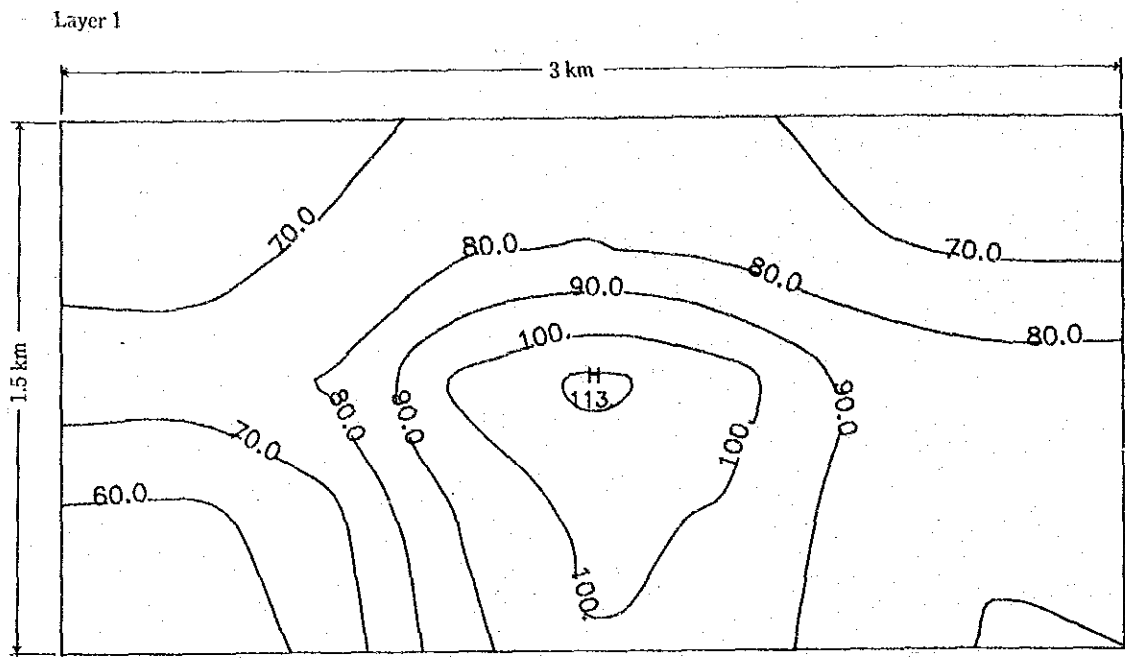


Fig. 6.2-6 Distribution of Temperature after 10 years — Rate of Production 1,500 t/h

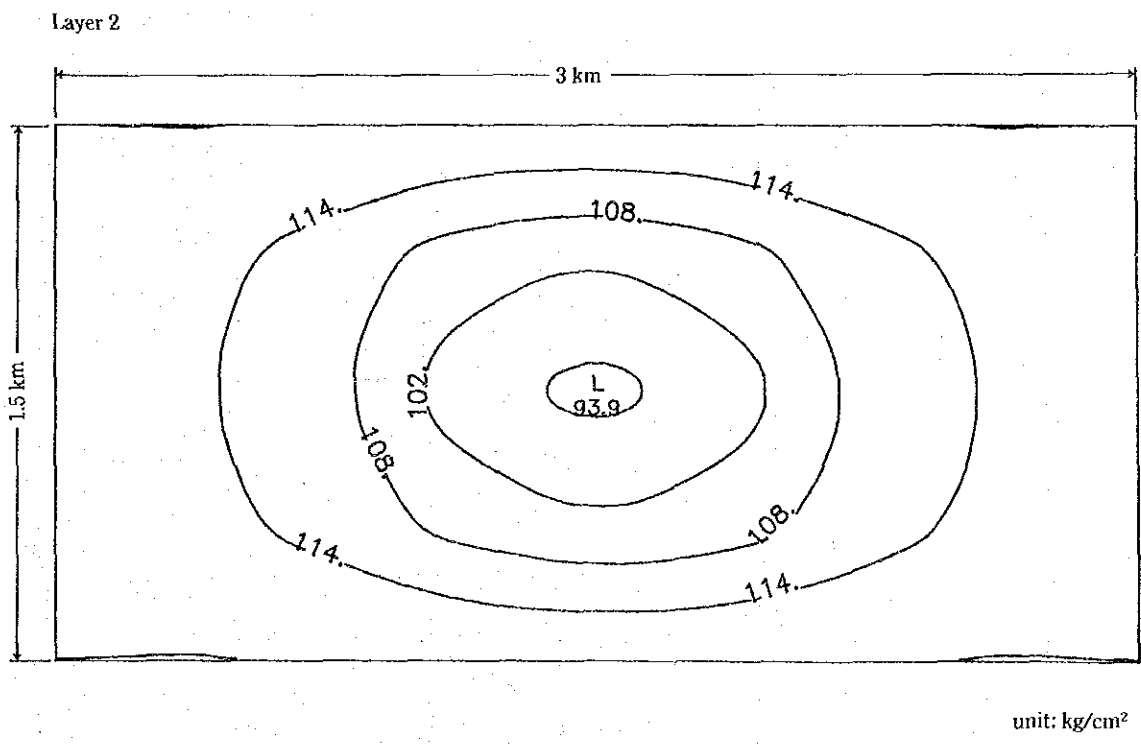
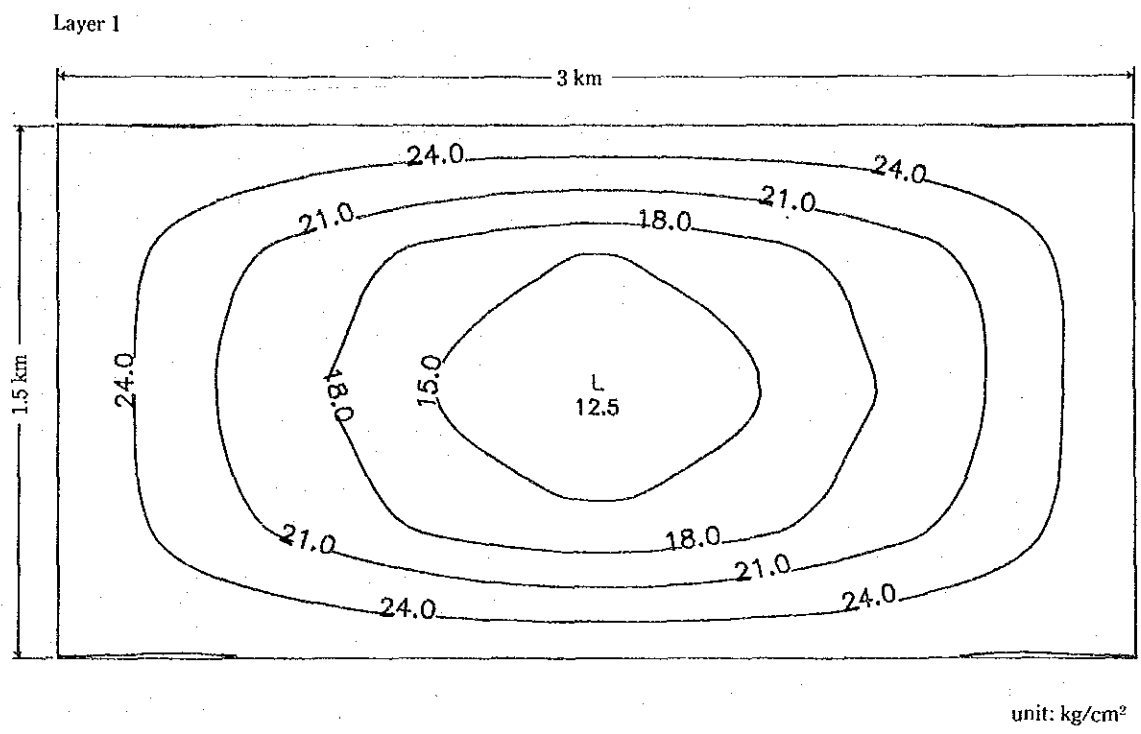


Fig. 6.2-7 Distribution of Pressure after 10 years — Rate of Production 1,500 t/h



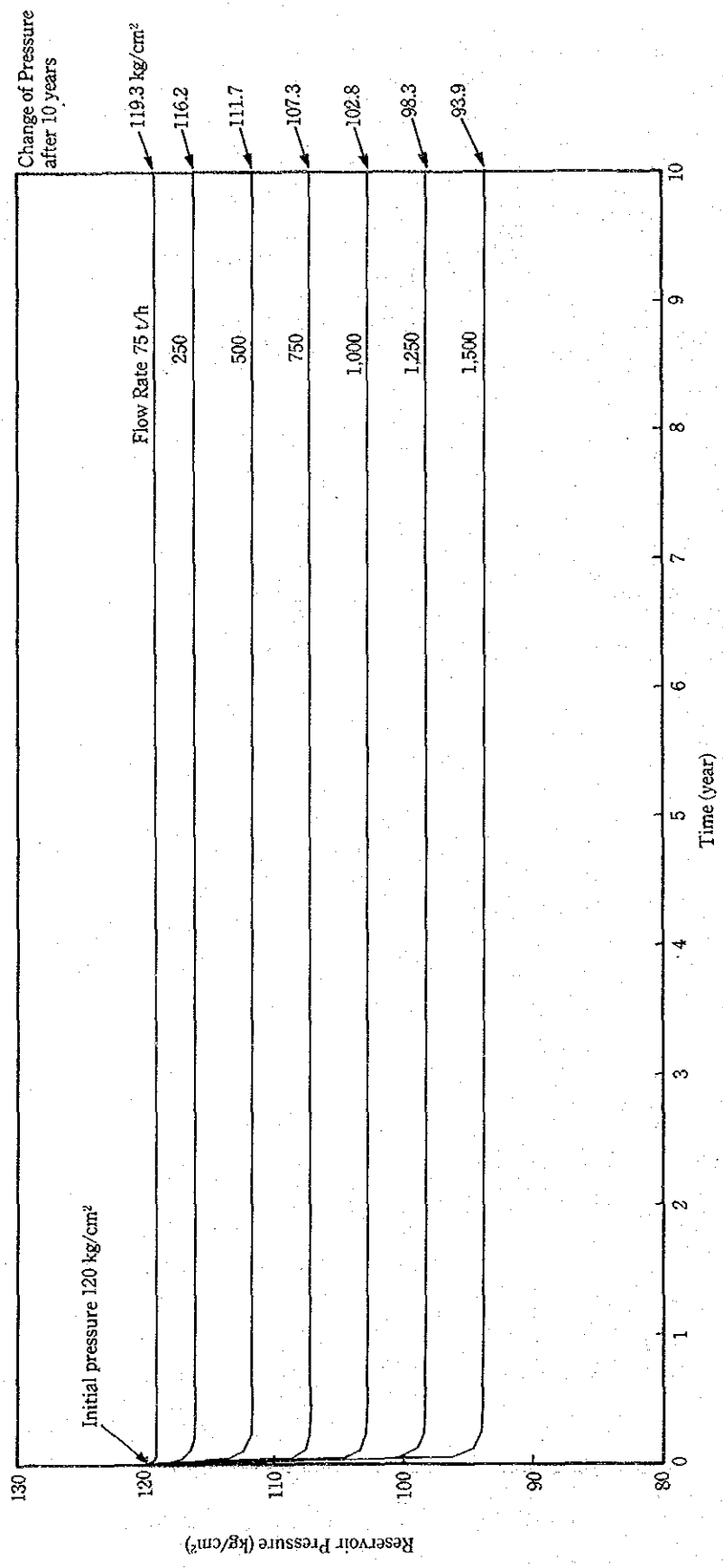
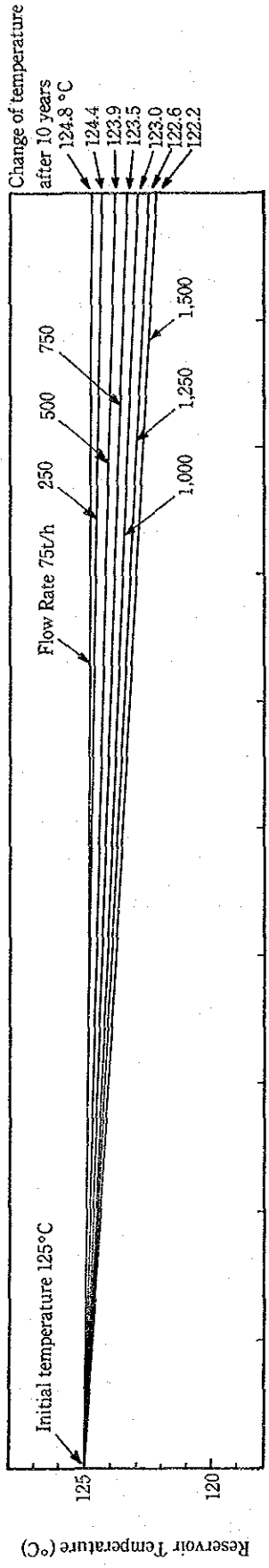


Fig. 6.2-8 Change of Reservoir Pressure and Temperature in Time in Production Zone

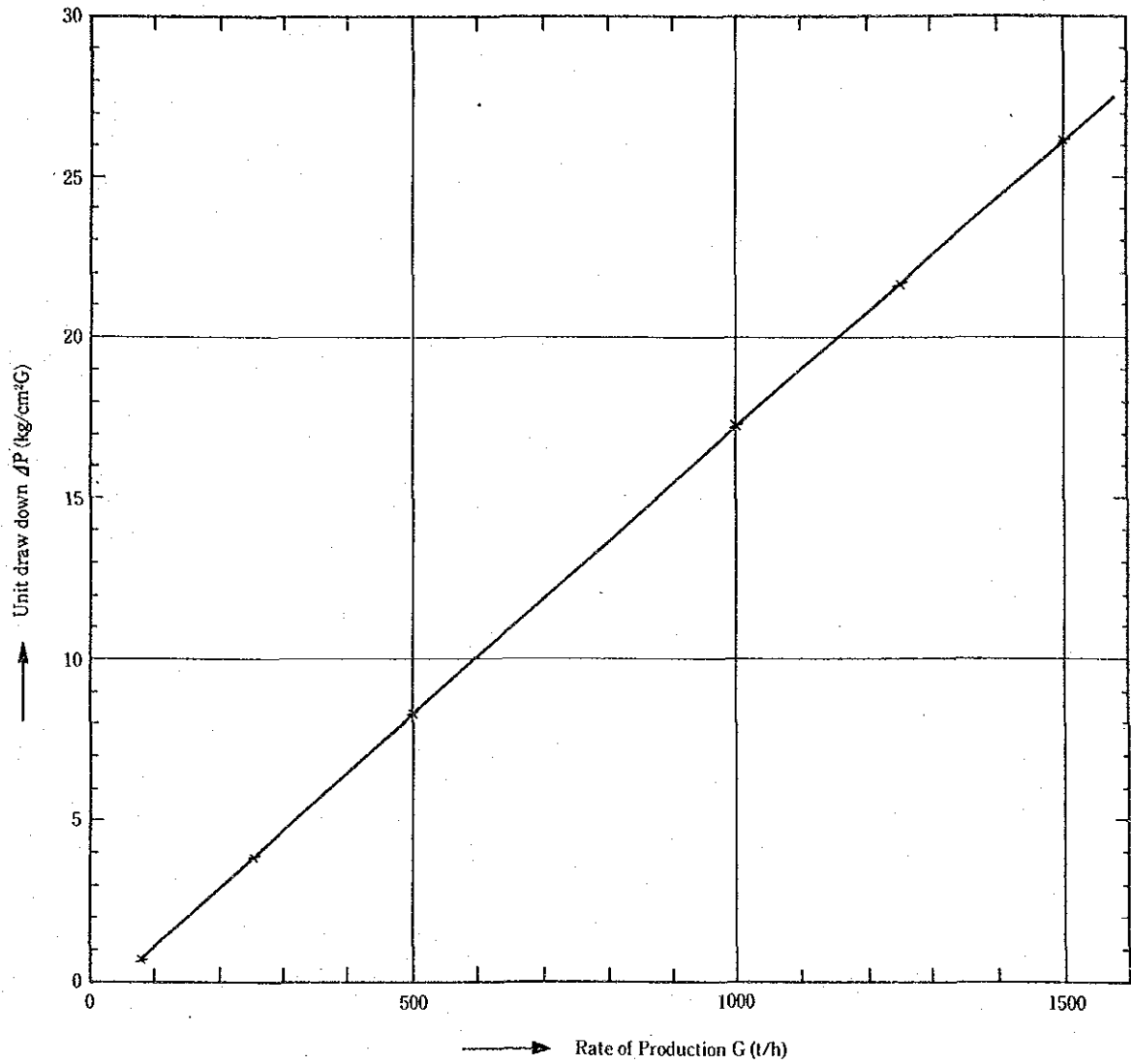


Fig. 6.3-1 Relation between Rate of Production and Unit Draw Down



### **III. SUMMARIZED EVALUATION OF RESULTS OF RURYVEY**



### III. SUMMARIZED EVALUATION OF RESULTS OF SURVEY

As stated in the preceding chapters pertaining to survey results in each year, the extent of the geothermal reservoir in the San Kampaeng area was detected by fault tracing survey applied by means of the Fingerprint method, in addition to 100m depth underground temperature survey carried out during 1985. After that, the exploratory well GTE-8 was drilled by EGAT during the period from 1986 to 1987 in the detected reservoir area. The purpose of the drilling is as follows:

- (1) To demonstrate whether the geothermal reservoir is rich in fractures and is filled by geothermal fluid,
- (2) To collect information and data necessary for reservoir analysis.

In order to evaluate possibility of geothermal development in the San Kampaeng area, it is necessary to obtain the following information furthermore:

- (3) To evaluate fluid temperature,  
and
- (4) To estimate the capacity of the fluid supply.

GTE-8 was drilled under technical guidance of a JICA engineer during the period from 1986 to 1987 as mentioned above. At the beginning of the drilling, the well was planned to drill to a depth of 1,500m, but owing to frequent lost circulation, encounter with hard rocks and shortage of drilling bits, drilling work was stopped at a depth of 1,049.84m. From the results of production logging and production test carried out before the end of drilling, necessary information and data for evaluation of the geothermal reservoir and possibility of geothermal development were obtained.

The results of the survey are as follows:

#### 1. Hydrologic Structure of the Reservoir

##### (1) Distribution of fractures

During the drilling, sometimes there occurred lost circulation and after that, occurred emission of geothermal fluid. From this fact, it has become clear that the geothermal reservoir detected by fault tracing survey and underground temperature survey is dominant in fractures. However, almost no fractures were found at the drilling of GTE-7 which is located northeast of the reservoir. Accordingly, the fractures are assumed to be developed in a limited area and be scarce at the surrounding area. Because of a few wells drilled in the reservoir area, it is difficult to clarify the extent of the geothermal reservoir in detail, but, judging from the results of fault tracing survey and underground temperature survey, it may have a dimension of about 500m wide and 1,000m long with the direction from northwest to southeast.

Considering from the results that down hole temperature of GTE-8 decreased, as well as no fractures at deeper than 930m, and also GTE-2 encountered with the fractures at about 300m in depth, but bore hole temperature decreased, as well as no fracture at deeper than 300m, it is

suggested that the fractures incline to east side. Although there remain some unsolved problems on reservoir structure yet, it can be said that the result of drilling of GTE-8 proved the existence of the geothermal reservoir rich in fractures in the San Kampaeng area.

(2) Permeability of the fractures

Production logging in a well is carried out to obtain productivity index and transmissibility related to permeability of the fractures.

During the drilling, GTE-8 encountered with fractures at depths of 707m, 907m and 915m to 930m and geothermal fluid emitted from those fractures. In order to continue drilling, fractures at 707m and 907m were filled by cement. Therefore, production logging and production test were carried out while geothermal fluid was emitting from the fractures at depths of 915m to 930m. As mentioned before, pressure difference ( $\Delta P$ ) and production difference ( $\Delta G$ ) were measured to obtain the value of production index (PI). Transmissibility (Kh) could be obtained from calculation using the value of productivity index. The calculated transmissibility shows 9 darcy-m ( $9 \times 10^{-12} m^3$ ), but this value is multiplier of permeability (K) and effective thickness of formation with fractures (h), then this value can not be used for judging the relative scale of permeability of fractures. On the other hand, productivity index reflects the relative scale of the permeability of fractures in some degree. The calculated productivity index indicated 17t/h/kg/cm<sup>2</sup> which means that by lowering (or raising) pressure each 1kg/cm<sup>2</sup>, 17t/h of the produced fluid increases (or decreases). Thus, figure of 17 of the productivity index shows fairly good permeability of the fractures. This value was that obtained from the fractures developed between 915m and 930m in depth. Besides them, GTE-8 encountered with another fractures with emission of geothermal fluid at deeper than 500m as shown in the following table:

Depth	Amount of discharge of geothermal fluid
707m	68t/h
907m	58t/h
(915m-930m)	(45t/h)

Because all geothermal fluid emitted from the fractures are assumed to be under the same pressure condition as that of 915m to 930m in depths, productivity indexes of the fractures at 707m and 907m may take almost the same values as that of 915m to 930m in depths. This means that many fractures are developed not only at deeper than 500m, but those have good permeability. From the drilling of GTE-8 which is located near the center of the geothermal reservoir detected by fault tracing survey and underground temperature survey, it was found that the reservoir is composed of rocks rich in fracture with high permeability.

As conclusion, the geothermal reservoir in the San Kampaeng area is evaluated to have favourable hydrologic structure.

## 2. Possibility of Geothermal Development

### (1) Evaluation of fluid temperature

Among geochemical thermometers using chemical components as indicators, silica geothermometer is widely used for detecting fluid temperature in depths.

Silica contents of thermal water collected from the geothermal manifestation area in San Kampaeng were analyzed by the Thai Team before commencement of this project, indicating temperature of 160°C as that of geothermal fluid in depths.

In this time, silica contents of hot water emitted from GTE-8, GTE-2 and EGAT-1 wells were collected and analyzed by the JICA Study Team, indicating temperature of 152-161°C. The values coincide with that obtained by the Thai Team.

However, the actual maximum temperature measured in GTE-8 was 125°C at 900m level in depth. So, it is expected that higher fluid temperature will be obtainable if deep drilling will be undertaken in future.

Considering geothermal power generation from standpoint of fluid temperature. It must be said that geothermal fluid in the San Kampaeng area is essentially not available for power generation using geothermal steam. However, recently, binary-cycle system power generation has been developed for practical use. This is a system that secondary fluid characterized by low boiling temperature is used as medium which plays a role as heat exchanger. In this system, fluid temperature ranging from 180°C to 80°C can be used for power generation. So, it can be said that geothermal fluid produced from geothermal reservoir in the San Kampaeng area has sufficient temperature necessary for binary-cycle system power generation. Fig.1 shows output of electricity obtained from 1t/h of fluid with temperature ranging from 160°C to 80°C. From Fig.1, it is pointed out that about 4kW of output will be obtained from 1t/h of geothermal fluid with temperature of 125°C in the San Kampaeng area. This means that about 180kW power generation will be expected by using 45t/h of geothermal fluid which is emitting from GTE-8 at present.

However, in case of commercial power generation, a large scale of output will be required. Therefore, prior to planning to construct a commercial power plant in the San Kampaeng area, it is necessary to examine the following problem: how much output can be expected, that is, how much geothermal fluid can be produced from the geothermal reservoir in the San Kampaeng area.

These are the problem closely connected with estimation of capacity of fluid supply from the geothermal reservoir, namely evaluation of geothermal reservoir.

### (2) Capacity of fluid supply

When geothermal fluid is produced from geothermal reservoir, there occur changes of temperature and pressure according to amount of fluid supply from the surrounding area.

As the values of transmissibility, initial temperature and pressure were obtained from the production logging carried out in GTE-8, changes of temperature and pressure with time according to amount of production was predicted by method of computer simulation.

The result of simulation was described in the preceding chapter already. Then, here, some supplementary explanation about the values used for calculation is added briefly.

#### 1) Permeability



Permeability of the production zone (Layer 2,  $i=2, j=2$ ) was set up as 15 m darcy. This is due to the following reason:

The value of transmissibility (Kh) calculated from data of GTE-8 was 9 darcy m, namely  $9 \times 10^{-12} \text{m}^3$ . As the thickness of the production layer (Layer 2) is regarded as 1,500m, K takes the following value:

$$K = \frac{9 \times 10^{-12} \text{m}^3}{1,500\text{m}} = 6 \times 10^{-15} \text{m}^2 = 6 \text{ m darcy}$$

However, GTE-8 encountered with several fractures during drilling, so, permeability of Layer 2 was regarded as 15 m darcy which is as much as 2.5 times of 6 m darcy.

Compared to the production zone, permeabilities at the surrounding areas take smaller values. This is due to the reason that those areas are considered to be scarce in the fractures.

## 2) Pressure

As mentioned already, pressure of Layer 1 was set up as  $27 \text{kg/cm}^2$  at 250m in depth and that of Layer 2 as  $120 \text{kg/cm}^2$  at 1,250m. This is due to the following reason:

According to measurement of static pressure in GTE-8, it was recorded that pressure at 250m in depth which is intermediate point of Layer 1 shows  $27 \text{kg/cm}^2$ , and at 1,000m,  $96 \text{kg/cm}^2$ . The pressure increases linearly along the line connecting  $27 \text{kg/cm}^2$  and  $96 \text{kg/cm}^2$ , showing  $120 \text{kg/cm}^2$  at 1,250m in depth which is intermediate point of Layer 2 (Fig. 2). This is the reason why pressures of Layer 1 and 2 were set up as  $27 \text{kg/cm}^2$  and  $120 \text{kg/cm}^2$  respectively.

As described already, reservoir performance with time according to amount of production of geothermal fluid was shown by changes of temperature and pressure drop after 10 years. Among examples, in case of production of fluid of 75t/h,  $1 \text{kg/cm}^2$  pressure drop was shown while almost no temperature change. On the other hand, in case of production of 1,500t/h,  $26 \text{kg/cm}^2$  pressure drop was shown while about  $3^\circ \text{C}$  temperature drop.

As mentioned above, relatively a large scale of pressure drop was shown in this simulation. This is due to the reason that, although geothermal fluid is supplied from the surrounding areas to production zone horizontally, permeabilities of the surrounding areas was set up on a small scale.

However, the actual reservoir structure in the San Kampaeng area is considered to be characterized by vertical fractures, along which geothermal fluid is supplied from depths in form of up-flow. Accordingly, although there is structural difference between reservoir model used for simulation and actual reservoir structure, the same scale of pressure drop as in the reservoir model will be shown in the actual geothermal reservoir because lateral flow in case of reservoir model is regarded as vertical up-flow along fractures in the actual reservoir. Therefore, so far as pressure drop is concerned, it may be considered that the result of simulation can be applied for the geothermal reservoir in the San Kampaeng area.

On the contrary, since fluid supply is characterized by up-flow in the San Kampaeng area, it is expected that fluid temperature will be kept constant or be increased even if a large amount of fluid is produced.

GTE-8 is characterized by high well-head pressure, showing about  $4 \text{kg/cm}^2$  as shut-in pressure. Then, it is possible to use 75t/h of geothermal fluid for 300kW power generation without installing down-hole pump. However, because of pressure drop with increase of amount of production, it is necessary to install down-hole pump in order to keep the flow rate of production constant. It is

said that, in general, down-hole pump is installed at depths of 300m to 500m. If it is installed at depth of 300m, the pressure at depth of 300m is regarded as  $32\text{kg/cm}^2$ . Accordingly, it is estimated that pressure drop by production must be kept within about  $25\text{kg/cm}^2$ . Considering amount of production from standpoint of pressure drop, maximum production rate is regarded as 1,500t/h which results in pressure drop of  $26\text{kg/cm}^2$ .

Of course, it is possible to produce geothermal fluid more if down-hole pump is installed deeper than 300m. However, since an excess of water lift by pumping brings pressure drop which goes on increasing, 1,000t/h of production is regarded as reasonable figure, which corresponds to 4,000kW of output. This is the result of estimation of limit of production, namely capacity of fluid supply to keep the flow rate or output stable.

As higher fluid temperature than  $125^\circ\text{C}$  is expected to be obtainable by deep drilling, it can be said that 5,000kW binary-cycle system power generation is obtainable in the San Kampaeng area by using 1,000t/h of geothermal fluid.

From the results mentioned above, it is concluded that 5,000kW power generation can be obtained by utilizing the geothermal fluid from the geothermal reservoir in the San Kampaeng area. However, the problem is whether such development is economically viable or not.

In the case of generation by the binary-cycle system, design of equipment, including the heat exchanger, becomes complicated since secondary fluid is used as the medium. Also, auxiliary power consumption is greater than in the case of steam generation. Consequently, facility cost including turbine, generator and subsequent power cost at the transmission terminus is relatively higher for the binary-cycle system than for steam power generation. Furthermore, as in the case where the geothermal reservoir is to be developed as a power source in an area such as San Kampaeng requiring well drilling to produce geothermal fluid, the cost for drilling and installation of down-hole pump(s) must also be considered. This requirement additionally increases overall construction cost and auxiliary power consumption, further raising power cost at generation.

On the basis of the points presented above, there are a number of constraints to the economic utilization of geothermal fluid in the San Kampaeng area for commercial power generation.

However, if this geothermal resource can be utilized in a multipurpose manner, i.e., using discharged hot water from a binary power plant for crop drying, tourism, irrigation etc., its socio-economic advantages will certainly off set the economic constraints, if any, of commercial power generation only.

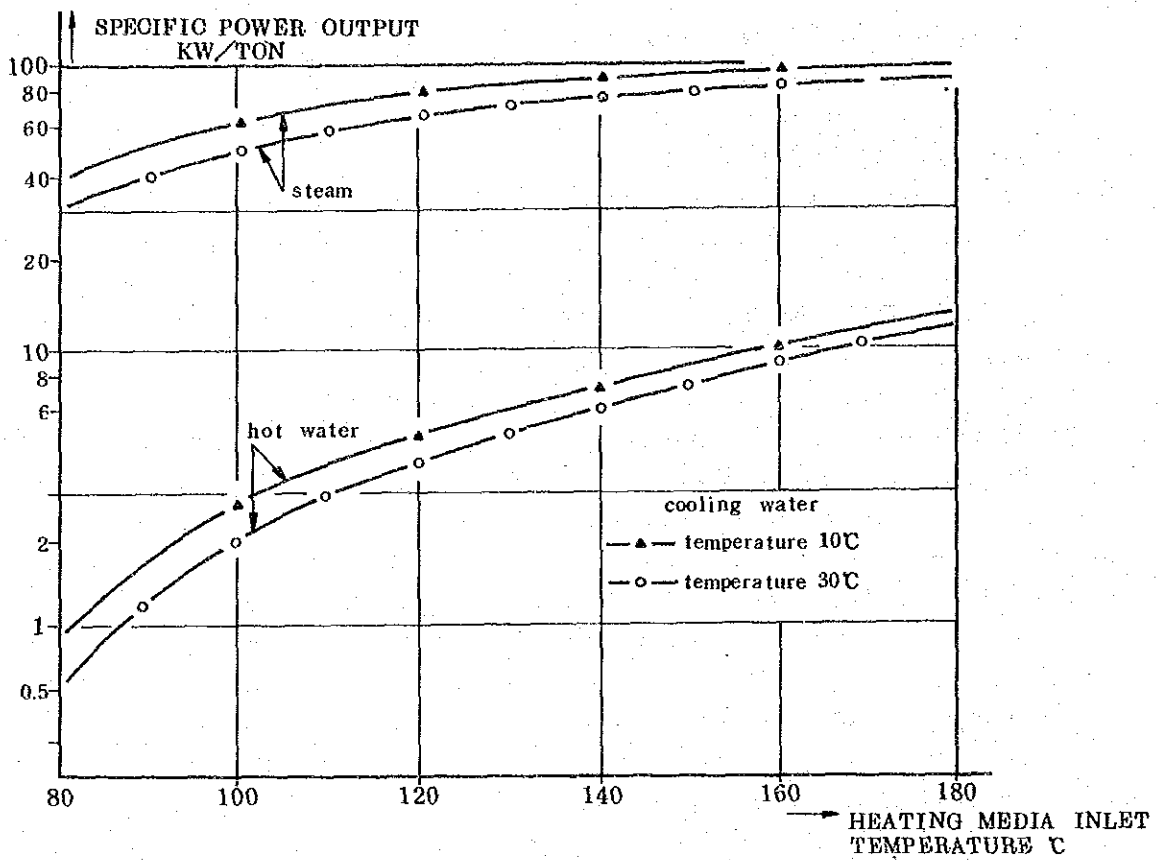


Fig. 1 OEC Specific Performance

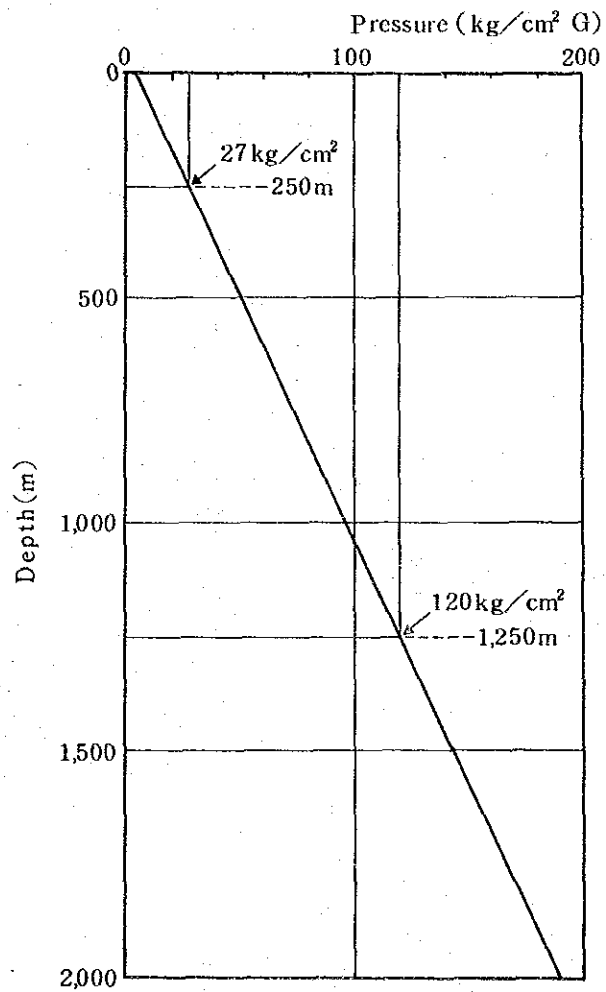
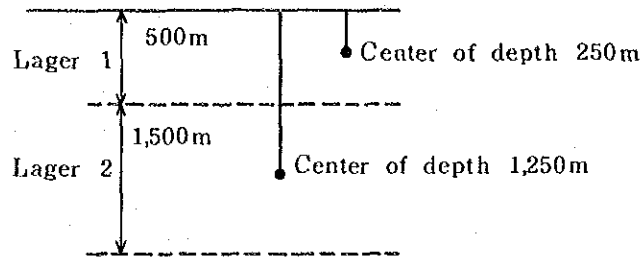


Fig. 2 Estimate of Reservoir Pressure





JICA